2016

The relationship of microRNAs to clinical features of Huntington's and Parkinson's disease

BOSTON UNIVERSITY

SCHOOL OF MEDICINE

Dissertation

THE RELATIONSHIP OF MICRORNAS TO CLINICAL FEATURES OF

HUNTINGTON'S AND PARKINSON'S DISEASE

by

ANDREW G HOSS

B.A., Binghamton University, 2006
M.S., Tufts University, 2010

Submitted in partial fulfillment of the

requirements for the degree of

Doctor of Philosophy

2016

Approved by

First Reader _____
Richard H. Myers, Ph.D.
Professor of Neurology

Second Reader _____
Jeanne C. Latourelle, Ph.D.
Assistant Professor of Neurology

DEDICATION

I would like to dedicate this work to my wife, Jenn - without your constant

encouragement, love and self-sacrifice, this process would never have been

possible ☺

ACKNOWLEDGMENTS

THE RELATIONSHIP OF MICRORNAS TO CLINICAL FEATURES OF

HUNTINGTON'S AND PARKINSON'S DISEASE

ANDREW G HOSS

Boston University School of Medicine, 2016

Major Professor: Richard H. Myers, Ph.D., Professor of Neurology

ABSTRACT

MicroRNAs (miRNAs) represent a major system of post-transcriptional regulation, by either preventing translational initiation or by targeting messenger RNA transcripts for storage or degradation. miRNA deregulation has been reported in neurodegenerative disorders, such as Huntington's disease (HD) and Parkinson's disease (PD), which may impact gene expression and modify disease progression and/or severity. To assess the relationship of miRNA levels to HD, small RNA sequence analysis was performed for 26 HD and 36 non-disease control samples derived from human prefrontal cortex. 75 miRNAs were differentially expressed in HD brain as compared to controls at genome-wide significance (FDR q<0.05). Among HD brains, nine miRNAs were significantly associated with the extent of neuropathological involvement in the striatum and three of these significantly related to a continuous measure of striatal involvement, after statistical adjustment for the contribution of HD gene length. Five miRNAs were identified as having a significant, inverse relationship to age of motor onset, in particular, miR-10b-5p, the mostly strongly over-expressed

miRNA in HD cases. Although prefrontal cortex was the source of tissue profiled in these studies, the relationship of miR-10b-5p levels to striatal involvement in the disease was independent of cortical involvement. In blood plasma from 26 HD, 4 asymptomatic HD gene carriers and 8 controls, miR-10b-5p levels were significantly elevated in HD as compared to non-diseased and preclinical HD subjects, demonstrating that miRNA alterations associated with diseased brain may be detected peripherally. Using small RNA sequence analysis for 29 PD brains, 125 miRNAs were identified as differentially expressed at genome-wide significance (FDR $q<0.05$) in PD versus controls. A set of 29 miRNAs accurately classified PD from non-diseased brain (93.9% specificity, 96.6% sensitivity, 4.8% absolute error). In contrast to HD, among PD cases, miR-10b-5p was significantly decreased and had a significant, positive association to onset age independent of age at death. These studies provide a detailed miRNA profile for HD and PD brain, identify miRNAs associated with disease pathology and suggest miRNA changes observed in brain can be detected in blood. Together, these findings support the potential of miRNA biomarkers for the diagnosis and assessment of progression for neurodegenerative diseases.

TABLE OF CONTENTS

LIST OF TABLES

LIST OF FIGURES

LIST OF ABBREVIATIONS

ANOVA .... Analysis of variance

BA9 .... Brodmanns Area 9

CAG .... Cytosine – adenine – guanine

CNS .... Central nervous system

FDR .... False discovery rate

GO .... Gene Ontology

HD .... Huntington's disease

HTT .... Huntingtin

H-V score .... Hadzi-Vonsattel score

mHTT .... Mutant HTT

miRNA .... MicroRNA

MSN .... Medium spiny neurons

PD .... Parkinson's disease

PDD .... Parkinson's disease with dementia

PMI .... Post-mortem interval

ROC .... Receiver operator characteristic

SNCA .... Alpha-synuclein

UHDRS .... Unified HD rating scale

UPDRS .... Unified PD rating scale

Chapter 1: INTRODUCTION

Background

Huntington's disease (HD) is a neurodegenerative disease caused by a cytosine-adenine-guanine (CAG) repeat expansion in the HTT gene located on chromosome 4p16.3 [1]. HD is a chronic, progressive, and fatal disease, with motor, cognitive and psychiatric symptoms. Most individuals diagnosed with HD first present symptoms at middle age, beginning with the emergence of insidious movement abnormalities, which progresses into abrupt, nonrandom, involuntary choreiform movements. Chorea is a key symptom of HD and defines disease diagnosis. Psychological problems, such as depression or psychosis are commonly observed [2]. Cognitive decline and loss of executive function in advanced stage HD is inevitable. Survival from onset to death averages 17 to 20 years.

The disease is autosomal dominant transmitted, affecting an estimated four to eight people per 100,000 in Western countries [3]. The normal range of the CAG repeat region of HD gene is 8 to 26 repeats, where 40 or more repeats is pathogenic [4, 5]. Individuals with an intermediate repeat range between 27 and 35 [6], and range of reduced repeats between 36 and 39, may also develop symptoms [7]. The CAG repeat size is inversely related to age of onset, where individuals with longer CAG repeat sizes are predicted to have earlier onset than individuals with short CAG repeat sizes [8] (**see Figure 1.1**). Although all HD is

caused by the same mutation, variability among individuals with HD is widely seen, with different degrees of motor and cognitive symptoms.

Neuropathology

The key neuropathologic feature of HD is selective neuronal loss of medium spiny neurons (MSNs) in the caudate nucleus and putamen, substructures of the striatum. Striatal atrophy begins at the tail of the caudate, which progresses in a rostral to caudal direction. Neuronal loss in the head of the caudate, near the lateral ventricle, and in the putamen, at the region closest to the internal capsule, occurs medially [9, 10]. Several imaging-based studies have identified a strong relationship between clinical features and the extent of brain atrophy in HD [11], indicating the loss of the inhibitory GABAergic MSNs in the striatum is associated with the motor aspects of the disease. Volumetric measurements of the caudate and putamen by MRI suggest that atrophy in the striatum begins 9 to 20 years prior to diagnosis [12].

By clustering neuropathological evaluations of 41 brain regions (rated 0-4, "0" being absent of change, "4" representing the highest degree of change), quantitative scores were created to represent the combined involvement of the disease within the striatal and cortical brain regions [13]. Termed the "Hadzi-Vonsattel" score, 523 brains from the Myers lab were scored by a neuropathologist and assessed for their relationship to disease features. Hadzi-Vonsattel striatal score was found to be strongly related to the size of the CAG expansion, where larger repeats are associated with more severe involvement at

time of death [10]. Cortical atrophy, however, did not relate to the extent of striatal involvement nor to CAG repeat size [10]. Variability in the relative to the involvement of cortical and subcortical regions likely influences the wide range of motor versus cognitive and psychiatric symptoms recognized among HD patients. While both cortical and subcortical regions are involved in HD [9, 14, 15], the cortex is considerably less involved than the striatum. The mechanisms that lead to patient-to-patient variability in cortical and CAG-independent striatal neurodegeneration remain unknown.

Molecular pathogenesis of HD

The HD mutation produces a neurotoxic, mutant HTT protein (mHTT). The polyglutamine tract expansion caused by the HD mutation exists within the N-terminal region of the HTT protein [4], which leads to aggregate formation in the brains of HD patients [16] as well as in HD *in vitro* models [17].

Cytosolic and intranuclear inclusions containing mHTT fragments in neurons of the striatum and cerebral cortex are a histopathological hallmark of HD [18]. In post-mortem HD brains, extensive aggregation is observed in the striatum and in sub-layers of the cerebral cortex, and to a lesser extent, in the basal ganglia, hippocampus, and cerebellum [18]. Striatal MSNs and cortical pyramidal interneurons exhibit extensive aggregation, where aggregates initially localize to the soma and dendritic processes and later as the disease progresses, intranuclear formation occurs [18].

Aberrant nuclear localization of mHTT fragments precedes cell death in neurons [19]. However, the process by which preferential death of striatal MSNs occurs is not fully understood. HD pathogenesis is likely caused by a gain-of-function of mHTT, where the polyglutamine repeat expansion contributes to the misfolding and aggregate form of HTT, resulting in a protein with new, toxic function [20] or by the loss of wildtype HTT function through a loss-of-function or dominant-negative effect.

Gain-of-function is the most well accepted hypothesis for HD pathogenesis. Transcription factors, such as CREB-binding protein (CBP) [21], specificity protein 1 (SP1) [22], TATA-binding protein (TBP) [23] and p53 [21], and transcriptional repressors such as REST/NSRF [24], spuriously bind to mHTT intranuclear inclusions impairing their normal activity, leading to transcriptional dysregulation [25]. The transcription factor nuclear factor kappa-light-chain-enhancer of activated B cells (*NFkB*), which is particularly related to immune function, has shown altered activity in HD due to direct, aberrant interactions with soluble mHTT [26, 27].

The HD gene encodes a large, 348 kDa cytosolic protein (HTT) that is widely distributed throughout the body, with its highest levels in the brain [28, 29]. The protein structure of HTT suggests it is a multifunctional scaffolding protein, with multiple HEAT repeats and hydrophobic alpha-helices that assist in protein-protein interactions, and a nuclear export signal [30] which aids in nuclear transport. HTT directly associates with the microtubule motor dynenin [31], and

indirectly binds kinesin-1 through Huntingtin-associated protein 1 [32],

modulating the bidirectional transport of endocytic and exocytic vesicles along

cytoskeletal tracks [33]. Within RNA transport granules, HTT colocalizes with

Argonaute 2, a component of the RNA-induced silencing complex, indicating it

may play a role in localized translational control through the silencing of RNA

transcription [34, 35]. HTT is critical for nervous system development [36] and

embryonic lethal in knockout huntingtin mice [37]. HTT may also play a role in

cytokine production in monocytes and macrophages under normal and HD

settings [38].

HD is associated with the disruption of an assortment of cellular

processes, impairing cell adhesion[39], mitochondrial energetics [40], cellular

transport [41], autophagic processing [42], ubiquitin–proteasome system [43],

synaptic plasticity [44] and enhancement of glutamate-related excitotoxicity [45].

HTT cleavage is mediated by caspases to produce an amino-terminal polyQ

containing fragment [46], and mHTT is more susceptible to cleavage than its

normal counterpart. The N-terminal region is cleaved by caspases and calpains

to produce N-terminal fragments in both normal and HD cells, where only the

expanded polyQ fragments of HD self-associate and seed aggregates [47-49].

Activation of caspases induces apoptosis; thus, overactive caspases have

deleterious effects on already stressed neurons.

Parkinson's disease

Background

Parkinson's disease (PD) is the second most common neurodegenerative disease, characterized by resting tremor, rigidity, bradykinesia and postural instability [50]. The loss of dopamine-producing neurons in the substantia nigra par compacta, a substructure of the basal ganglia, is a hallmark of PD neuropathology. Reduction of dopaminergic neurons results in dopamine depletion, improper regulation of the nigrostriatal pathways, consequently hypokinesia.

Neuronal cytoplasmic inclusions, termed Lewy bodies, and Lewy neurites found in neuronal processes, are observed throughout the brain [51]. Lewy bodies predominantly consist of α-synuclein protein, and to a lesser extent, ubiquitin, calbindin, and tubulin [51]. α-synuclein is a small, 140 amino-acid protein found in high abundance at the presynaptic terminal of neurons, representing up to 1% of all cytosolic protein found in the brain [52]. A predictable topography of pathological changes in the central nervous system is observed, as annotated by Braak [53], beginning in olfactory bulb and medulla oblongata, then progressing rostrally from the medulla to the pons, then to the substantia nigra and midbrain, limbic structures, and neocortical structures.

α-synuclein has the ability to generate β-sheet structures under specific physiological conditions, creating amyloid-like fibrils. Soluble, oligomeric α-synuclein can transition into spherical, string-like, protofibrils, which gradually

6

assemble into insoluble, neurotoxic fibrils [51]. Injection of protofibrils into PD

mouse models results in widespread aggregate deposition in the brain [54],

which indicates transmission of the protofibrils through neural connectivity.

The mechanism by which dopaminergic neurons preferentially degenerate

likely occurs through several converging pathways. α-synuclein accumulation is

neurotoxic. Oligomeric α-synuclein may lead to dopamine leakage of

neurotransmitter filled vesicles into the cytosol, which could lead to oxidative

stress-induced death [55]. Cytosolic dopamine contributes to oxidative stress and

cellular damage, by disrupting glutathione homeostasis, enhancing calcium

influx, increasing calcium-mediated calpain activation and supporting in free

radical production [56]. Neurotoxins, such as 6-hydroxydopamine (6-OHDA),

MPTP, and the pesticide paraquat, have been shown to destroy DA neurons, and

individuals that have exposure to these chemicals display Parkinsonism [57].

These toxins infer with complex I of the electron transport chain, causing the

increase of free radicals and halting mitochondrial metabolism, leading to cell

death [58]. In PD, impaired energetics by mitochondrial dysfunction may be

aggravated by abnormal proteostasis, as normal clearance of proteins by

chaperone-mediate autophagy or other proteolytic mechanisms may be impaired

[59]. Both neuronal and glial sources have been implicated in the contribution of

oxidative stress, and chronic neuroinflammatory activity from dying cells or

inclusion bodies may play a role in the degenerative process [60].

Genetic heterogeneity

The underlining mechanism of α-synuclein misfolding and insoluble

aggregation is poorly understood. However, the discovery of genetic forms of PD

caused by mutations of the α-synuclein gene (*SNCA*) [61-67], have led to its

identification and insight into PD pathogenic mechanisms. Multiplication of *SNCA*

(duplication and triplication of the gene) leads a dominant forms of PD, and

SNCA levels of gene expression inversely related to age of onset of PD [68]. A

missense substitution (A53T) impacts protein clearance and also leads to

dominant inheritance.

Mendelian and complex forms of PD [61] may provide novel insight into

disease etiology and pathological mechanisms. Mutations of the leucine-rich

repeat kinase 2 gene (*LRRK2)* represent the most common inherited form of PD

[68]. 13 other Mendelian forms have been identified, and this number will

continue to grow as genome-wide methods are continually applied [68]. Many of

these genes, including parkin, DJ-1, and PINK, are linked to respiration and

mitochondrial function.

Due to the occurrence of reduced penetrance, variable expressivity, and

environmental phenocopy effects, pedigrees often lack Mendelian patterns of

inheritance. Genome-wide association studies illustrate the complex etiology of

PD and genetic heterogeneity of the disease. The results from the mega-meta

PD GWAS over (~13,000 PD, 80,000 control), identified 24 loci, and the second

most significant locus, microtubule-associated protein tau (*MAPT*), also encodes

for the protein which when phosphorylated, is present in aggregates in tauopathies and Alzheimer's disease [61]. However, GWAS variants only account for an estimated 30% of familial and 5% of sporadic, non-familial cases [69, 70].

Preclinical and progressive biomarkers for neurodegenerative disease

Huntington's disease biomarkers

Although genetic testing allows for reliable detection of HD (by sequencing of the CAG repeat of the HD gene), there remains a need for biomarkers of disease progression in premanifest individuals. The mechanism by which premanifest HD gene carriers transition to manifest HD remains unknown. Slowing disease progression may delay the onset of disease symptoms.

Clinical progression of HD can be measured by a number of clinical tests. The Unified Huntington Disease Rating Scale (UHDRS) is the gold standard, which assesses of the degree of motor, cognitive, and behavioral involvement as well as total functional capacity (TFC) and degree of independence [2]. Although UHDRS may be able to determine the extent of deterioration of executive functioning (as measured by TFC), its utility is limited to symptomatic, early and mid-stage HD patients.

As HD progresses, the brain loses significant volume, and these early structural changes are observable using magnetic resonance imaging (MRI) in premanifest individuals. A 50% reduction in volume of the putamen and 28% reduction of the caudate nucleus has been observed in early stage HD patients

[71]. TRACK-HD, a large (n=366) cross-sectional study aimed to discover baseline predictors of HD progression, observed volumetric changes in premanifest HD across a 36 month period, and in early symptomatic HD patients, these changes correlated with progression [72]. Results from PREDICT-HD, another large HD cohort, estimated that volumetric brain changes might be detectable up to 15–20 years prior to diagnosis [73]. The severity of HD clinical manifestations relate to the loss of neurons, but also to neuronal dysfunction and synaptic changes as measured by functional MRI (fMRI). Increased activation of the dorsolateral prefrontal cortex was observed in presymptomatic individuals as they approached disease onset, independent of cortical atrophy [74]. Increased neuroinflammation, measured by microglial activation [75, 76] or proinflammatory cytokines (such as TNF-α, IL-6, IL-8) in blood has been observed in premanifest and early stage HD [77].

Altered dopamine signaling may play a role in HD pathogenesis. Positron emission tomography (PET) based imaging using radiolabeled striatal dopamine receptors (D1, D2) and well as dopamine transporter (DAT), have shown decreased postsynaptic receptor density and binding in asymptomatic HD gene carriers and HD patients [78]. Brain metabolism can also be measured using PET. Reduced glucose uptake was first observed in mice with neostriatal lesions, using 14C-2-deoxyglucose (DG) autoradiography [79] and later, glucose hypometabolism in human neostriatum was shown to preceded degeneration and correlate with motor impairments [80-83].

10

Increased levels of leukocyte 8-hydroxydeoxyguanosine (8-OHdG), a marker of free radical oxidative damage to DNA, have been observed in the caudate and parietal cortex [84], serum [85], and leukocytes [86]. Increased 8-OHdG levels were observed in premanifest individual in longitudinal studies, with higher levels in those with larger repeats or older ages [87]. However, these results were not repeatable in an independent cohort, assayed by two separate using two assay protocols (LCECA, LC-MSMS) [88]. Phosphodiesterase 10A (PDE10A) using [^{18}F]MNI-659, PET imaging tracer selective for the striatum, has shown promise in preliminary cross-sectional and longitudinal studies, where reduced PDE10A levels correlate with clinical measures of disease severity [89].

Although precise and accurate anatomical or functional endpoints can be measured using neuroimaging, poor reproducibility can result due to the lack of standardization. Imaging is susceptible to unreliability across centers, due to differences in data acquisition, the handling of motion artifacts, scanner models, image processing, the software for normalization, the reference for spatial mapping and overall analysis [90].

Ideally, assays that predict the continuum of HD would be derived from peripheral biofluids, due to cost effectiveness, simplicity and ease of clinical adoption. As immunoassays improve, mHTT may be a tractable biomarker for HD progression. The extent of accumulation of mHTT protein in peripheral fluids such as sorted blood cells [91] and cerebrospinal fluid [92], can be measured

using high-resolution immunoassays. In cerebrospinal fluid, using single

molecular counting for mHTT, mHTT was detectable only in HD gene carriers,

was three times higher in symptomatic HD as compared to premanifest HD gene

carriers, and was associated with of cognitive and motor dysfunction in

symptomatic HD patients [92]. However, these results, while encouraging, are

relatively new and yet to be reproduced.

Several studies describe the early and chronic elevation of

proinflammatory cytokines in HD blood cells but these signals do not provide the

resolution needed to track disease progression [31-33]. Researchers have

attempted to use a candidate gene approach, in particular in probing

inflammatory cytokine genes, with little success [34,35].

Genome-wide genomic profiling is an attractive option for HD diagnostics,

as these tests have the ability to measure cellular state with high-resolution. A

set candidate genes identified in genome-wide studies can be easily

standardized with PCR-based tests or as DNA sequencing technologies continue

to improve, a set of genes could efficiently tested with a single assay. H2A

histone family, member Y (H2AFY) mRNA was found to overexpressed in HD

prefrontal cortex and HD patients compared to controls, and was recent validated

by an independent study [93], which used RNA-sequencing of peripheral blood

cells to identify 167 genes that related to clinical motor scores [93]. Although

these results lacked concordance to a previous blood study [94], the

concordance of H2AFY mRNA is encouraging. Discrepancies could be due to the

12

technologies used (microarray versus sequencing), the susceptibility of RNA to nucleases and the relatively short half-life of messenger RNA, estimated from 15 minutes to 17 hours *in vitro* [36]. Other representative genomic markers, such as miRNAs, with high stability and long half-lives [38-40] may be more useful for HD prediction.

Parkinson's disease biomarkers

PD diagnostics apply similar strategies as in HD, however isolating preclinical PD patients is difficult. Additionally, the diagnosis of idiopathic PD is encumbered by the heterogeneous presentation of symptoms, distinctive clinical subtypes (PD, PDD), and variable rates of progression. 30% of PD patients have PD-related dementia [95]. Monogenic, familial forms only represent a small sample of PD patients.

Three phases have been proposed – preclinical, premotor, and motor phases of PD [96]. In the preclinical phase, no symptoms are present. Nonmotor manifestations are detectable in the premotor phase. Prodromal or premotor markers include olfactory dysfunction [97], neuropsychiatric, and autosomal changes such as gastrointestinal complications [98], or sleep abnormalities (excessive sleepiness [99], idiopathic REM sleep behavior disorder [100]). Over 90% of patients with PD have olfactory dysfunction [97], and using the Brief Smell Identification Test in 2,267 healthy males, longitudinal tests found the odds of PD development within 4 years in the lowest quartile of olfactory acuity to be 5.2 times that observed in the highest two quartiles [101]. Clinical measures of

PD progression of motor symptoms and cognitive decline can be assessed by the Unified Parkinson's Disease Rating Scale (UPDRS), a battery of tests comprised of six tests, measuring cognitive health, complications of therapy, extent of motor involvement, level of independence as severity of PD symptoms as measured by the Hoehn and Yahr scale [102].These measures are used for diagnosis, clinical evaluation and monitoring of the rate of functional decline in PD.

The onset of DA loss precedes motor symptoms. Image based analysis using radioligands for DA transporter to assess the integrity of the dopaminergic system have been successful in some instances of differentiating the degree of PD severity [103]. In a longitudinal 3-center observational study with 37 months of prospective follow-up, a 17-fold increased for the relative risk for developing PD was observed among those with transcranial sonography substantia nigra hyperechogenicity [104], occurring in over 90% of PD patients, compared to 10% of healthy older adults. Histopathological evidence from gastrointestinal tract neurons, from colonic submucosa of PD patients, was positive for α-synuclein accumulation [105]. Biochemical screening methods for Lewy body related proteins in peripheral fluids like CSF and blood might act as high-resolution biomarkers. In postmortem CSF from PD and control subjects, assaying six proteins (fibrinogen, transthyretin, apolipoprotein E, clusterin, apolipoprotein A-1, and glutathione-S-transferase-Pi), using two-dimensional difference gel electrophoresis, PD samples differed by 1.5-fold in protein concentration [106].

Comparing protein levels in the CSF of 42 PD and 69 controls, in PD, increased α-synuclein levels were associated with progression of motor symptoms and cognitive decline over 2 years, lower levels of Aβ was associated with worsening of performance on delayed memory recall, and high levels of phosphorylated tau were associated with worsening in motor symptoms [107].

Genome-wide transcriptomics have been used for PD biomarker discovery. In an RNA-seq study of blood, asymptomatic individuals with the G2019S LRRK2 mutation were compared to idiopathic PD and health controls, to identify genes that may be specifically altered in LRRK-related PD [1]. In a study of 105 total patients, microarrays were used to create a detail transcriptomic profile of early-stage PD peripheral blood, and though differentially expressed genes were identified, classification of PD based on RNA expression failed in validation [2]. Reanalysis of these data identified a set of 10 genes that may predict PD using PCA [3]. Levels of seven brain-relate genes were measured in blood samples from 62 early-stage PD patients and 64 controls, and using a stepwise multivariate logistic regression analysis, five genes were identified as disease predictors of PD (sensitivity 90.3, specificity 89.1, ROC AUC=0.96, validated AUC=0.95) [4]. After induction of deep brain stimulation, RNA changes were observed in PD leukocytes [108, 109]. Using network analysis from four independent microarray studies, hepatocyte nuclear factor 4 alpha (*HNF4A*) and polypyrimidine tract binding protein 1 (*PTBP1*) were significantly altered in blood from two independent cohorts, and based on their levels, exhibited significant
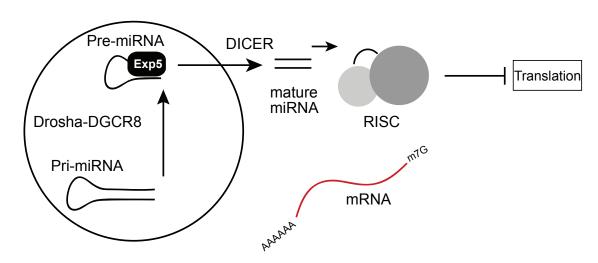
longitudinal changes over the course of the 3 year follow-up period and classified

PD with 90% sensitivity and 80% specificity [110]. mRNA biomarkers in blood

may be informative for identifying PD-related genes, but due to their inherent

lability and patient-to-patient variability, other markers, such as microRNAs, may

be representative of mRNA changes but more biochemically stable.

Role of miRNAs in neurodegenerative diseases

MicroRNAs (miRNAs) are small non-coding RNAs, 18-25 nucleotides in

length, which bind complementary sites within the 3' untranslated regions of

messenger RNA. Through the assembly of the RNA-induced silencing complex

(RISC), the duplexed transcript signals for degradation by endonuclease

cleavage, or preventing translation of the gene product by stalling protein

synthesis machinery [111] (**see Figure 1**). As translational regulators of mRNA

expression, miRNAs can directly control cell fate decisions, and consequently,

miRNAs are involved in numerous aspects of embryonic and neurodevelopment

[112].

Figure 1. Schematic of miRNA biogenesis.
Primary transcripts are transcribed and processed by DROSHA, exported from the nucleus by Exportin 5, trimmed by DICER and loaded into RISC to become active silencers. Insoluble aggregates can affect normal miRNA mechanisms, by increasing mRNA content due to spurious protein binding or impairing miRNA complex activity.
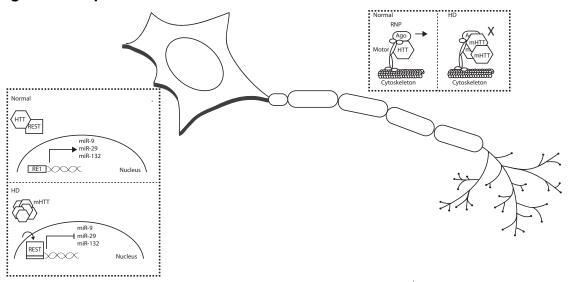
Dysregulation of miRNAs has been linked to neurological and neurodegenerative disorders [113] and several studies have explored the role of miRNAs in HD (see Figure 2). In targeted study, Parker et al 2008 observed miRNAs predicted to target RE1-silencing transcription factor (*REST*), a transcriptional repressor which has enhanced function as mHTT fails to prevent its nuclear translocation and subsequent downstream repressive effects of neuroprotective genes [114]. Marti et al [115] performed miRNA-sequencing for two pooled HD samples and two pooled control samples, and while a number of miRNA differences were observed, differential expression could not be performed. Altered expression of miRNAs, quantified using microarray technology, has been reported in cellular models of HD [114, 116, 117] and in mouse models of HD [117-120], which either focus on REST/CoREST-related

miRNAs or miRNAs which are predicted to target *HTT*. Most telling may be the interaction of HTT with important miRNA-related machinery. Wildtype HTT was found to colocalize with Argonaute 2, the endonuclease required for RNA-mediated gene silencing by the RNA-induced silencing complex (RISC), within neuronal transport RNA granule [121, 122], suggesting HTT may facilitate miRNA-mediated mRNA degradation and/or localized translation of specific mRNAs.
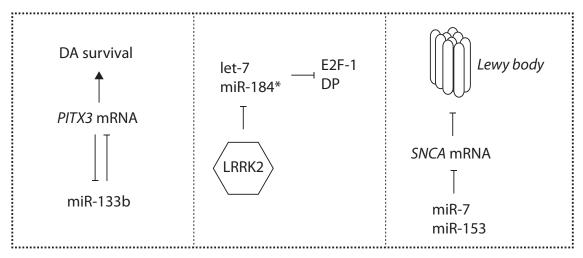
Figure 2. Proposed HD miRNA mechanisms.

Kim et al. 2007 was the first to highlight the importance of miRNA function within the dopaminergic system [123]. Dicer, the enzyme responsible for the cleavage of primary miRNA into their mature, active form, was genetically removed exclusively in post-mitotic, dopaminergic neurons. Dicer-null neurons in these transgenic mice into lived into adulthood, but later in life, mice displayed PD-like phenotypes and dopamine-expressing neurons were progressively lost.

In vitro, these neurons were unable to mature but were effectively rescued with the addition of small endogenous RNAs [123]. While specific miRNAs were altered in the midbrain of these mice, subsequent genetic studies have found no association of these miRNAs or their target to PD [124]. However, miRNAs have been observed to modulate of alpha-synuclein protein expression, and single nucleotide polymorphisms (SNPs) in the 3'UTR of SNCA [125], as well as SNCA 3'UTR length, may be associated with PD, revealing a potential role of SNCA-binding miRNAs in PD [126-128]. Several miRNAs that we reported altered in PD brain may have an indirect relationship to PD-related genes (see Figure 3). Genetic forms of PD include mutations within the α-synuclein gene (SNCA), as well in Leucine-rich Repeat Kinase 2 (LRRK2), one of the most common causes of familial PD [61]. miR-34b/c was identified as being altered in brain from microarray, however genome-wide changes were not reported [129]. A number of PD blood studies have been performed with little concordance [130-134], although miRNA in blood of PD patients after Levodopa treatment showed suggestive alterations [135]. In Burgos et al. 2014, small RNA sequencing was performed for blood serum and CSF from 67 PD and 78 control postmortem subjects [136], a number of changes were reported, but without information from brain, were difficult to interpret.

Figure 3. Proposed PD miRNA mechanisms.

Commonly, miRNA biomarker studies have been initiated in blood or other peripheral biofluids, and their relationship to neuropathological involvement has not been considered. As noted above, both HD and PD are known to have physiological complications such as gastrointestinal problems, weight loss, sleep disorders, as well as autonomic and sensory dysfunctions. It is likely that some of these changes produce alterations in blood that are not indicative of the underlying neurodegenerative process and thus would not predict the neurologically dependent disease processes. By using primarily affected tissue, such as prefrontal cortex, from postmortem patient samples as an initial miRNA screening approach, candidate miRNAs can be selected for studying the periphery, decreasing noise and irrelevant signals such as physiological changes which do not explain disease progression. A comprehensive evaluation of the correspondence of brain miRNA and miRNA detectible in biofluids is the logical first in the effective detection of HD and PD biomarkers.

Biochemically, miRNAs are relatively stable. The half-life of the majority miRNA has been predicted to be on average 5 days [137]. Plasma miRNAs have been observed unaffected by extreme heat or pH, long-time storage at room temperature, or multiple freeze-thaw cycles [38-40]. The small size of miRNA allow higher potential for neuropathologically specific miRNA to cross the blood-brain barrier in exosomes [138] and circulate stably in peripheral fluids as cell free molecules [139]. The ability of miRNA to circulate provides a unique opportunity to monitor the neurological disease processes from the periphery.

miRNA sequencing offers high-resolution detection over a wide dynamic range of miRNA levels to create a detailed miRNA profile. miRNA sequence analysis would provide the most accurate and comprehensive miRNAs signature in HD or PD, to identify neuropathologically and potentially clinically relevant miRNA for biomarker discovery.

Hypothesis and Specific Aims

Hypothesis

We hypothesize miRNAs are altered in Huntington's and Parkinson's disease brain. As key post-transcriptional regulators, miRNAs associated with disease may also help describe neuropathology or disease features, such as the age of motor onset. Due to their stability and extracellular transport, brain-related miRNA changes may be observed in the blood, and therefore function as potential disease classifiers or predictors of disease phenotypes.

Specific Aims

Aim 1: Characterize miRNA expression in HD brain. We will perform Illumina small non-coding next-generation sequencing on 42 Brodmann Area 9 (BA9) prefrontal cortex samples (16 HD, 26 controls), and combine this cohort with our initial study of 12 HD and 9 controls to identify disease-related miRNA. Additional samples will provide statistical power and confidence needed to find differentially expressed miRNA, as well as model relationships of clinical features of HD, such as age of disease onset, age at death, and extent of neurodegeneration in striatum and prefrontal cortex, to miRNA expression.

Aim 2: **Evaluate blood plasma miRNAs as circulating biomarkers for HD disease progression.** We will assess whether brain-specific miRNA changes are peripherally observable. Using blood plasma-derived RNA collected from a cohort of 26 HD, 4 asymptomatic HD gene carriers and 8 controls, we will measure levels of miR-10b-5p, miR-486-5p, miR-132-3p and miR-363-3p, four miRNAs with associations to the extent of striatal involvement and/or onset age. We will compare the levels across the three groups to identify whether miRNA levels associate with disease stage.

Aim 3: Characterize miRNA levels in Parkinson's disease brain. We will perform sequencing in 29 PD prefrontal cortex and using our existing controls, compare the two groups to identify genome-wide miRNA alterations in PD brain. We will use classification analysis to find a miRNA profile for PD, and

identify miRNAs that relate to disease phenotypes, such as onset age and

dementia.

CHAPTER 2: MICRORNAS LOCATED IN THE HOX GENE CLUSTERS ARE IMPLICATED IN HUNTINGTON'S DISEASE PATHOGENESIS

Abstract

Transcriptional dysregulation has long been recognized as central to the pathogenesis of Huntington's disease (HD). MicroRNAs (miRNAs) represent a major system of post-transcriptional regulation, by either preventing translational initiation or by targeting transcripts for storage or for degradation. Using next-generation miRNA sequencing in prefrontal cortex (Brodmann Area 9) of twelve HD and nine controls, we identified five miRNAs (miR-10b-5p, miR-196a-5p, miR-196b-5p, miR-615-3p and miR-1247-5p) up-regulated in HD at genome-wide significance (FDR q-value <0.05). Three of these, miR-196a-5p, miR-196b-5p and miR-615-3p, were expressed at near zero levels in control brains. Expression was verified for all five miRNAs using reverse transcription quantitative PCR and all but miR-1247-5p were replicated in an independent sample (8HD/8C). Ectopic miR-10b-5p expression in PC12 HTT-Q73 cells increased survival by MTT assay and cell viability staining suggesting increased expression may be a protective response. All of the miRNAs but miR-1247-5p are located in intergenic regions of Hox clusters. Total mRNA sequencing in the same samples identified fifteen of 55 genes within the Hox cluster gene regions

as differentially expressed in HD, and the Hox genes immediately adjacent to the four Hox cluster miRNAs as up-regulated. Pathway analysis of mRNA targets of these miRNAs implicated functions for neuronal differentiation, neurite outgrowth, cell death and survival. In regression models among the HD brains, huntingtin CAG repeat size, onset age and age at death were independently found to be inversely related to miR-10b-5p levels. CAG repeat size and onset age were independently inversely related to miR-196a-5p, onset age was inversely related to miR-196b-5p and age at death was inversely related to miR-615-3p expression. These results suggest these Hox-related miRNAs may be involved in neuroprotective response in HD. Recently, miRNAs have shown promise as biomarkers for human diseases and given their relationship to disease expression, these miRNAs are biomarker candidates in HD.

Introduction

Huntington's disease (HD) (OMIM: 143100) is an inherited neurodegenerative disorder characterized by involuntary movement, dementia, and changes in personality. HD is transmitted as an autosomal dominant disorder, for which an expansion of a CAG trinucleotide repeat within the coding region of the huntingtin gene (*HTT)* is the disease causing mutation [1]. The CAG repeat codes for a polyglutamine domain in the Htt protein and results in neuronal cell death predominantly affecting the caudate nucleus and putamen although neuronal loss is widespread in the HD brain [2,3]. While the biological processes leading to neurodegeneration in HD are poorly understood,

transcriptional dysregulation has long been proposed as central to the pathogenesis of HD. Widespread alterations in gene expression have been reported [4] and several studies suggest that gene expression may be altered at one or more of the stages of RNA processing, translation, protein post-translational modification or trafficking [5,6].

MicroRNAs (miRNAs) are small non-coding RNAs that function as translational regulators of mRNA expression. miRNAs may inhibit gene expression either by repressing translation, or by targeting mRNA for either storage or degradation [7]. Recently, dysregulation of miRNAs has been linked to neurological and neurodegenerative disorders [8] and several studies have explored the role of miRNAs in HD. Marti et al [9] performed miRNA-sequencing for two pooled HD samples and two pooled control samples and reported altered expression for a large number of miRNAs. Altered expression of miRNAs, quantified using microarray technology, has been reported in cellular models of HD [10-12] and in mouse models of HD [12-15] but a comprehensive study of miRNA and mRNA expression obtained through next-generation sequencing technology in human HD samples has not been performed.

In order to investigate (1) the presence of altered miRNA expression and (2) the potential role of miRNAs on the altered mRNA expression seen in HD, we performed both miRNA-sequencing and mRNA sequencing, using Illumina massively parallel sequencing in twelve HD and nine neurologically normal control brains. To our knowledge this is the first genome-wide quantification of

miRNA expression comparing human HD and control brain, and the first to combine total miRNA expression with total mRNA expression obtained through massively parallel sequencing.

Results

Selection of prefrontal cortex and BA9. While the striatum is the region most heavily involved neuropathologically in HD [3], 80% to 90% of the neurons in that region will have degenerated by the time of death. These changes, together with the presence of reactive astrocytosis, alter the cellular composition of the striatum. In contrast, cortical involvement in HD is well defined [2,16] and while it does not experience dramatic neuronal degeneration, cortical neurons are known to exhibit the effects of protein aggregation and nuclear inclusion bodies characteristic of the disease. Therefore, we selected the prefrontal cortex for these studies.

Table 1. HD brain samples analyzed for mRNA-seq, miRNA-seq and RT-qPCR validation of miR-10b-5p.
All of the HD samples passed mRNA-seq QC. Scale of neuron loss: 0=absent, 1=mild, 2=moderate

Sample ID	miRNA-seq	RT-qPCR	PMI (hr.)	RIN or RQN	Death age	Onset age	Duration (yr.)	CAG repeat size	Neuron Loss in Neocortical Gray Matter
HD-01	Passed	Y	37	7.1	55	44	11	45	1
HD-02	Passed	Y	6	7.5	69	63	6	41	1
HD-03	Passed	Y	21	7	71	52	19	43	1
HD-05	Passed	Y	19	6.9	48	25	23	48	2
HD-06	Passed	Y	NA	6.2	40	34	6	51	1
HD-07	Passed	Y	8	8.5	72	55	17	41	1
HD-08	Passed	Y	21	7.4	43	NA	NA	49	1
HD-09	Passed	Y	4	7.8	68	45	23	42	1
HD-10	Passed	Y	6	8.3	59	35	24	46	1
HD-12	Passed	Y	13	6	68	52	16	42	0
HD-13	Passed	N	25	6.1	57	40	17	49	1
HD-14	Passed	Y	11	7.3	48	38	10	45	1
Mean	-	-	15.48	7.18	58.17	43.91	15.64	45.17	0.875

Table 2. Control brain samples analyzed for mRNA-seq, miRNA-seq and RT-qPCR validation of miR-10b-5p.
All the control samples passed mRNA-seq QC.
RIN = RNA Integrity Number, RQN = RNA Quality Number, PMI = Postmortem Interval

Sample ID	miRNA-seq	RT-qPCR	PMI (hr.)	RIN or RQN	Death age
C-14	Passed	Y	21	8	79
C-21	Passed	Y	26	7.3	76
C-29	Passed	Y	13	6.4	93
C-31	Passed	Y	24	7.3	53
C-32	Passed	Y	24	8.3	57
C-33	Passed	Y	15	7.5	43
C-35	Failed PCA	N	21	7.6	46
C-36	Passed	Y	17	7.5	40
C-37	Failed PCA	N	28	8.3	44
C-38	Passed	Y	20	7.7	57
C-39	Passed	Y	15	7.3	80
Mean	-	-	20.36	7.49	60.73

Five miRNAs are up-regulated in HD. After removing sample outliers using principal component analysis filtering, we identified five out of 1,417 detected mature miRNA species as differentially expressed between twelve HD and nine control prefrontal cortex samples using the R statistical package DESeq (**Tables 1, 2 and 3; Figure 4**). All five miRNAs were significantly up-regulated in HD. The largest effect between conditions was seen for miR-10b-5p, with a 28.41 fold increased expression in HD relative to control samples (mean control expression=915.81; mean HD expression=26,020.05, **Figure 4**). miR-1247-5p was expressed at moderate levels in both control (mean=49.44) and HD brain (mean=102.01). Three of the miRNAs, miR-196a-5p (mean control
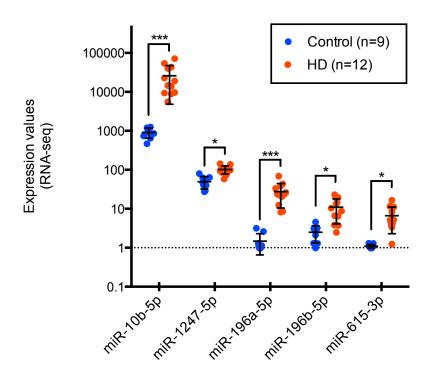
expression=1.47; mean HD expression=27.49), miR-196b-5p (mean control

expression=2.49; mean HD expression=11.01) and miR-615-3p (mean control

expression=1.09, mean HD expression=6.66), had near zero expression levels in

all nine control samples.

Table 3. Differentially expressed miRNAs from miRNA-seq
* FDR-adjusted q-value

miRNA	Control expression	HD expression	Fold Change	p-value	q-value *
miR-196a-5p	1.47	27.49	18.66	2.05E-10	2.91E-07
miR-10b-5p	915.81	26020.05	28.41	1.99E-08	1.41E-05
miR-615-3p	1.09	6.66	6.09	2.73E-05	1.29E-02
miR-1247-5p	49.44	102.01	2.06	7.67E-05	2.72E-02
miR-196b-5p	2.49	11.01	4.41	9.77E-05	2.77E-02

Figure 4. miR-196a-5p, miR-10b-5p and miR-615-3p were found significantly differentially expressed in Huntington's disease
miR-10b-5p, miR-1247-5p, miR-196a-5p, miR-196b-5p, and miR-615-3p were identified as differentially expressed in Huntington's disease prefrontal cortex compared to non-neurological disease controls by Illumina miRNA-sequencing. Normalized expression values quantified from DESeq analysis are shown on the y-axis. miR-196a-5p, miR-196b-5p and miR-615-3p were essentially not expressed in control samples, while the mean HD expression was 27.49, 11.01 and 6.66 respectively. miR-1247-5p was expressed at moderate levels in both control (mean=49.44) and HD brain (mean=102.01). miR-10b-5p was expressed in control (mean=915.81) and highly expressed in HD brain (mean=26,020.05). For miRNA, *p<0.05 and ***p<0.001, as determined by DESeq, followed by the Benjamini-Hochberg multiple comparison correction. (HD=Huntington's disease).
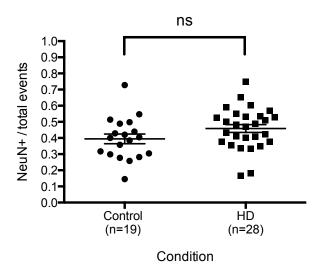
Validation and replication of miRNA findings. miRNA expression

differences were orthogonally validated using the Exiqon miRCURY LNA™

technology for reverse transcription quantitative PCR (RT-qPCR) in eleven of

twelve sequenced HD samples and nine control samples originally studied for

miRNA-seq. All five miRNAs were confirmed to be significantly up-regulated in

HD, consistent with our miRNA-sequencing findings.

To replicate our findings in an independent sample set, we performed RT-qPCR

in an additional eight control and eight HD prefrontal cortical samples. Four out

of five miRNA (miR-10b-5p, miR-196a-5p, miR-196b-5p, miR-615-3p) were

confirmed as significantly increased in expression in HD.

Similar proportion of neurons in HD and control cortical brain

homogenate samples. HD is characterized by progressive cortical atrophy, with

recognizable neuropathologic abnormalities in the neocortical gray matter [2,16-20] (<mark>Table 1</mark>). To address whether miRNA expression changes in HD may be due to altered ratios in brain cell-type abundance, such as a change in the ratio of neurons to glial cells, we compared the number of neuronal and non-neuronal nuclei across conditions. Suspensions of cell nuclei of prefrontal cortex from 28 HD cases and 19 controls were immunocytochemically labeled with anti-NeuN, a neuron-specific nuclear antigen, followed by flow cytometric analysis. The mean and range of NeuN+ ratios for controls and cases were not significantly different (t=1.67, p-value=0.10; <mark>Figure 5</mark>), suggesting cortical neuron loss in the BA9 area in HD is relatively modest and does not account for the dramatic alterations in miRNA levels reported here.

Figure 5. Neuron counts from prefrontal cortical tissue homogenate.
No significant difference is observed when comparing ratios of NeuN+ counts to total events quantified by flow cytometry.
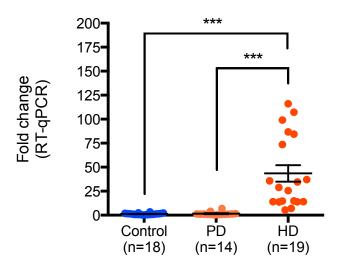
Increased miR-10b-5p expression is not observed in Parkinson's

disease (PD). To establish whether miR-10b-5p change is a generalized

response to neurodegeneration, we evaluated this miRNA in PD prefrontal

cortex. While cortical neuronal loss is variable in PD, both PD and HD are

neurodegenerative and caused by protein inclusions. We selected PD prefrontal

cortex samples that exhibited reported neuron loss on their neuropathological

evaluation (n=6) and PD samples without reported cortical neuronal loss (n=8).

From total RNA, RT-qPCR was performed for miR-10b-5p. No difference was

seen in miR-10b-5p expression when stratifying PD based on the extent of

neuron loss (t=0.59, p-value=0.58). Additionally, no significant difference in HD

miR-10b-5p expression from qPCR was observed when stratifying HD cases

based on a measure of cortical neuron loss (f=0.28, p-value=0.76).

Next, the relative expression of miR-10b-5p in PD was compared to all

nineteen HD and eighteen control samples assayed. While no significant

difference in miR-10b-5p expression was observed between control and PD

samples (q=0.05, p=0.99), a significant difference was seen in HD compared to

PD (q=7.30, p<0.0001; **Figure 6**), suggesting increased miR-10b-5p expression,

independent of neuron loss, is not a generalized response to neurodegeneration.

Figure 6. miR-10b-5p expression in control, Parkinson's disease and Huntington's disease prefrontal cortex.
Up-regulation of miR-10b-5p was confirmed in HD by performing RT-qPCR, comparing nineteen Huntington's disease prefrontal cortex samples to eighteen non-neurological disease control samples (***p<0.001) or fourteen Parkinson's disease samples (***p<0.001). $\Delta\Delta C_T$ values of miR-10b-5p in PD and HD as compared to controls are shown on the y-axis. The absence of up-regulation in PD frontal cortex suggests that up-regulation of miR-10b-5p may be HD specific. (C_T= cycle threshold; RT-qPCR=reverse transcription quantitative PCR; PD=Parkinson's disease; HD=Huntington's disease)

Ectopic miR-10b-5p expression protects HD cell lines from

polyglutamine-mediated cytotoxicity. To determine the functional importance

of miR-10b-5p up-regulation in HD, we ectopically expressed miR-10b-5p in

PC12 Q73 cells. These cell stably expressed huntingtin fragment derived from

exon 1 (1-90), contain a pathogenic, 73 long polyglutamine repeat and a MYC

epitope for protein identification. PC12 cells have been shown to terminally

differentiate and form neural processes upon nerve growth factor (NGF)

treatment [21], and HD models of these cells have been highly characterized,

exhibiting phenotypic changes such as aggregate formation and polyglutamine-dependent cell death [22-26].
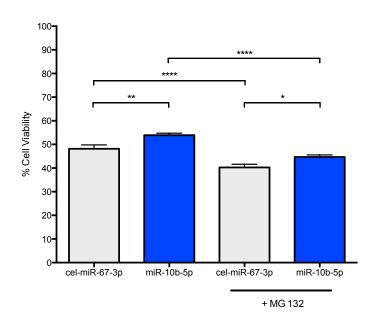
PC12 Q73 cells were transfected with miR-10b-5p mimic or a negative control mimic, cel-miR-67-3p, after 48 hours post-differentiation. Cell survival was quantified using a MTT cell viability assay 48 hours post-transfection. Increased survival, though modest (53.9% versus 48.2%), was statistically higher for cells transfected with miR-10b-5p compared to cells transfected with negative control miRNA (q=4.58, p-value<0.0001; **Figure 7**). The enhanced survival via ectopic miR-10b-5p expression was further substantiated in experiments using viable fluorescent cell staining, where miR-10b-5p transfected cells showed increased cell viability over cells transfected with negative control miRNA (t=2.381, p-value=0.018).

Thus, miR-10b-5p may play a protective role in enhancing cell survival during stress. To model stress, we treated miRNA transfected cells with 1uM MG 132, a potent proteasome inhibitor that increases huntingtin aggregation and cellular apoptosis in PC12 HD cell lines [27]. As expected, MG 132 treated cells had reduced cell viability as compared to untreated cells (cel-miR-67-3p, q=6.52, adjusted p-value<0.0001; miR-10b-5p, q=10.88, adjusted p-value<0.0001). However, MG 132 treated miR-10b-5p transfected PC12 Q73 cells exhibited improved survival over those transfected with negative control miRNA (q=3.728, adjusted p-value=0.045). No statistical difference was observed when comparing miR-10b-5p levels with MG 132 treatment to cel-miR-67-3p without treatment,

(q=2.95, adjusted p-value=0.16), suggesting miR-10b-5p may enhance survival

in times of cellular stress.

Figure 7. miR-10b-5p overexpressing PC12 Q73 cells exhibit reduced cytotoxicity.
PC12 cells expressing huntingtin exon 1 with a polyglutamine expansion spanning 73 repeats were transfected with miR-10b-5p or cel-miR-67-3p as a negative control. On day 3 post-differentiation, a subset of cells were treated with 1 uM MG 132. A MTT assay was used to measure cell viability after four days post differentiation. On the Y-axis, the viability percentage was calculated from the initial cell count. Error bars represent SEM. (****$p<0.0001$; **$p<0.001$ *$p<0.05$)

miRNA expression is related to clinical variables in HD. RNA

sequence count data may be non-normally distributed [28], and tests of normality

for miRNA expression levels in HD found that miR-10b-5p was negatively

skewed (see Materials and Methods). Therefore, to test the relationship of

miRNA expression to clinical variables such as CAG repeat size, age at onset of

motor symptoms, disease duration and age at death, as well as to the sample

quality information for RIN/RQN (RNA integrity number/RNA quality number), we

applied a step-wise backwards selection, negative binomial regression model.

Age at onset, duration and age at death are inter-dependent and could not

be simultaneously included in the models. Furthermore, age at onset and age at

death were strongly correlated with each other (Pearson r=0.85, p-value=5e-04)

and both were correlated with CAG repeat size (r=-0.84, p-value =6e-04, and r= -

0.89, p-value =1e-04 respectively) while duration was not correlated with age at

onset, age at death or CAG repeat size in this sample. To determine which

variables best modeled the relationship of the miRNAs to clinical variables, we

compared the Akaike information criterion (AIC) for each variable (onset age,

death age and duration) in regression analyses that adjusted for the effect of

CAG repeat size. Of these three variables, duration was found to have the

poorest fit with each of the five miRNAs and therefore we report analyses

containing age at onset and age at death.

Among the HD brains, CAG repeat size, age at onset and age at death

were all independently found to have a negative association with miR-10b-5p

(CAG, β= -0.18, p-value =2.7e-05; onset, β= -0.05, p-value=1.9e-05; death, β= -

0.07, p-value=6.8e-07). CAG repeat size and age at onset were found to be

independently, negatively related to miR-196a-5p (CAG, β= -0.15, p-value=1.7e-

02; onset, β=-0.07, p-value=1.4e-03). Age at death was significantly related to

miR-615-3p expression (β= -0.03, p-value=0.0045) and age at onset was

36

associated with miR-196b-5p (β= -0.04, p-value=9e-04). No association to any

clinical features was seen for miR-1247-5p. In order to fully evaluate whether

there was any effect of disease duration on the observed relationships to the

clinical features, duration was added back into final models. No substantial

changes to the effect estimates were observed with the addition of duration to

any of the models.

None of the miRNA levels was related to post-mortem interval in either

control or HD case samples. The essentially null level of expression in controls

prevented meaningful assessment of the relationship of miR-196a-5p, miR-196b-

5p and miR-615-3p with clinical variables, in particular age at death, or sample

variables, post-mortem interval (PMI), or RIN/RQN. Analysis of miR-10b-5p

showed no association to age at death (β=-0.002, p-value=0.60), or PMI (β=-

0.014, p-value=0.31), but did show association with RIN/RQN (β=0.54, p-value=

7.2e-05) in controls. miR-1247-5p showed association with later age at death

(β=-0.013, p-value=0.024) in controls.

Expression of miR-10b-5p, miR-196a-5p, miR-196b-5p and miR-615-

3p are correlated. Among the twelve HD samples, the levels of four out of the

five significantly differentially expressed miRNAs (miR-10b-5p, miR-196a-5p,

miR-196b-5p, miR-615-3p) were strongly correlated with each other, (Spearman

r range 0.71-0.88; p range 0.0002-0.01). miR-1247-5p was not significantly

correlated with these miRNAs (Spearman r range 0.13-0.51; p range 0.09-0.70).

Because the values of miR-615-3p and miR-196a-5p were essentially zero in the

control samples, correlations among the miRNAs were not performed for controls.

mRNA targets of miR-10b-5p, miR-196a-5p, miR-196b-5p and miR-615-3p may have similar functions. Watson-Crick base-pairing between nucleotide position 2 through 8 on the mature miRNA, termed the 'seed region,' and the 3' untranslated region (3' UTR) of target mRNA determine the recognition, specificity and efficiency of miRNA silencing [29]. Seed sequences differ for miR-10b-5p (ACCCUGU), miR-615-3p (CCGAGCC) and miR-1247-5p (CCCGUCC) suggesting these miRNA have different targets, while miR-196a-5p and miR-196b-5p share a seed sequence (AGGUAGU) and only differ by a single base difference in mature miRNA sequence.

Targets of the five miRNAs were obtained from miRWalk (http://www.umm.uni-heidelberg.de/apps/zmf/mirwalk/index.html), a repository of experimentally validated miRNA targets curated from literature and online resources [30]. miRWalk targets of miR-196a, miR-196b and miR-1247 were not strand specific. The miRWalk database contained 84 unique targets for miR-10b-5p, 80 for miR-196a, 40 for miR-196b, two for miR-1247 and twelve for miR-615-3p. Since miR-1247 had just two validated targets, it was removed from analysis.

Four target genes (*DICER1, HOXA7, HOXB4, HOXD1*) were shared across all four miRNAs. miR-10b-5p shared eleven targets with miR-196a-5p (*HOXB8, COX8A, HOXA10, NPC1, FLT3, AKT1, NPM1, DROSHA, AGO2, NFYC, PAX7*), and one with miR-615-3p (*MAPK8*). miR-196a and miR-196b

38

shared 28 targets. In all, eleven of the 167 unique validated targets were Hox cluster genes (*HOXA1, HOXA7, HOXA9, HOXA10, HOXB4, HOXB7, HOXB8, HOXC8, HOXD1, HOXD4, HOXD10*).

To understand the influence these miRNAs may be having on shared biological processes, targets of each miRNA were analyzed using IPA Core Analysis. To find overlap in biological functions and canonical pathways of each miRNA and its targets, the IPA Core Comparison Analysis tool was used. After correcting for multiple comparisons, targets of miR-10b-5p, miR-196a, miR-196b and miR-615-3p shared significant overlap in 33 biological functions; the top three functional categories were "*Cell Death and Survival*," (Benjamini-Hochberg adjusted p-value, range=3.5e-07 – 1.5e-04), "*Nervous System Development and Function*" (range=1.5e-07 – 1.5e-03) and "*Cellular Assembly and Organization*" (range=2.5e-05 – 1.7e-03). Twelve pathways were shared among all four sets of miRNA targets, including "*Huntington's Disease Pathway*" (range=7.6e-04 – 8.1e-03), (Gene set=*AKT1, BAX, CAPSN1, CLTC, CREB1, EGFR, HDAC9, JUN, MAPK8*).

Table 4. 22 differentially expressed targets of miR-10b-5p, miR-196a, miR-196b, miR-1247 and miR-615-3p.
* FDR-adjusted q-value for 167 targets of the five miRNAs.

Target gene	miRNA	Location	Mean Control Expression (n=9)	Mean HD Expression (n=12)	Fold Change	p-value	q-value *
SERPINE1	miR-10b-5p	7q22.1	22.91	140.82	6.15	3.03E-11	5.06E-09
CDKN1A	miR-196a	6p21.2	336.73	841.75	2.5	1.58E-04	1.22E-02
HOXD4	miR-10b-5p	2q31.1	1.74	18.33	10.51	2.38E-04	1.22E-02
ANXA3	miR-10b-5p	4q21.21	259.93	553.71	2.13	2.92E-04	1.22E-02
TWIST1	miR-10b-5p	7p21.2	43.43	105.16	2.42	5.63E-04	1.72E-02
CD33	miR-196a, miR-196b	19q13.3	16.58	46.63	2.81	6.75E-04	1.72E-02
DIO3	miR-1247	14q32	10.89	41.93	3.85	7.29E-04	1.72E-02
MMP2	miR-10b-5p	16q13-q21	58.67	137.83	2.35	8.26E-04	1.72E-02
MMP9	miR-10b-5p	20q11.2-q13.1	5.32	17.33	3.26	9.33E-04	1.73E-02
HOXA10	miR-10b-5p, miR-196a, miR-196b	7p15.2	1.06	17.06	16.12	1.21E-03	1.73E-02
RHOD	miR-10b-5p	11q14.3	12.71	37.96	2.99	1.23E-03	1.73E-02
COL1A1	miR-196a	17q21.33	30.19	220.28	7.3	1.31E-03	1.73E-02
HLA-E	miR-10b-5p	6p21.3	3703.47	7769.76	2.1	1.34E-03	1.73E-02
PPARA	miR-10b-5p	22q13.31	444.7	865.02	1.95	1.53E-03	1.73E-02
PAX6	miR-196a	11p13	693.52	1337.23	1.93	1.62E-03	1.73E-02
EGFR	miR-10b-5p	7p12	784.95	1762.88	2.25	1.66E-03	1.73E-02
HOXB7	miR-196a	17q21.3	1.63	6.99	4.28	2.83E-03	2.78E-02
PLAUR	miR-10b-5p	19q13	56.15	119.67	2.13	3.65E-03	3.38E-02
HOXD10	miR-10b-5p	2q31.1	1.25	9.33	7.45	4.73E-03	3.96E-02
RUNX1	miR-10b-5p	21q22.3	87.69	224.88	2.56	4.74E-03	3.96E-02
SOX2	miR-10b-5p	3q26.3-q27	1963.76	3492.72	1.78	5.32E-03	4.23E-02
KRT5	miR-196a	12q13.13	113.74	51.99	-2.19	6.00E-03	4.55E-02

mRNA targets of differentially expressed miRNAs are differentially expressed. Total mRNA-sequencing was performed in the same brain samples as miRNA-sequencing to examine whether gene expression was affected by miRNA up-regulation. Of the 169 unique gene targets for the five differentially expressed miRNAs, 167 were detected using mRNA-sequencing. 22 mRNA targets were significantly differentially expressed between the HD and control prefrontal cortex samples (False Discovery Rate (FDR) adjusted q-value=0.05

after adjusting for 167 comparisons). Only one gene (keratin 5, *KRT5*) was down-regulated in HD (<mark>Table 4</mark>), and four of these target genes were located in the Hox clusters (*HOXD4, HOXA10, HOXB7* and *HOXD10*).

Table 5. Differential expression of Hox cluster genes in HD.
* FDR-adjusted q-value for the 55 genes in the four Hox clusters

| Gene	Mean Control Expression (n=9)	Mean HD Expression (n=12)	Fold Change	p-value	q-value *
HOXA11	1.06	8.2	7.75	3.96E-05	2.07E-03
HOXA5	1.06	7.63	7.21	1.03E-04	2.07E-03
HOXD8	1.15	7.84	6.8	1.13E-04	2.07E-03
HOXD4	1.74	18.33	10.51	2.38E-04	3.22E-03
HOXB9	1.06	9.2	8.69	2.93E-04	3.22E-03
HOXA10	1.06	17.06	16.12	1.21E-03	1.11E-02
HOXC6	1.15	6.16	5.34	1.62E-03	1.27E-02
HOXA11-AS	1.25	7.39	5.9	2.49E-03	1.71E-02
HOXB7	1.63	6.99	4.28	2.83E-03	1.73E-02
HOXA13	1.45	8.74	6.03	4.07E-03	2.24E-02
HOXD10	1.25	9.33	7.45	4.73E-03	2.36E-02
HOXD1	55.91	22.8	-2.45	8.55E-03	3.92E-02
HOXC10	1.36	8.04	5.9	1.06E-02	4.14E-02
HOXC4	3.57	10.77	3.02	1.12E-02	4.14E-02
HOTAIRM1	3.52	12.52	3.56	1.13E-02	4.14E-02
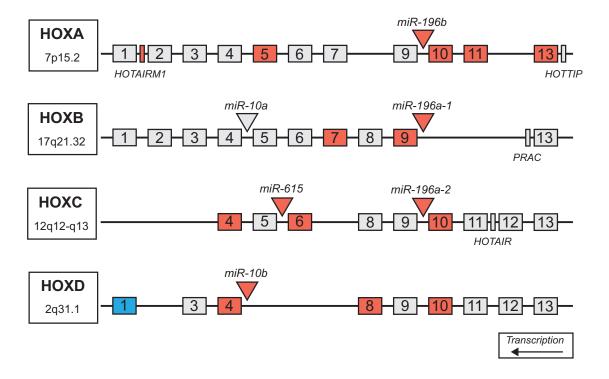
miR-10b-5p, miR-196a-5p, miR-196b-5p and miR-615-3p expression is related to Hox cluster gene expression. Four of the five up-regulated miRNAs are located intergenic to Hox gene clusters (<mark>Figure 8</mark>). Because of gene duplication, miR-196a is derived from both the HOXB and HOXC clusters; miR-10b is located in the HOXD cluster and miR-615 is found in the HOXC cluster

[31,32]. A total of 55 genes (40 protein-coding genes, eleven antisense transcripts, three functional lncRNAs and one pseudogene) are located in the four Hox clusters [33,34]. To evaluate evidence for a general regional up-regulation of Hox cluster genes, an expression analysis of the mRNA-sequence data was performed for all annotated genes within the Hox loci (==Table 5==). Fifteen out of 55 genes within the Hox loci were differentially expressed in HD. Fourteen Hox genes were significantly up-regulated (FDR-adjust q-value<0.05, mean fold-change = 6.73, range 3.02 to 16.12) and a single Hox gene was down-regulated (*HOXD1*, FDR-adjust q-value=3.92e-02, fold change = -2.45). The majority of differentially expressed Hox genes (13 out of 15) were essentially unexpressed in controls.

The genes adjacent to the four differentially expressed miRNAs were highly expressed. Two genes immediately adjacent to miR-10b-5p were significantly up-regulated in HD (*HOXD4*, FDR-adjusted q=3.22e-03; *HOXD8*, FDR-adjusted q=2.07e-03), (==Figure 8==). *HOXB9* (FDR-adjusted q-value=3.22e-03) immediately downstream of miR-196a-1 and *HOXC10* (FDR-adjusted q-value=4.14e-02) immediately upstream of miR-196a-2 were also up-regulated. Furthermore, all three Hox genes located upstream of miR-196b were significantly up-regulated in HD (*HOXA10*, FDR-adjusted q-value=1.11e-02*; HOXA11*, FDR-adjusted q-value=2.07e-03; *HOXA13*, FDR-adjusted q-value=2.24e-02). *HOXC6* (FDR-adjusted q-value=1.27e-02) immediately upstream of miR-615 was also up-regulated.

Figure 8. Differentially expressed miRNAs in HD are located in Hox gene clusters.
Schematic representation of Hox clusters. Hox genes are represented as numbered boxes (labeled 1-13), miRNA are represented by triangles and other genes in the regions (functional lncRNA, *PRAC*) are represented by rectangles. Antisense transcripts and pseudogenes are not pictured. Nineteen genes within Hox cluster regions were found significantly differentially expressed in HD prefrontal cortex using mRNA-sequencing (FDR-adjusted p-value<0.05). Four miRNAs, one lncRNA, and fourteen Hox genes were significantly up-regulated in HD (indicated by red), many of which are adjacent to differentially expressed miRNAs. A single Hox gene (*HOXD1)* was down-regulated in HD (indicated by blue) (HD=Huntington's disease).

Discussion

Up-regulation of expression for five miRNAs in HD brain. We report a next-generation sequencing study of small RNAs, identifying 1,417 mature miRNA species in the prefrontal cortex (Brodmann Area 9) of twelve HD and nine control brains. Five of these, miR-10b-5p, miR-196a-5p, miR-196b-5p, miR-615-3p and

miR-1247-5p, were up-regulated in HD at genome-wide significance (FDR q-value <0.05), and three of these five, miR-196a-5p, miR-196b-5p and miR-615-3p, were expressed at near zero levels in the control brains. Up-regulation of miR-10b-5p was validated in the miRNA-sequencing samples and confirmed in an independent replication sample set. Several studies implicating a role for miRNAs in HD have been performed, although, to our knowledge this is the first genome-wide quantification of miRNA expression comparing individual human HD and control brain samples.

Packer et al. [11], studying an array of 365 mature miRNAs, had previously reported miR-196a-5p to be significantly increased by nearly six-fold in Brodmann Area 4 of HD grade 1 brains. Recently, a study by Cheng et al. [13] found increased miR-196a expression suppressed mutant *HTT* expression in both HD neuronal cell models and HD transgenic mouse models. These findings suggest increased expression of miR-196a may be an adaptive response, promoting neuronal survival and may have therapeutic implications for HD. Miyazaki et al. [35] studied miR-196a in spinal and bulbar muscular atrophy (SBMA), a neurodegenerative disease caused by a similar polyglutamine repeat expansion in the androgen receptor (*AR*) gene. They found increased miR-196a expression via adeno-associated virus vector-mediated delivery reduced *AR* mRNA levels leading to improved neurological function in transgenic SBMA mouse models. Together, these findings suggest a neuroprotective role for miR-196a and its targets and possible therapeutic implications across multiple

44

polyglutamine-expansion neurodegenerative diseases. miR-196a-5p and miR-10b-5p were among the 56 miRNAs found to be elevated in response to mutant *HTT* over-expression in undifferentiated NT2 cells [36]. According to the miRNA search program "PubmiR," [37] miR-196b-5p, miR-1247-5p and miR-615-3p have not been previously reported in HD miRNA studies.

A number of past studies have examined miRNA levels in HD, HD transgenic mice or cellular models; however, we did not replicate the results obtained in these studies. Gaughwin et al. [36] reported miR-34b elevated in plasma samples in HD, but we found neither miR-34b-3p nor miR-34b-5p to be altered in HD brain at genome-wide levels. We were not able to confirm any of the miRNAs reported in past microarray studies that examined targeted subsets of miRNAs, including the nine miRNAs reported as down-regulated in two mouse models of HD (YAC128 and R6/2) by Lee et al. [14] using a 567 miRNA microarray or the 38 miRNAs with altered expression in HD transgenic mice in a 382 miRNA microarray [15]. Johnson et al. [10-12] reported miR-29a and miR-330 to be significantly up-regulated in HD samples, neither of which was found to be altered in this study [10]. In a RT-qPCR study comparing 90 miRNAs in mouse Hdh (Q111/Q111) striatal cells to control mice [12,38], none of the 27 reported differentially expressed miRNAs was different at genome-wide levels in our study. The most commonly reported altered miRNA in HD studies, miR-132, has been reported as both down-regulated [10,14,39] and up-regulated [11], but was not differentially expressed in our study.

45

While some of the lack of concordance may be a consequence of the differences between human and animal models of HD, it is also likely that some of the differences are a consequence of the different technologies employed by these studies. Microarrays may have different levels of detection for some miRNAs from that seen by miRNA sequencing. Finally, nearly all of the studies employ microarray methods. Microarrays that study only 365 (e.g. Packer et al. [11],) to 567 miRNAs (e.g. Lee et al. [14]) are not performing as many contrasts and thus do not adjust for as many contrasts as our genome wide analysis (e.g. 1,417 miRNAs detected) demands.

miR-10b-5p, miR-196a-5p, miR-196b-5p and miR-615-3p implicate Hox cluster genes. Four (miR-10b-5p, miR-196a-5p, miR-196b-5p and miR-615-3p) of the five differentially expressed miRNAs are related to Hox cluster genes as follows: (1) these four are located in intergenic regions of the Hox clusters, (2) eleven Hox genes are validated targets of these four miRNAs, (3) Hox genes adjoining differentially expressed miRNAs are differentially expressed and (4) multiple Hox cluster genes are differentially expressed in HD versus control brains (Table 4).

Of the eleven Hox gene targets, eight did not differ in their expression across condition. A single target, *HOXD1* was seen to be down-regulated in HD (FC=-2.45). *HOXD1* is a reported target of four of the five miRNAs [40] which may explain its repression in HD.

46

Three Hox gene targets were up-regulated in HD (*HOXB7, HOXD4 HOXD10*). It is possible these up-regulated Hox genes share similar regulatory mechanisms, as the increased miRNA expression does not produce the expected miRNA-mediated gene silencing and suppress the observed up-regulation of the miRNA target genes. Coevolution of Hox genes and Hox-related miRNAs may further suggest that they share regulatory elements or mechanisms [41]. Furthermore, Hox genes and related miRNAs have been observed to have similar patterns of transcriptional activation and both are activated by retinoic acid [42-46]. Although miR-10b-5p has been validated as targeting *HOXD4*, they may exhibit patterns of co-expression. Specifically, Phua et al. [45] report miR-10b and *HOXD4* are temporally co-expressed during neurodifferentiation. Here, we see a similar up-regulation and co-expression pattern in HD, where miR-10b and *HOXD4* are both highly expressed.

Hox genes are a family of transcription factors that contribute to major morphological changes during embryonic development and are required for anterior-posterior body axis in bilaterally developing species [47]. They are highly involved in most aspects of early development, and are prominently expressed in the developing brain [48]. Hox-related miRNAs may also follow similar spatio-temporal patterns of expression during embryogenesis [49].

Hox genes are regulated by retinoic acid but also other factors, including basic fibroblast growth factor [50], steroid hormones [51,52] and polycomb repressive complex group [53]. Polycomb group (PcG) proteins assemble into

47

large silencing complexes and control histone-modifying activity. Hox genes are repressed by PcG complexes, specifically Polycomb Repressive Complex 2 (PRC2), which trimethylates histone H3 at lysine 27 (H3K27me3) [53]. Seong et al [54] observed knockout huntingtin mouse embryos lacked repression of *HOXB1, HOXB2,* and *HOXB9* and showed diminished global H3K27me3, while a knock-in expanded repeat mouse exhibited increased H3K27me3 signal, suggesting mutant huntingtin may alter proper PRC2 activity. These findings raise the possibility that the increased expression of miRNAs and Hox genes reported here are related to enhanced H3K27me3 or impaired PcG repression. However, the role of Hox in the adult, HD brain is still unclear. Increased transcriptional activity of Hox may be compensatory, helping to preserve or re-establish cell polarity, or an indirect result of impaired epigenetic regulation.

miR-10b-5p response in HD may be protective. To functionally validate our miRNA-sequencing findings, we chose to assess miR-10b-5p. We believed this miRNA to be the most biologically active of the differentially expressed miRNAs. miR-10b-5p had the highest basal expression levels and the highest fold change between conditions. Additionally, miR-10b-5p levels were not increased in PD, a comparable protein aggregate, neurodegenerative disease, nor in PD samples with pathology in the prefrontal cortex equivalent to HD.

To determine whether miR-10b-5p had a protective or deleterious effect on neuron viability, we ectopically expressed miR-10b-5p in terminally differentiated PC12 Q73 cells. Since the levels the five differentially expressed

48

miRNA were up-regulated, we felt overexpression of miR-10b-5p best represented the phenotype observed in HD brain.

We reported increased miR-10b-5p expression enhanced the survival of PC12 Q73 cells. Furthermore, we found that increased miR-10b-5p expression enhanced survival in the presence of apoptosis-inducing compound, MG 132. In this experiment, survival in cells with increased miR-10b-5p expression was comparable to that of unchallenged cells and significantly greater than untreated cells exposed to toxin. These finding provide support for the hypothesis that increased miR-10b-5p may be a neuroprotective response to the expanded polyglutamine repeat seen in HD and speaks to the role of this microRNA in the pathology of HD.

miR-10b-5p, miR-196a-5p, miR-196b-5p and miR-615-3p have overlapping biological functions. pathway analysis, we showed that miR-10b-5p, miR-196a-5p, miR-196b-5p and miR-615-3p targeted genes are predicted to be involved in apoptosis as well as nervous system development and function. In neuroblastoma SH-SY5Y cell lines, miR-10a, miR-10b and miR-615-5p expression levels significantly increased during all-trans-retinoic-acid (ATRA) treatment, indicating miR-10a/b and miR-615-5p may have a role in neurodifferentiation [44]. SH-SY5Y cells treated with antisense miR-10a or miR-10b had impaired neurite outgrowth and morphology but did not show changes in overall cell proliferation [44]. miR-10a and miR-10b were highly expressed in SK-N-BE, LAN5 and SH-SY5Y cell lines during ATRA treatment and ectopic

expression of miR-10ab mirrored the phenotype of the ATRA treatment [42]. Taken together, these studies implicate these miRNAs in neuron differentiation, migration, and outgrowth.

In our past studies [16], we found increased neurite outgrowth in HD prefrontal cortex. Relative to controls, HD pyramidal neurons had a significantly increased number of primary dendritic segments, increased total dendritic length, and more dendritic branches than control neurons. Here, we report four miRNAs that have been observed in cell models to present a similar phenotype. It is possible that increased expression of these miRNAs and related targets represent an adaptive response of neurons stressed by a toxic expanded polyglutamine protein fragment.

miR-10b-5p, miR-196a-5p, miR-196b-5p and miR-615-5p are related to HD pathogenesis. Four of the five up-regulated miRNAs showed association to clinical features of HD (CAG repeat size, age of motor onset and age at death for miR-10b-5p; CAG repeat size and age at onset for miR-196a-5p, age at onset for miR-196b-5p and age at death for miR-615-3p). Due to the near zero level of expression in controls, it was not possible to assess the relationship of miR-196a-5p, mir-196b-5p and miR-615-3p to age at death, but miR-10b-5p was not correlated with age at death in controls. Thus, the increased expression of these miRNAs did not appear to be related to normal aging, but rather a component of gene regulation and transcription in the context of neurodegeneration. A growing body of literature points to the presence of toxic effects of the HD gene

50

substantially before the onset of symptoms, perhaps from the time of conception [55-57].

Because age at death represents the lifetime exposure of the individual to the effects of the HD gene, we hypothesize that the association of miR-10b-5p and miR-615-3p with age at death may represent the lifetime exposure to the effects of the HD mutation. If the relationship of altered miRNA expression to age at death supports the view that the HD gene may have a life-long effect among expanded CAG-repeat carriers, this raises the possibility that the HD mutation may influence neuronal development in the developing brain through the action of one or more of these miRNAs and Hox cluster genes.

Target genes of over-expressed miRNAs show increased expression in HD. We report five miRNAs as being highly up-regulated in HD and though our expectation was to see the mRNA targets of these miRNAs as decreased, we observe increased expression of many of their shared mRNA targets. We believe these effects are not attributable to differences in cell populations studied, since flow cytometric analysis measuring neuron abundance found no significant difference across condition. Rather, we hypothesize positive miRNA-mRNA target relationships are a result of HD-specific alterations in mRNA processing. Translation is a highly dynamic process. Cytoplasmic mRNA actively engaged in translation can cycle to a non-translated state and accumulate in stress granules or processing bodies (P-bodies). During cellular stress, mRNA can be sequestered to P-bodies or stress granules, to stall translation through

translational repression machinery or miRNA silencing, until stress conditions have been resolved [7,58-60]. P-bodies may also serve an important role in RNA transport. Because neurons are highly polarized, cytoplasmic transport of mRNA is essential for localized translation to discrete regions of the cell. During transport, it is believed that mRNAs are silenced by miRNA, upon rapid exchange at the synapse [60-62].

In HD cortical neurons, excitotoxicity, oxidative damage, aberrant gene expression and energetic defects lead to stress conditions and in response, cells may sequester mRNA to P-bodies and stress granules. Among the 55 Hox locus genes studied, only one of the fifteen significantly differentially expressed genes is down regulated (Table 4). Thus, the increased levels of most of the validated gene targets of these four miRNAs may be reactionary, as they are sequestered to P-bodies for storage as part of a protective process to enhance cell viability [7].

To the best of our knowledge, no study has addressed the role of P-bodies or stress granules in HD. However, it was observed in live cortical neurons that wildtype huntingtin co-localized in P-bodies, specifically in neuronal RNA granules, along with Argonaute 2, the endonuclease required for RNA-mediated gene silencing by the RNA-induced silencing complex (RISC) [63,64]. Therefore, it is reasonable to suggest mutant huntingtin may impair miRNA-mediated mRNA degradation and/or localized translation of specific mRNAs.

There is evidence that miRNA-mRNA regulatory mechanisms may be altered in other neurodegenerative diseases as well. In a joint examination of miRNA-mRNA expression in Alzheimer's disease (AD) and control prefrontal cortex, an overwhelming number of miRNA to mRNA targets were found to be positive correlated. Genomic variants in TDP-43 and FUS, genes that encode stress granule proteins, were found to cause familial Amyotrophic lateral sclerosis [65,66] and several other stress granule proteins (TIA-1, G3BP) may also be pathogenic [67].

miRNAs as potential biomarkers in HD. These studies suggest potential relationships of these miRNAs to CAG repeat expansion, age at onset or age at death. If these findings hold up on further examination, these miRNAs may hold potential to provide insight into important biological and disease expression for HD. miRNA are extremely stable. The half-life of the majority miRNAs has been predicted to be on average five days and plasma miRNAs have been found to be stable after being subjected to high heat, extreme pH, long-time storage at room temperature, or multiple freeze-thaw cycles [68-70]. If these miRNAs cross the blood-brain barrier and can be detected at reasonable levels in serum/plasma from mutant HD gene carriers, they may serve as biomarkers of disease expression.

Materials and Methods

Sample Information. Frozen brain tissue from prefrontal cortex Brodmann Area 9 (BA9) was obtained from the Harvard Brain and Tissue

53

Resource Center (HBTRC) McLean Hospital, Belmont MA. Twelve Huntington's disease (HD) samples and eleven neurologically-normal control samples were selected for the study (<mark>Table 1</mark>). The HD subjects had no evidence of Alzheimer or Parkinson disease (PD) comorbidity based on neuropathology reports. For microscopic examination, 16 tissue blocks were systematically taken and histologically assessed as previously described [3]. All samples were male. HD samples and controls were not different for postmortem interval (PMI) (t=1.07, p=0.30), RNA integrity number (RIN) (t=0.83, p=0.41) or death age (t=0.40, p=0.69). CAG repeat size was known for all HD samples and onset age and disease duration was unknown for a single sample (<mark>Table 1</mark>). Eight additional HD, nine control and fourteen PD cases were studied as part of validation and replication studies, and were obtained from the HBTRC and the Sun Health Research Institute Sun City, Arizona.

RNA extraction. Total RNA, for all samples studied, was isolated using QIAzol Lysis Reagent and purified using miRNeasy MinElute Cleanup columns (Qiagen Sciences Inc., Germantown, MD). RNA quality for sequencing was assessed using either Agilent's BioAnalyzer 2100 system and RNA 6000 Nano Kits to find RNA Integrity Number (RIN) or Agilent 2200 TapeStation and DNA ScreenTape assay RNA Quality Number (RQN; Agilent, Foster City, CA). Both methods calculate the area under the peak for 18S and 28S RNA as a ratio of total RNA as well as the relative height of the 18S and 28S peaks to determine

RNA quality [71]. The RIN/RQN values were similar for the twelve HD and eleven control specimens studied for miRNA and mRNA (t=0.95, p=0.36).

Illumina miRNA sequencing (miRNA-seq). For each brain sample, 1 ug of RNA was used to construct sequencing libraries using Illumina's TruSeq Small RNA Sample Prep Kit, according to the manufacturer's protocol (Illumina, San Diego, CA). In brief, small RNA molecules were adapter-ligated, reverse transcribed, PCR amplified and gel purified to generate the library. Multiplexed samples were equimolarly pooled into sets of eight samples per flowcell lane and sequenced using 1x50 bp single-end reads on Illumina's HiSeq 2000 system at Tufts University sequencing core facility (http://tucf-genomics.tufts.edu/). Demultiplexing and FASTQ file generation (raw sequence read plus quality information in Phred format) were done using Illumina's Consensus Assessment of Sequence and Variation (CASAVA) pipeline.

Primary processing of Illumina miRNA-seq reads. Sequence read quality was evaluated using the FASTQ quality filter module from the FASTX-toolkit version 0.0.13 (http://hannonlab.cshl.edu/fastx_toolkit/), and only those reads with at least 80% of the base calls above Q20 (Phred score) were retained. The 3' adapter sequence (5'-TGGAATTCTCGGGTGCCAAGG-3') was removed from all reads using the FASTA/Q clipper module from the FASTX-toolkit. A minimum length threshold of 15 nucleotides was set for clipped reads because miRNAs of this length will contain the seed sequence. To avoid redundancy amongst identical read species, the reads were collapsed using the FASTA/Q

collapser module from FASTX-toolkit to generate a FASTA file of only the unique read species.

Alignment and mapping of miRNA-seq reads. Quality-filtered, 3' adapter-clipped reads were aligned to the UCSC human reference genome (build hg19) using Bowtie version 0.12.3 [72]. Alignment parameters were set to allow for no mismatch alignments and no limits on multiple mapping instances. Multiple-mapped identical sequences were summed for a single count for that annotated mature miRNA. The default settings were used for all other alignment options.

The miRNA aligned data are available on ArrayExpress as follows: Experiment name: RNA-seq of micro RNAs (miRNAs) in Human prefrontal cortex to identify differentially expressed miRNAs between Huntington's Disease and control brain samples. ArrayExpress accession: E-MTAB-2206, Release date: 2014-01-30 https://www.ebi.ac.uk/arrayexpress/experiments/E-MTAB-2206/

miRNA abundance estimation. Aligned reads that overlapped with the human miRNA annotation version 19 from miRBase (http://www.mirbase.org/ftp.shtml) were identified using default BEDTools' *IntersectBed* functionality [73]. To select for mature miRNA reads, sequences more than 27 bases in length were removed. Only those reads for which the aligned 5' start-nucleotide matched exactly to the 5' start-nucleotide of the annotated miRNA were retained for the analysis. After filtering, collapsed read counts were summed per annotated mature miRNA.

miRNA differential expression. The R (http://www.R-project.org) package DESeq version 1.10.1 [28] was used to perform the differential expression analysis between HD and control samples using the read counts generated for each sample as described above. miRNAs with zero read counts across all case and control samples were removed from analysis. To accommodate the analysis of miRNAs with read counts of zero for some samples, a pseudo-count of one was added to all raw counts for every miRNA across all the samples, prior to performing DESeq's estimateSizeFactors and estimateDispersions functions with default options. DESeq assumes that count data follow a negative binominal distribution and factors in technical and biological variance when testing for differential gene expression between groups. DESeq's function, estimateSizeFactors, was used to obtain normalization factors for each sample and to normalize miRNA read counts.

The normalized counts were evaluated by principal component analysis (PCA) with the FactoMineR R package for all HD and control samples. The samples identified to be three or more standard deviations away from the mean on the first or second principal component were considered outliers and were removed from analysis. The first two principal components were used because they each explained more than 10% of the variance, while the remaining principal components explained less than 10% of the variance. Two control samples (C-35 and C-37) were identified as outliers based on PCA analysis.

miRNA differential expression analysis was performed with DESeq's nbinomTest function for the remaining nine control and twelve HD samples. All analyses were performed on DESeq normalized counts.

miRNA quantitative PCR*.* miRNA were assayed using Exiqon's miRCURY LNA Universal RT miRNA PCR following the manufacturer's protocol (Exiqon Inc, Denmark). In brief, reactions were incubated for 60 min at 42˚C followed by heat-inactivation of reverse transcription for 5 min at 95˚C and stored at 4˚C. After cDNA synthesis, samples were diluted to 0.2 ng/ul in water. Brain samples were assayed using Exiqon ExiLENT SYBR Green master mix and LNA primer sets containing UniRT and miR-10b-5p, miR-196a-5p, miR-196b-5p, miR-615-3p or miR-1247. Reference primer hsa-SNORD48 PCR/UniRT was used for brain samples; U6 snRNA for cell lines. Samples were run in triplicate for each primer set in 384-well format (5 ul PCR Master mix, 1ul PCR primer mix, 4 ul 0.2 ng cDNA). Reactions were cycled using Applied Biosystems 7900HT Fast Real-Time PCR System using manufacturer's instructions (Life Technologies, Carlsbad, CA). For analysis, threshold cycle (C_T) was generated by ABi SDS v2.4 software. C_T values for triplicate wells were normalized by average RNU48 value for brain or U6 for cells. miRNA fold change was calculated using the 2-ΔΔCT method [74].

Neuron abundance quantification. 0.5-1.0 g of tissue in 5 ml of lysis buffer was homogenized using a dounce tissue grinder. Lysates were transferred to ultracentrifugation tubes, loaded on top of sucrose solution and centrifuged at

24,400 RPM for 2.5 hr at 4°C (Beckman Coulter, Pasadena, CA; L8-70 M with SW80 rotor). Nuclei pellets were resuspended in 500 ul PBS and incubated at 4°C in a staining solution containing 0.72% normal goat serum, 0.036% BSA, 1:1200 anti-NeuN (Millipore, Germany), 1:1400 Alexa488 goat anti-mouse secondary antibody (Life Technologies, Carlsbad, CA), for 45 min. Flow cytometry was performed at the Boston University Medical School Flow Cytometry Core Lab on a FACSVantage SE flow cytometer.

Illumina messenger RNA sequencing (mRNA-seq). For each brain sample, 1 ug of RNA was used to construct sequencing libraries using Illumina's TruSeq RNA Sample Prep Kit according to the manufacturer's protocol. In brief, mRNA molecules were polyA selected, chemically fragmented, randomly primed with hexamers, synthesized into cDNA, 3' end-repaired and adenylated, sequencing adapter ligated and PCR amplified. Each adapter-ligated library contained one of twelve TruSeq molecular barcodes. Multiplexed samples were equimolarly pooled into sets of three samples per flowcell lane and sequenced using 2x100 bp paired-end reads on Illumina's HiSeq 2000 system at Tufts University sequencing core facility (http://tucf-genomics.tufts.edu/). Demultiplexing and FASTQ file generation were accomplished using Illumina's CASAVA pipeline.

Primary processing of Illumina mRNA-seq reads. Forward and reverse sequencing reads were independently quality-filtered using the FASTQ quality filter module from the FASTX-toolkit version 0.0.13

59

(http://hannonlab.cshl.edu/fastx_toolkit/) with the same criteria as that applied for the processing of the miRNA-seq reads. Reads failing the quality threshold, as well as their corresponding mate reads, were removed.

Alignment and mapping of mRNA-seq reads. Quality-filtered paired-end reads were aligned to the UCSC human reference genome (build hg19) using TopHat version 2.0.4 [75,76]. This version of TopHat incorporates the Bowtie version 2.0.0.7 algorithm to perform the alignment [72] as well as SAMtools version 0.1.18.0 for alignment file formatting [77]. For efficient read mapping, TopHat requires the designation of the mean and standard deviation of the distance between paired-end reads, the read inner-distance. To estimate the appropriate read inner-distance, we aligned a subset of 5 million reads from four HD and four control samples to the Ensembl human reference transcriptome (release 66) using Bowtie version 2.0.0.7. Using the CollectInsertSizeMetrics function from picardTools version 1.76 (http://sourceforge.net/projects/picard/files/picard-tools/), we estimated the average mean inner-distance per condition and subsequently applied these values for the TopHat alignment; 22 for HD samples 25 for controls respectively, (the current TopHat default setting is 20). To account for read variability, the standard deviation for inner-distance was set to 100. The number of allowed splice mismatches was set to 1. Default settings were used for all other alignment options.

60

mRNA gene abundance estimation. Gene expression quantification was performed using htseq-count version 0.5.3p9 (http://www-huber.embl.de/users/anders/HTSeq) and the GENCODE version 14 annotation gtf file as reference (http://www.gencodegenes.org/releases). Intersection non-empty mode and unstranded library type were specified as parameters for htseq-count. Default settings were used for all other options.

mRNA differential expression analysis. The mRNA differential expression analysis between HD and control samples was performed using DESeq version 1.10.1 [28]; the workflow was the same as described for the miRNA differential expression analysis. No outliers were found based on the PCA of the DESeq-normalized count data. The nbinomTest function was run for eleven control samples and twelve HD samples to assess differentially expressed genes. Multiple comparison adjustment for multiple testing with the Benjamini-Hochberg correction was used to control for false discovery rate. For Hox gene differential expression analysis, 55 comparisons were used. Genes located within HOX-gene containing regions were queried through the Ensembl database (release 72), interfacing through the R package BiomaRt [78,79]. Genes that were between *HOXA1-HOXA13*, *HOXB1-HOXB13, HOXC4-HOXC13* and *HOXD1-HOXD13* start sites were regarded as "Hox genes." For miRNA target differential expression, 154 comparisons were used for Benjamini-Hochberg correction.

miRNA-mRNA target analysis. Information on experimentally validated miRNA targets of miR-10b-5p, miR-196a-5p and miR-615-3p were extracted from the miRWalk "Validated Targets" module [30]. Strand specificity was preserved. Targets for miR-196a-1 and miR-196a-2 were merged for analysis. IPA Core Analysis (analysis.ingenuity.com) was run as nervous system and CNS cell line specific across all species, using target gene lists imported from miRWalk output. "Bio Functions" and "Canonical Pathway" analyses were used. Right-tailed Fisher's Exact Tests were run through IPA software and p-values with FDR-adjusted q-values ($p<0.05$) were considered significant. Biological functions across the 3 significant miRNA were compared using the IPA Core Comparison Analysis tool. Benjamini-Hochberg Multiple Testing Correction p-values ($p<0.05$) were considered significant.

Linear modeling of miRNA relationship to clinical covariates. To account for the non-normality in the miRNA data, negative binominal general linear regressions were performed using Proc genmod in SAS. DESeq normalized counts were rounded to the nearest integer before running the model. To test the normality of gene expression data, Shapiro-Wilk tests were performed. Differentially expressed miRNA data trended as non-normally distributed in HD (miR-10b-5p, $p=0.04$; miR-196a-5p, $p=0.05$; miR-615-3p, $p=0.06$), but not in controls (miR-10b-5p, $p=0.71$; miR-196a-5p and miR-615-3p were essential zero).

Generation of transgenic cell lines. PC12 (rat adrenal gland

phaeochromocytoma) cells were grown at 37°C and 5% CO_2 in Dulbecco's

modified Eagle's medium (DMEM; Life Technologies, Carlsbad, CA) with 20%

fetal bovine serum (FBS; Atlanta Biologicals, Flowery Branch, GA), 100 units/ml

penicillin and 100 units/ml streptomycin (Life Technologies, Carlsbad, CA).

pcDNA3.1mycC expressing human huntingtin fragment (1-90) containing 73

polyglutamine repeats (Coriell Institute; CHDI-90000034) was used for stable

transfection. Cells were seeded to 70% confluency and grown overnight. 15 µl of

Attractene Transfection Reagent (Qiagen, Gaithersburg, MD) was added to 4 µg

plasmid DNA diluted in 300 µl Opti-MEM (Life Technologies, Carlsbad, CA). Cells

were grown in complete media and selected for four weeks using 500 mg/ml

G418 (Life Technologies, Carlsbad, CA). To create monoclonal cultures, single

colonies were isolated using dilution cloning, picked with filter paper, grown in a

6-well plate and screened for transgenic expression by Western blot analysis

using mouse Anti- c-Myc (Novex, R950-25, Life Technologies, Carlsbad, CA).

Cell differentiation and miRNA overexpression. 96-well culture plates

were seeded with 10,000 cells per well. For differentiation, culture medium was

replaced with medium composed of DMEM with 0.5% FBS, 100 mg/ml G418,

100 units/ml penicillin and 100 units/ml streptomycin and 100 ng/ml nerve growth

factor (R&D Systems, Minneapolis, MN). After 48 hr, miRNA was transfected into

HD cells using 0.25 ul Lipofectamine 2000 (Life Technologies, Carlsbad, CA) and

6.25 pmol miR-10b-5p or miRIDIAN microRNA Mimic Negative Control #1 (cel-

miR-67-3p, Thermo Scientific, Waltham, MA) per well, following manufacturer's

protocol. miR-10b-5p overexpression was verified using qPCR.

   Cell viability assays. For MTT assays, 1 uM MG 132 (Tocris Bioscience,

United Kingdom) was added to select wells containing 10,000 cells per well at 72

hr post-differentiation. Cell viability was assessed at 96 hr post-differentiation.

Following manufacturer's protocol, CellTiter 96 Non-Radioactive Cell Proliferation

Assay kit (Promega; Madison, WI) was used to determine cell number. Cells

were incubated for 1.5 hr at 37°C and 5% CO_2 with MTT dye solution.

Undifferentiated HD cells were serially diluted across a 96-well plate to create a

standard curve for cell number calculation. Absorbance was measured using Bio-

Tek Synergy H1 spectrophotometer at 540 nm for miR-10b-5p transfected wells,

with MG 132 (n=44) and without MG 132 (n=35) and cel-miR-67-3p transfected

wells with MG 132 (n=40) and without MG 132 (n=40). One-way ANOVA way

used for statistical analysis. For cell viability staining, miR-10b-5p and negative

control mimic were transfected after 48 hours of differentiation in 12-well culture

plate with 4 replicates each, 250,000 cells per well. Molecular Probes Neurite

Outgrowth Staining Kit (Life Technologies, Carlsbad, CA) was used according to

manufacturer's protocol. Using Bio-Tek Synergy H1 microplate reader,

fluorescent area scans were taken at 530 nm excitation/590 nm emission with a

5x5 matrix per well.

References

1. HDCRG (1993) A novel gene containing a trinucleotide repeat that is expanded and unstable on Huntington's disease chromosomes. . Cell 72: 971-983.

2. Hadzi TC, Hendricks AE, Latourelle JC, Lunetta KL, Cupples LA, et al. (2012) Assessment of cortical and striatal involvement in 523 Huntington disease brains. Neurology 79: 1708-1715.

3. Vonsattel JP, Myers RH, Stevens TJ, Ferrante RJ, Bird ED, et al. (1985) Neuropathological classification of Huntington's disease. Journal of neuropathology and experimental neurology 44: 559-577.

4. Hodges A, Strand AD, Aragaki AK, Kuhn A, Sengstag T, et al. (2006) Regional and cellular gene expression changes in human Huntington's disease brain. Human molecular genetics 15: 965-977.

5. Cha JH (2000) Transcriptional dysregulation in Huntington's disease. Trends in neurosciences 23: 387-392.

6. Cha JH (2007) Transcriptional signatures in Huntington's disease. Progress in neurobiology 83: 228-248.

7. Lavut A, Raveh D (2012) Sequestration of highly expressed mRNAs in cytoplasmic granules, P-bodies, and stress granules enhances cell viability. PLoS genetics 8: e1002527.

8. Junn E, Mouradian MM (2012) MicroRNAs in neurodegenerative diseases and their therapeutic potential. Pharmacology & therapeutics 133: 142-150.

9. Marti E, Pantano L, Banez-Coronel M, Llorens F, Minones-Moyano E, et al. (2010) A myriad of miRNA variants in control and Huntington's disease brain regions detected by massively parallel sequencing. Nucleic acids research 38: 7219-7235.

10. Johnson R, Zuccato C, Belyaev ND, Guest DJ, Cattaneo E, et al. (2008) A microRNA-based gene dysregulation pathway in Huntington's disease. Neurobiology of disease 29: 438-445.

11. Packer AN, Xing Y, Harper SQ, Jones L, Davidson BL (2008) The bifunctional microRNA miR-9/miR-9* regulates REST and CoREST and is downregulated in Huntington's disease. The Journal of neuroscience : the official journal of the Society for Neuroscience 28: 14341-14346.

12. Sinha M, Ghose J, Bhattarcharyya NP (2011) Micro RNA -214,-150,-146a and-125b target Huntingtin gene. RNA biology 8: 1005-1021.

13. Cheng PH, Li CL, Chang YF, Tsai SJ, Lai YY, et al. (2013) miR-196a Ameliorates Phenotypes of Huntington Disease in Cell, Transgenic Mouse, and Induced Pluripotent Stem Cell Models. American journal of human genetics.

14. Lee ST, Chu K, Im WS, Yoon HJ, Im JY, et al. (2011) Altered microRNA regulation in Huntington's disease models. Experimental neurology 227: 172-179.

15. Jin J, Cheng Y, Zhang Y, Wood W, Peng Q, et al. (2012) Interrogation of brain miRNA and mRNA expression profiles reveals a molecular regulatory network that is perturbed by mutant huntingtin. Journal of neurochemistry 123: 477-490.

16. Sotrel A, Williams RS, Kaufmann WE, Myers RH (1993) Evidence for neuronal degeneration and dendritic plasticity in cortical pyramidal neurons of Huntington's disease: a quantitative Golgi study. Neurology 43: 2088-2096.

17. Cudkowicz M, Kowall NW (1990) Degeneration of pyramidal projection neurons in Huntington's disease cortex. Annals of neurology 27: 200-204.

18. Gu X, Li C, Wei W, Lo V, Gong S, et al. (2005) Pathological cell-cell interactions elicited by a neuropathogenic form of mutant Huntingtin contribute to cortical pathogenesis in HD mice. Neuron 46: 433-444.

19. Rosas HD, Hevelone ND, Zaleta AK, Greve DN, Salat DH, et al. (2005) Regional cortical thinning in preclinical Huntington disease and its relationship to cognition. Neurology 65: 745-747.

20. Rosas HD, Liu AK, Hersch S, Glessner M, Ferrante RJ, et al. (2002) Regional and progressive thinning of the cortical ribbon in Huntington's disease. Neurology 58: 695-701.

21. Greene LA, Tischler AS (1976) Establishment of a noradrenergic clonal line of rat adrenal pheochromocytoma cells which respond to nerve growth factor. Proceedings of the National Academy of Sciences of the United States of America 73: 2424-2428.

22. Kita H, Carmichael J, Swartz J, Muro S, Wyttenbach A, et al. (2002) Modulation of polyglutamine-induced cell death by genes identified by expression profiling. Human molecular genetics 11: 2279-2287.

23. Wyttenbach A, Swartz J, Kita H, Thykjaer T, Carmichael J, et al. (2001) Polyglutamine expansions cause decreased CRE-mediated transcription and

early gene expression changes prior to cell death in an inducible cell model of Huntington's disease. Human molecular genetics 10: 1829-1845.

24. Igarashi S, Morita H, Bennett KM, Tanaka Y, Engelender S, et al. (2003) Inducible PC12 cell model of Huntington's disease shows toxicity and decreased histone acetylation. Neuroreport 14: 565-568.

25. Apostol BL, Illes K, Pallos J, Bodai L, Wu J, et al. (2006) Mutant huntingtin alters MAPK signaling pathways in PC12 and striatal cells: ERK1/2 protects against mutant huntingtin-associated toxicity. Human molecular genetics 15: 273-285.

26. Sugars KL, Brown R, Cook LJ, Swartz J, Rubinsztein DC (2004) Decreased cAMP response element-mediated transcription: an early event in exon 1 and full-length cell models of Huntington's disease that contributes to polyglutamine pathogenesis. The Journal of biological chemistry 279: 4988-4999.

27. Li X, Wang CE, Huang S, Xu X, Li XJ, et al. (2010) Inhibiting the ubiquitin-proteasome system leads to preferential accumulation of toxic N-terminal mutant huntingtin fragments. Human molecular genetics 19: 2445-2455.

28. Anders S, Huber W (2010) Differential expression analysis for sequence count data. Genome biology 11: R106.

29. Bartel DP (2009) MicroRNAs: target recognition and regulatory functions. Cell 136: 215-233.

30. Dweep H, Sticht C, Kharkar A, Pandey P, Gretz N (2013) Parallel analysis of mRNA and microRNA microarray profiles to explore functional regulatory patterns in polycystic kidney disease: using PKD/Mhm rat model. PLoS One 8.

31. Swalla BJ (2006) Building divergent body plans with similar genetic pathways. Heredity (Edinb) 97: 235-243.

32. Yekta S, Tabin CJ, Bartel DP (2008) MicroRNAs in the Hox network: an apparent link to posterior prevalence. Nat Rev Genet 9: 789-796.

33. Flicek P, Ahmed I, Amode MR, Barrell D, Beal K, et al. (2013) Ensembl 2013. Nucleic acids research 41: D48-55.

34. Rinn JL, Kertesz M, Wang JK, Squazzo SL, Xu X, et al. (2007) Functional demarcation of active and silent chromatin domains in human HOX loci by noncoding RNAs. Cell 129: 1311-1323.

35. Miyazaki Y, Adachi H, Katsuno M, Minamiyama M, Jiang YM, et al. (2012) Viral delivery of miR-196a ameliorates the SBMA phenotype via the silencing of CELF2. Nature medicine 18: 1136-1141.

36. Gaughwin PM, Ciesla M, Lahiri N, Tabrizi SJ, Brundin P, et al. (2011) Hsa-miR-34b is a plasma-stable microRNA that is elevated in pre-manifest Huntington's disease. Human molecular genetics 20: 2225-2237.

37. Windemuth AS, I; Pregibon, D; Marini. D. (2012) PubmiR: A Literature Search Tool for MicroRNA Research. Firefly BioWorks, Inc.

38. Sinha M, Ghose J, Das E, Bhattarcharyya NP (2010) Altered microRNAs in STHdh(Q111)/Hdh(Q111) cells: miR-146a targets TBP. Biochemical and biophysical research communications 396: 742-747.

39. Soldati C, Bithell A, Johnston C, Wong K-Y, Stanton LW, et al. (2013) Dysregulation of REST-regulated coding and non-coding RNAs in a cellular model of Huntington's disease. J Neurochem 124: 418-430.

40. Woltering JM, Durston AJ (2008) MiR-10 represses HoxB1a and HoxB3a in zebrafish. PLoS One 3.

41. Tehler D, Hoyland-Kroghsbo NM, Lund AH (2011) The miR-10 microRNA precursor family. RNA Biol 8: 728-734.

42. Foley NH, Bray I, Watters KM, Das S, Bryan K, et al. (2011) MicroRNAs 10a and 10b are potent inducers of neuroblastoma cell differentiation through targeting of nuclear receptor corepressor 2. Cell death and differentiation 18: 1089-1098.

43. Huang H, Xie C, Sun X, Ritchie RP, Zhang J, et al. (2010) miR-10a contributes to retinoid acid-induced smooth muscle cell differentiation. J Biol Chem 285: 9383-9389.

44. Meseguer S, Mudduluru G, Escamilla JM, Allgayer H, Barettino D (2011) MicroRNAs-10a and -10b contribute to retinoic acid-induced differentiation of neuroblastoma cells and target the alternative splicing regulatory factor SFRS1 (SF2/ASF). J Biol Chem 286: 4150-4164.

45. Phua SL, Sivakamasundari V, Shao Y, Cai X, Zhang LF, et al. (2011) Nuclear accumulation of an uncapped RNA produced by Drosha cleavage of a transcript encoding miR-10b and HOXD4. PloS one 6: e25689.

46. Weiss FU, Marques IJ, Woltering JM, Vlecken DH, Aghdassi A, et al. (2009) Retinoic acid receptor antagonists inhibit miR-10a expression and block

metastatic behavior of pancreatic cancer. Gastroenterology 137: 2136-2145 e2131-2137.

47. Lemons D, McGinnis W (2006) Genomic evolution of Hox gene clusters. Science 313: 1918-1922.

48. Pearson JC, Lemons D, McGinnis W (2005) Modulating Hox gene functions during animal body patterning. Nature reviews Genetics 6: 893-904.

49. Wienholds E, Kloosterman WP, Miska E, Alvarez-Saavedra E, Berezikov E, et al. (2005) MicroRNA expression in zebrafish embryonic development. Science 309: 310-311.

50. Diez del Corral R, Storey KG (2004) Opposing FGF and retinoid pathways: a signalling switch that controls differentiation and patterning onset in the extending vertebrate body axis. Bioessays 26: 857-869.

51. Svingen T, Tonissen KF (2006) Hox transcription factors and their elusive mammalian gene targets. Heredity (Edinb) 97: 88-96.

52. Taylor HS, Arici A, Olive D, Igarashi P (1998) HOXA10 is expressed in response to sex steroids at the time of implantation in the human endometrium. J Clin Invest 101: 1379-1384.

53. Schuettengruber B, Chourrout D, Vervoort M, Leblanc B, Cavalli G (2007) Genome regulation by polycomb and trithorax proteins. Cell 128: 735-745.

54. Seong IS, Woda JM, Song JJ, Lloret A, Abeyrathne PD, et al. (2010) Huntingtin facilitates polycomb repressive complex 2. Human molecular genetics 19: 573-583.

55. Humbert S (2010) Is Huntington disease a developmental disorder? EMBO reports 11: 899.

56. Kirkwood SC, Siemers E, Hodes ME, Conneally PM, Christian JC, et al. (2000) Subtle changes among presymptomatic carriers of the Huntington's disease gene. Journal of neurology, neurosurgery, and psychiatry 69: 773-779.

57. Myers RH, Vonsattel JP, Paskevich PA, Kiely DK, Stevens TJ, et al. (1991) Decreased neuronal and increased oligodendroglial densities in Huntington's disease caudate nucleus. J Neuropathol Exp Neurol 50: 729-742.

58. Liu J, Valencia-Sanchez MA, Hannon GJ, Parker R (2005) MicroRNA-dependent localization of targeted mRNAs to mammalian P-bodies. Nature cell biology 7: 719-723.

59. Balagopal V, Parker R (2009) Polysomes, P bodies and stress granules: states and fates of eukaryotic mRNAs. Current opinion in cell biology 21: 403-408.

60. Bhattacharyya SN, Habermacher R, Martine U, Closs EI, Filipowicz W (2006) Relief of microRNA-mediated translational repression in human cells subjected to stress. Cell 125: 1111-1124.

61. Cougot N, Bhattacharyya SN, Tapia-Arancibia L, Bordonne R, Filipowicz W, et al. (2008) Dendrites of mammalian neurons contain specialized P-body-like structures that respond to neuronal activation. The Journal of neuroscience : the official journal of the Society for Neuroscience 28: 13793-13804.

62. Zeitelhofer M, Karra D, Macchi P, Tolino M, Thomas S, et al. (2008) Dynamic interaction between P-bodies and transport ribonucleoprotein particles in dendrites of mature hippocampal neurons. The Journal of neuroscience : the official journal of the Society for Neuroscience 28: 7555-7562.

63. Savas JN, Ma B, Deinhardt K, Culver BP, Restituito S, et al. (2010) A role for huntington disease protein in dendritic RNA granules. The Journal of biological chemistry 285: 13142-13153.

64. Savas JN, Makusky A, Ottosen S, Baillat D, Then F, et al. (2008) Huntington's disease protein contributes to RNA-mediated gene silencing through association with Argonaute and P bodies. Proceedings of the National Academy of Sciences of the United States of America 105: 10820-10825.

65. Sreedharan J, Blair IP, Tripathi VB, Hu X, Vance C, et al. (2008) TDP-43 mutations in familial and sporadic amyotrophic lateral sclerosis. Science 319: 1668-1672.

66. Kwiatkowski TJ, Jr., Bosco DA, Leclerc AL, Tamrazian E, Vanderburg CR, et al. (2009) Mutations in the FUS/TLS gene on chromosome 16 cause familial amyotrophic lateral sclerosis. Science 323: 1205-1208.

67. Wolozin B (2012) Regulated protein aggregation: stress granules and neurodegeneration. Molecular neurodegeneration 7: 56.

68. Gantier MP, McCoy CE, Rusinova I, Saulep D, Wang D, et al. (2011) Analysis of microRNA turnover in mammalian cells following Dicer1 ablation. Nucleic acids research 39: 5692-5703.

69. Mitchell PS, Parkin RK, Kroh EM, Fritz BR, Wyman SK, et al. (2008) Circulating microRNAs as stable blood-based markers for cancer detection.

Proceedings of the National Academy of Sciences of the United States of America 105: 10513-10518.

70. Chen X, Ba Y, Ma L, Cai X, Yin Y, et al. (2008) Characterization of microRNAs in serum: a novel class of biomarkers for diagnosis of cancer and other diseases. Cell research 18: 997-1006.

71. Schroeder A, Mueller O, Stocker S, Salowsky R, Leiber M, et al. (2006) The RIN: an RNA integrity number for assigning integrity values to RNA measurements. BMC molecular biology 7: 3.

72. Langmead B, Trapnell C, Pop M, Salzberg SL (2009) Ultrafast and memory-efficient alignment of short DNA sequences to the human genome. Genome Biol 10.

73. Quinlan AR, Hall IM (2010) BEDTools: a flexible suite of utilities for comparing genomic features. Bioinformatics 26: 841-842.

74. Livak KJ, Schmittgen TD (2001) Analysis of relative gene expression data using real-time quantitative PCR and the 2(-Delta Delta C(T)) Method. Methods 25: 402-408.

75. Kim D, Pertea G, Trapnell C, Pimentel H, Kelley R, et al. (2013) TopHat2: accurate alignment of transcriptomes in the presence of insertions, deletions and gene fusions. Genome Biol 14.

76. Trapnell C, Pachter L, Salzberg SL (2009) TopHat: discovering splice junctions with RNA-Seq. Bioinformatics 25: 1105-1111.

77. Li H, Handsaker B, Wysoker A, Fennell T, Ruan J, et al. (2009) The Sequence Alignment/Map format and SAMtools. Bioinformatics 25: 2078-2079.

78. Durinck SH, W. (2013) biomaRt: Interface to BioMart databases (e.g. Ensembl, COSMIC ,Wormbase and Gramene). R. 2.10.0 ed.

79. Kasprzyk A (2011) BioMart: driving a paradigm change in biological data management. Database (Oxford) 2011.

CHAPTER 3: MIR-10B-5P EXPRESSION IN HUNTINGTON'S DISEASE BRAIN

RELATES TO AGE OF ONSET AND THE EXTENT OF STRIATAL

INVOLVEMENT

Abstract

Background. MicroRNAs (miRNAs) are small non-coding RNAs that recognize sites of complementarity of target messenger RNAs, resulting in transcriptional regulation and translational repression of target genes. In Huntington's disease (HD), a neurodegenerative disease caused by a trinucleotide repeat expansion, miRNA dysregulation has been reported, which may impact gene expression and modify the progression and severity of HD.

Methods. We performed next-generation miRNA sequence analysis in prefrontal cortex (Brodmann Area 9) from 26 HD, 2 HD gene positive, and 36 control brains. Neuropathological information was available for all HD brains, including age at disease onset, CAG-repeat size, Vonsattel grade, and Hadzi-Vonsattel striatal and cortical scores, a continuous measure of the extent of neurodegeneration. Linear models were performed to examine the relationship of miRNA expression to these clinical features, and messenger RNA targets of associated miRNAs were tested for gene ontology term enrichment.

Results. We identified 75 miRNAs differentially expressed in HD brain (FDR q-value <0.05). Among the HD brains, nine miRNAs were significantly associated with Vonsattel grade of neuropathological involvement and three of these, miR-10b-5p, miR-10b-3p, and miR-302a-3p, significantly related to the Hadzi-Vonsattel striatal score (a continuous measure of striatal involvement) after adjustment for CAG length. Five miRNAs (miR-10b-5p, miR-196a-5p, miR-196b-5p, miR-10b-3p, and miR-106a-5p) were identified as having a significant relationship to CAG length-adjusted age of onset including miR-10b-5p, the mostly strongly over-expressed miRNA in HD cases. Although prefrontal cortex was the source of tissue profiled in these studies, the relationship of miR-10b-5p expression to striatal involvement in the disease was independent of cortical involvement. Correlation of miRNAs to the clinical features clustered by direction of effect and the gene targets of the observed miRNAs showed association to processes relating to nervous system development and transcriptional regulation. ***Conclusions.*** These results demonstrate that miRNA expression in cortical BA9 provides insight into striatal involvement and support a role for these miRNAs, particularly miR-10b-5p, in HD pathogenicity. The miRNAs identified in our studies of postmortem brain tissue may be detectable in peripheral fluids and thus warrant consideration as accessible biomarkers for disease stage, rate of progression, and other important clinical characteristics of HD.

Background

Huntington's disease (HD) is an inherited disorder caused by a CAG trinucleotide repeat expansion in *HTT* which leads to progressive motor and cognitive impairment due to the gradual loss of neurons within striatal and cortical brain regions [1]. Although monogenic, HD displays remarkable variation in clinical expression, most readily observed by the range in age at clinical onset as determined by the manifestation of motor symptoms, varying from age 4 years to age 80 [2]. While onset age is unequivocally related to the size of the expanded CAG repeat, with longer repeats leading to earlier onset, only 50% to 70% of the variation can be attributed to repeat size [3,4]. The remaining variation is highly heritable (h^2 = 0.56), suggesting a strong role for genes that modify disease progression [3].

MicroRNAs (miRNAs) are small non-coding RNAs that negatively regulate the expression of genes in a sequence-specific manner, binding to the 3′-untranslated region (3′UTR) to initiate cleavage or translational repression of target transcripts [5,6]. miRNAs influence a diverse range of cellular processes [7] and consequently, their altered expression may lead to or influence disease-related pathological phenotypes, or reveal unknown aspects of the disease process. In the central nervous system (CNS), miRNAs are abundant, as brain-

specific miRNAs assist in various neuronal processes such as synaptic

development, maturation and plasticity [8,9]. Altered miRNA expression has been

observed in diseases of the CNS, particularly in age-dependent

neurodegenerative diseases, which suggests that the expression of miRNAs may

contribute to neuropathogenesis [10,11].

In HD, the dysregulation of miRNAs has been reported in HD *in vitro*

models, transgenic HD animals and human HD brain [12-24]. We hypothesize

that post-transcriptional regulation by miRNAs plays a role in modifying the

progression and severity of HD. Recently, we completed a study of miRNA

expression obtained through next-generation sequencing technology in human

HD and control brain samples to investigate the presence of altered miRNA

expression in HD and its role in transcriptional dysregulation [13]. The original

study provided sample power to detect large miRNA changes, but the sample

size was not sufficient to detect more subtle changes in miRNA expression and

did not represent a wide enough range of HD pathology to investigate

relationships to clinical features of HD. Therefore, to follow-up on these findings,

we have sequenced small RNAs in an additional 16 HD brains, two of which are

gene positive asymptomatic Vonsattel grade 0 cases, and 27 control samples, for

a combined study of 28 HD and 36 control samples. The increased sample size

enables the detection of significantly altered miRNAs with lower levels of

differential expression as well as more comprehensive characterization of the

relationship of these miRNAs to relevant clinical features of the disease,

including the age at motor onset of the disease, disease duration (the time between onset and death), age at death and extent of pathological involvement in the striatum and cerebral cortex. A deeper understanding of the global miRNA expression in HD may elucidate pathogenic mechanisms of disease progression in HD and suggest new therapeutic targets.

Results

Differential expression analysis highlights disrupted miRNA expression in HD brain. To evaluate the relationship of miRNA expression to salient clinical and pathological features of HD, we profiled miRNA expression using small RNA-sequencing of prefrontal cortex (Brodmann Area 9) of 26 symptomatic HD and 36 control samples (**see Table 6**). Although the striatum is the most affected brain region in HD, differences in miRNA expression between HD and unaffected controls, independent of cellular composition, would be difficult to assess due to the extent of neuron loss and the increase of reactive astrocytosis in HD striatal tissue [25]. Therefore, prefrontal cortex, which exhibits hallmark characteristics of HD pathology [26], relates to striatal involvement (Pearson r = 0.44, p < 2e-16) [27], but experiences less extreme changes than the striatum [28,29], was used for sequencing. In addition, previous studies have found no difference in cell counts between HD and controls from similar BA9 brain samples [13,30].

The HD samples consisted of Grade 2 (n = 4), Grade 3 (n = 15), and Grade 4 (n = 7) brains as determined by Vonsattel grade, an assessment of

striatal involvement classified as 0 through 4 in order of the severity of neuropathological involvement [25]. Sequenced samples were also among the 523 HD brains characterized by the recently established measure of pathological involvement termed the Hadzi-Vonsattel score (H-V score), which independently characterizes both striatal and cortical pathological involvement in each brain [28]. While Vonsattel grading and H-V striatal score are closely related, (Pearson r = 0.90, measured using 346 HD brains), H-V scores are a continuous metric and therefore more amenable to adjustment of covariates such as CAG repeat size in modeling of neuropathological involvement and independently assesses striatal and cortical involvement. H-V scores ranged from 0–4, where 0 indicates no detectable neuropathological involvement and 4 indicates severe neuropathological involvement. Samples from symptomatic individuals had striatal scores ranging 1.43–3.82 and cortical scores ranging from 0.40–2.36 (see Table 6). Additionally, two Grade 0 brains (both with CAG repeat expansions of 42 repeats) were small-RNA sequenced and analyzed separately from the 26 HD brains used in differential expression analysis. Grade 0 brains were neuropathologically normal and asymptomatic at the time of death (see Table 1).
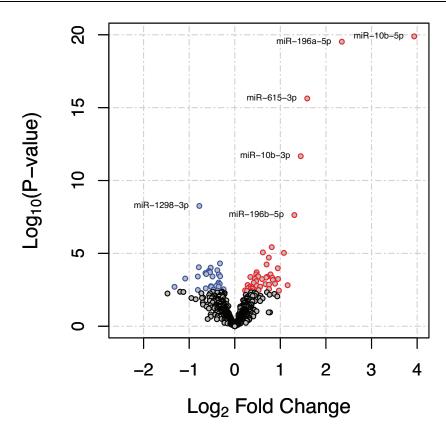
Table 6. Summary of the brain samples used for miRNA-sequence analysis.

Variable	HD, Grades 2 - 4	Asymptomatic Grade 0	Control
N	26	2	36
Age at death	59.5 ± 10.7	67.5 ± 26.1	68.6 ± 14.3
RNA integrity number	7.3 ± 0.9	7.7 ± 0.6	7.7 ± 0.7
Post mortem interval	15.7 ± 7.7	28.0 ± 7.9	14.4 ± 8.8
CAG repeat size	44.6 ± 2.9	42.0 ± 0	
Age of onset	44.5 ± 11.8		
Disease duration	15.0 ± 6.1		
Striatal score	2.70 ± 0.65		
Cortical score	1.25 ± 0.50		

After processing sequencing data to remove sequencing artifacts, normalize using variance stabilization transformation, and adjust for batch effects (see Methods), 938 miRNAs were reliably quantified and 75 of these were significantly differentially expressed in HD versus control brains after adjusting for multiple comparisons (FDR q-value < 0.05, see Appendix Table 1). In HD, 46 miRNAs were identified as significantly up-regulated and 29 as down-regulated in their expression. Hox-related miRNAs had the most extreme, positive fold changes, where miR-10b-5p was 3.9 log2 fold increased, miR-196a-5p was 2.4 log2 fold increased, miR-615-3p was 1.6 log2 fold increased, miR-10b-3p was 1.5 log2 fold increased, and miR-196b-5p was 1.3 log2 fold increased (see Figure 9, see Table 7). Both the 5′ and 3′ mature miRNAs were differentially expressed for eight miRNA precursors (miR-10b, miR-129, miR-1298, miR-142, miR-144, miR-148a, miR-302a, and miR-486). In HD and controls, most 5′-3′ miRNA pairs were positively correlated in their expression, with the exception of miR-1298 in HD and miR-10b and miR-302a in controls.

Appendix Table 1. Differentially expressed miRNAs in Huntington's disease prefrontal cortex

Figure 9. Characterization of miRNA in Huntington's disease brain.
Volcano plot of 75 significantly differentially expressed miRNA after FDR-adjustment for 938 comparisons. Points labeled red were up-regulated in HD and points labeled as blue were down-regulated in HD. Hox-related miRNA points are labeled and represent the top differentially expressed miRNA in HD.

To confirm our previously published findings, we re-analyzed the twelve HD and nine controls samples from our original study using our updated sequence analysis pipeline (see Methods) and then used the newly sequenced samples, consisting of 14 HD and 27 control brains, as a replication set. Fourteen miRNAs were significantly differentially expressed (FDR q-value < 0.05) in the original set using the updated analysis pipeline, compared to five differentially expressed

miRNA in the original study. Fourteen differentially expressed miRNAs were significantly differentially expressed in the replication set and thirteen of these fourteen were significant in the combined sequence analysis. As previously reported, Hox-related miRNA, including miR-10b-5p, were among the most strongly differentially expressed across all three studies (**see Appendix Table 1**). Firefly Bioworks microRNA assay, a multiplexed, particle-based technology using flow cytometry to measure miRNA levels, was used to quantify and orthogonally validate miRNA differential expression from sequencing (see Methods). A subset of 21 controls and 15 HD samples from the sequencing study were selected for the assay. Sixteen miRNAs with moderately high expression levels were selected for testing and an additional six miRNAs were used as input normalizers. miR-10b-5p was confirmed as significant after correcting for multiple corrections (p-value = 3.0e-10, q-value = 6.6e-9). Seven out of sixteen miRNAs assayed approached but did not reach significance after adjustment in this subset (unadjusted *p*-value < 0.05, miR-10b-5p, miR-194-5p, miR-223-3p, miR-132-3p, miR-144-5p, miR-148a-3p, miR-486-5p). Eight of the remaining nine miRNAs that failed to achieve significance had the same direction of effect. These results were consistent with the reduced power available from this subset.
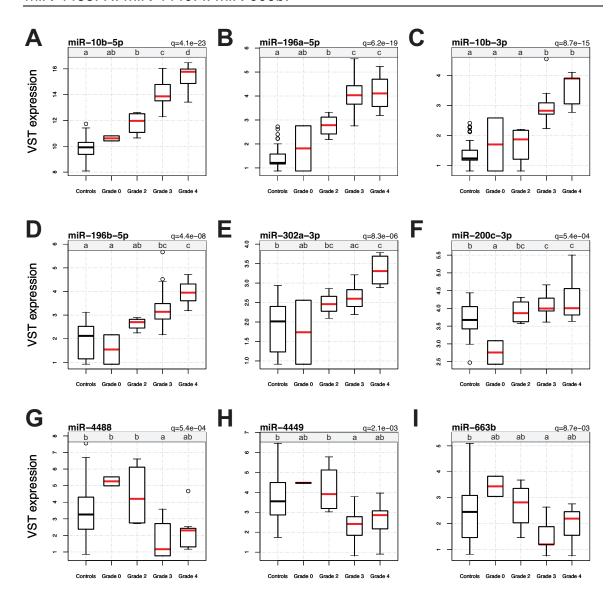
Nine miRNAs relate to Vonsattel grade. To explore the relationship of miRNA expression to principal clinical aspects of the disease, we next modeled the expression of the 75 differentially expressed miRNAs to the Vonsattel grade of neuropathological involvement. Analysis of variance (ANOVA) was performed

to compare the expression of the 75 differentially expressed miRNAs across Vonsattel grade in all 28 (Grade 0–4) HD gene-positive and control brains. 65 miRNA were found to be significant in the ANOVA (FDR-adjusted q-value < 0.05), indicating differential expression may be driven by the difference of controls to specific grades. Next, ANOVA was performed exclusively in HD brains to find whether miRNA differences exist across Vonsattel grades. Nine miRNAs were significant in both ANOVA tests after adjusting for multiple comparisons, indicating a significant difference in the expression of these miRNAs across Vonsattel grades (both FDR q-values < 0.05). Last, pairwise comparisons of each grade with the control group were performed using post-hoc Tukey's HSD (honestly significant different) tests to find specific groups that significantly differed from one another. **Figure 10** highlights the nine miRNAs that are associated with grade in order of statistical significance from the ANOVA inclusive of control brains in the test. In **Figure 10**, significant differences across grade and control groups as determined by Tukey HSD are denoted by letters (a-d) in the grey banner above each boxplot, whereby groups with different letters are significantly different from one another while those which share letters are not.

Figure 10. Nine miRNAs are associated with Vonsattel grade.
In HD brains, expression of differentially expressed miRNA was compared across Vonsattel grades 0–4. Boxplots represent nine FDR-significant miRNAs (FDR q < 0.05, adjusted for 75 contrasts) associated with Vonsattel grade by analysis of variance (ANOVA). X-axes represent Vonsattel grade, classified 0–4 in order of the severity of striatal involvement and Y-axes show the VST expression values after batch correction. Significant differences across grades and controls are denoted by letters in the grey banner above the boxplot, labeled

a-d. Groups with different letters are significantly different from one another while those with the same letter are not, after correcting for multiple comparisons. For example, group "a" would be significantly different from group "b" and "c." Conditions represented by multiple letters indicate no significant difference among those groups. For example, group "ab" would not be significantly different than groups "a" and "b," but would be different group "c." A. miR-10b-5p. B. miR-196a-5p. C. miR-10b-3p. D. miR-196b-5p. E. miR-302a-3p. F. miR-200c-3p. G. miR-4488. H. miR-4449. I. miR-663b.
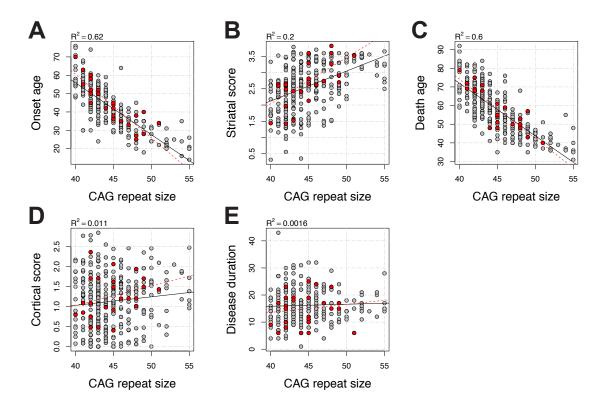
Several patterns in the relationship of grade to miRNA expression were observed. First, the expression of miR-10b-5p was significant in nearly all comparisons; pairwise contrasts between all grades as well as with the control group were different except for grade 0, although grade 0 was different than grades 2, 3 and 4 (**see Figure 10A**). Second, the expression of miRNAs in grade 0 brains was rarely different than controls, with the exception of miR-200c-3p, where its expression in grade 0 brains was significantly lower than both controls and grades 2–4 brains (**see Figure 10G**). Third, the expression of miRNAs in grade 3 and 4 brains appeared relatively similar to one another, with the exception of miR-10b-5p, as mentioned above, and miR-4488, where grade 3 brains were significantly lower than all other groups (see **Figure 10D**). Although not significant in the HD-only ANOVA, significant pairwise differences between grade 3 and 4 were observed for miR-1298-5p (Bonferroni q-value = 3.6e-2) and miR-615-3p (Bonferroni q-value = 2.2e-2).

To assess the sensitivity and specificity of miR-10b-5p for predicting HD, area under the curve (AUC) values were calculated using receiver operating characteristic curves (ROC). When comparing HD to controls to predict HD, the AUC was 99.47% (95% confidence level was 98.46%-100%). In a comparison of asymptomatic HD to HD to predict HD status, the AUC was 98.08% (95% confidence level was 92.75-100%) and comparing asymptomatic HD to controls, the AUC was 84.72% (95% CI: 71.09%-98.36%).

miRNA expression relates to striatal involvement and age of onset in

HD. To further elucidate the meaning of the associations of the miRNAs to HD,

we examined the relationship between the 75 differentially expressed miRNAs

and other salient features of the disease (age at motor onset, disease duration,

age at death, and H-V scores of striatal and cortical involvement). To avoid

confounding the analysis of these clinical features by the known, strong

relationship between *HTT* CAG repeat size and disease pathology and onset

[4,28,31,32], CAG-adjusted residuals were calculated for all continuous clinical
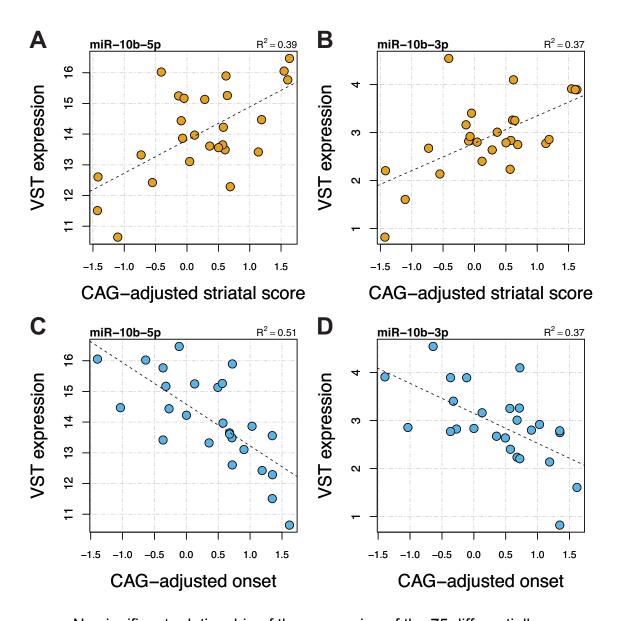
traits (see Figure 11).

Figure 11. Association of clinical features to HD CAG repeat size.
CAG-adjusted residuals for onset age, death age, duration, H-V striatal score
and H-V cortical score were computed from data derived from 346 HD brain
samples with CAG repeat sizes <56 from Hadzi et al. [28]. Red dots represent
samples studied in these analyses.

Using linear regression analysis and applying FDR-adjustment for the 75

comparisons, three miRNAs (miR-10b-5p, miR-10b-3p, miR-302a-3p) were

observed to have a significant relationship to CAG-adjusted striatal score (FDR

q-values = 2.28e-2). All three were significant in the analysis of miRNA

expression to Vonsattel grade (see above). Additionally, five miRNAs were

identified as having significant association to CAG-adjusted age of onset (miR-

10b-5p, FDR *q*-value = 3.49e-3; miR-196a-5p, FDR *q*-value = 1.32e-2; miR-

196b-5p, FDR *q*-value = 1.71e-2; miR-10b-3p, FDR *q*-value = 1.71e-2; miR-

106a-5p, FDR *q*-value = 1.71e-2). **Figure 12** highlights the relationship of miR-

10b to CAG-adjusted striatal score and onset, where both 3p and 5p mature

sequences of miR-10b were the only miRNA species to have significant, linear

association to these two clinical features independent of CAG effect. No FDR-

significant relationships of miRNA to disease duration or death age were

observed.

Figure 12. miR-10b is associated with age of onset and striatal involvement.
In 26 Vonsattel grade 2, 3 and 4 HD brains, both mature miR-10b sequences (-5p and -3p) have FDR-significant relationships to clinical features of HD. Y-axes show the variance stabilizing transformation expression values after batch correction. Grade 0 cases are not included, as they have neither onset age nor Hadzi-Vonsattel (H-V) striatal score. A. Scatterplot of miR-10b-5p expression and CAG-adjusted H-V striatal score. B. Scatterplot of miR-10b-3p expression and CAG-adjusted H-V striatal score. C. Scatterplot of miR-10b-5p expression and CAG-adjusted onset age. D. Scatterplot of miR-10b-3p expression and CAG-adjusted onset age.

No significant relationship of the expression of the 75 differentially expressed miRNA to CAG-adjusted cortical score was observed, although nominal associations were seen. In order to account for the potential impact of cortical involvement on the relationship of miRNA expression to striatal involvement, we performed a multivariate regression analysis modeling miRNA expression to striatal H-V score while correcting for cortical H-V score. After
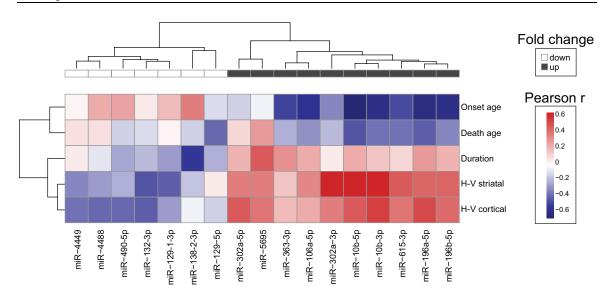
CAG-adjusted cortical score correction, CAG-adjusted striatal score remained significant (miR-10b-5p *p*-value = 0.04, miR-10b-3p *p*-value = 0.01, miR-302a-3p *p*-value = 0.005).

Last, to characterize the patterns of association of miRNAs to clinical features, Pearson coefficients of the correlation of the expression of the differentially expressed miRNAs to five CAG-adjusted features (onset age, disease duration, death age, striatal score and cortical score) were hierarchically clustered. Grade 0 and controls samples were not included in these analyses. Correlation coefficients rather than beta coefficients were used in order to standardize the direction of effect. Here, we observed differentially expressed miRNAs with correlation *p*-values < 0.05 clustered into distinguishable patterns of association to clinical variables (see Figure 13). Differentially expressed miRNAs increased in HD compared to controls tended to have negative correlations with onset and death, and positive correlations with striatal and cortical score. Conversely, differentially expressed miRNAs with negative relative fold changes had positive correlations with onset and death, and negative correlations with striatal and cortical scores.

Figure 13. CAG-adjusted clinical features of HD show patterns of association with miRNA expression.
CAG-adjusted measures of onset age, disease duration, death age, Hadzi-Vonsattel (H-V) striatal and cortical score were correlated with differentially expressed miRNAs in HD brains. miRNAs with at least one nominal *p*-value < 0.05 are shown. Pearson correlation coefficients and features were independently hierarchically clustered. Red boxes indicate positive correlations and blue boxes indicate negative correlations. Seven miRNAs in the left section are down-regulated in HD and the ten miRNAs in the right section are up-

regulated. Unsupervised clustering separated miRNA by their direction of fold change.

Targets of HD-related miRNAs are associated with nervous system development and transcriptional regulation. To attempt to understand the potential functional impact of miRNA dysregulation in HD, gene ontology enrichment was performed using predicted targets for miRNAs that correlated with clinical features and were suitably annotated in Targetscan (twelve miRNAs in total). 5712 unique mRNA targets for miRNAs with positive fold change in HD (miR-106a/302a-5p, miR-196a/miR-196b, miR-302a-3p, miR-363, miR-10b, miR-615-3p), and 6572 mRNA targets for negative fold change in HD (miR-129-3p, miR-129-5p, miR-132-3p, miR-4449, miR-4488, miR-490-5p) were found using Targetscan [33], and stratified by fold change for gene ontology term (GO) enrichment analysis. Using TopGO's weight algorithm with Fisher's Exact Test for gene ontology term enrichment and a weighted p-value cutoff less than $p <$ 0.05, 354 GO Biological Processes, 86 GO Molecular Functions and 62 GO

Cellular Component terms for mRNA targets of down-regulated miRNA were significant. 260 GO Biological Processes, 78 GO Molecular Functions, 48 GO Cellular Component terms for mRNA targets of up-regulated miRNA were significant.
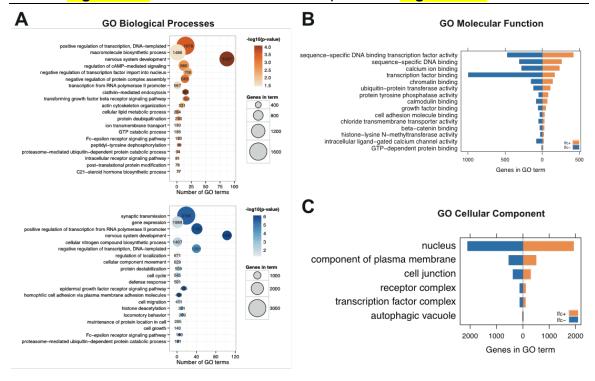
To make these long lists of GO terms more intelligible, terms were summarized using semantic similarity measures to remove gene-set and GO term redundancy (see Methods).

Targets of up- and down-regulated miRNAs had substantial overlap in their overall function. Three of the top twenty collapsed GO Biological Processes terms were shared between the two sets of targets (see Figure 14A). These terms were "nervous system development," "Fc-epsilon receptor signaling pathway," and "proteasome − mediated ubiquitin − dependent protein catabolic process." "Nervous system development" was the most significant term in both sets (Up p = 8.5e-5, Down p = 9.9e-7). The top enriched term was "positive regulation of transcription, DNA-templated", (N = 1678, p = 2.7e-4) for the positive gene set and "synaptic transmission", (N = 3166, p = 3.4e-6) for the negative gene set. Of the 78 up-regulated Molecular Function terms and 86 down-regulated terms, fifteen terms were the same (see Figure 14B). Top terms were included "sequence-specific DNA binding transcription factory activity", "sequence-specific DNA binding" and "calcium ion binding". Though shared between the two groups, "transcription factor binding" was enriched higher in down-regulated miRNAs than positive ones. For GO Cellular Component, six

90

terms were the same between the two gene sets. These terms included

"nucleus" and "cytoplasm" as well as "cell junction" (see Figure 14C).

Figure 14. Gene ontology terms are similar for mRNA targets of clinically relevant deregulated miRNAs.
Figure 14A illustrates the overlap in GO Biological Processes between targets of increased miRNA (in orange) and decreased miRNA (in blue) in HD. The x-axis shows the number of gene ontology terms that fall within a given semantic term set, and the y-axis lists the top twenty enriched terms for each set of miRNA targets. Darker colored points represent terms with higher significance and the size of the points represents the union of all genes that fall within a given the term. A number of terms, including "nervous system development" as well as terms relating to transcriptional regulation are shared across up- and down-regulated miRNA target groups. The similarity targets of up-regulated miRNA (in orange) and down-regulated miRNA (in blue) for GO Molecular Function are seen in Figure 14B and for GO Cellular Component in Figure 14C.

Discussion

In a next-generation sequence analysis of small non-coding RNAs in 26

HD and 36 control brains we detected 938 miRNAs and 75 of these were

91

differentially expressed. All five miRNAs reported as differentially expressed in our previous study (miR-10b-5p, miR-196a-5p, miR-196b-5p, miR-615-3p and miR-1247-5p) were significantly differentially expressed in this study [13]. These results were independently validated in the 41 (14 HD and 27 control brains) newly studied brains (**see Appendix Table 1**), and support the presence and robust up-regulation of Hox-related miRNAs in HD brain [13]. The increased number of differentially expressed miRNAs is likely due to an increase in sample size. Increasing our sample size (from N = 21 to N = 62) enhanced the statistical power to detect additional miRNAs with smaller but significant changes in miRNA expression. We believe these miRNA signals are not attributed to a change in BA9 architecture, influenced by neuronal cell death or reactive glial response, because cell numbers between HD and controls from the same brain samples were indistinguishable [13,30].

Dysregulation of several miRNAs from our study have been observed in HD in other contexts. Concordant with our findings, miR-132-3p down-regulation in human HD parietal cortical tissue [15] and in brains of R6/2 and YAC128 HD mouse models has been observed [15,18]. miR-132 is highly enriched in the brain [34,35] and its expression has been shown to affect neuron morphogenesis and enhance neurite outgrowth by suppressing the GTPase-activating protein p250GAP (*p250GAP/RICS*) [36]. Another target of miR-132 is acetylcholinesterase (*ACHE*), which encodes an enzyme responsible for the breakdown of the neurotransmitter acetylcholine at the neural synapse [37].

Acetylcholinesterase is critically involved in cognition, and acetylcholinesterase inhibitors are FDA-approved for the treatment of cognitive impairments in Alzheimer's disease [37]. Thus, decreased miR-132 levels may negatively impact brain health, through the dysregulation of *p250GAP* (limiting its suppression) and *ACHE* (indirectly decreasing acetylcholine levels).

Differentially expressed miRNAs may also target *HTT* transcripts as a response to mutant *HTT* to reduce *HTT* transcriptional levels and limit toxicity. miRNAs that target the *HTT* 3′UTR and reduce *HTT* transcript levels in vitro, miR-148a-5p, miR-150-5p and miR-214-5p, were significantly up-regulated in their expression [21,38]. Although miR-196a does not directly target *HTT* [33], increased miR-196a expression was observed in a primate model of HD and its over-expression *in vitro* and in animal transgenic models suppressed mutant *HTT* expression [24]. The miRNAs with the largest effect in our study, miR-10b-5p, putatively targets *HTT* by binding to two 3′UTR sites (both 7mer-1A seed, positions 2742–2748 and 3301–3307) and may reduce expression of *HTT* although it is not clear whether or not this would be neuroprotective [33]. However, miR-10b-5p also targets brain-derived neurotrophic factor (*BDNF*) [39], a growth factor required for the survival and differentiation of striatal neurons [40]. *BDNF* has been extensively studied in HD [41], as normal huntingtin protein is reported to up-regulate *BDNF* levels, while mutant huntingtin impairs BDNF protein abundance which may consequently lead to death of striatal neurons [42]. Because of the potential biological importance of *BDNF*, and the possibility that

miR-10b-5p may diminish translation of *BDNF*, over-expression of miR-10b-5p might be harmful to neuronal cells. However, in Hoss et al. [13], we showed that ectopic expression of miR-10b-5p in PC12 cells expressing a mutant huntingtin fragment enhanced cell survival [13], and miR-10b-5p has been observed to facilitate neurodifferentiation [43]. Given its high levels of differential expression, strong relationship to striatal involvement and age at onset, more research into miR-10b-5p is justified to understand its role in the pathogenesis of HD, its potential as a biomarker of disease progression and its potential as a therapeutic target.

The cell type most responsible for miRNA changes cannot be determined from these data. Tissue homogenate was used for sequencing, so the source of miRNA signal is likely both neuronally and non-neuronally derived. To determine the miRNA cellular specificity in the brain, Jovicic et al. [16] measured miRNA expression in cultured neurons, oligodendrocytes, microglia and astrocytes to find miRNAs enriched for each cell type. Based upon this study, miRNAs found to be specifically enriched in neuronal cultures (miR-129-3p, miR-129-5p, miR-132, miR-135b, miR-431, miR-433) were all down-regulated in our study whereas miRNAs enriched in microglial cultures (miR-126-5p, miR-126-3p, miR-141, miR-142-3p, miR-142-5p, miR-150, miR-200c and miR-223) were all were up-regulated. According to these enrichment categories, microglial activation miRNAs do not relate to clinical features of the disease. Conversely, three neuronal-related miRNAs, miR-129-3p/5p and miR-132, were associated with

pathological involvement (see Figure 13). Therefore, we hypothesize that differential expression of those miRNAs related to neuron function may also relate to the HD pathology.

The relationship of the expression of miRNAs with Vonsattel grade suggests expression changes may occur early in the disease process (see Figure 10). Many of these miRNA changes appear present ordinal trends with an increase (miR-10b-5p, miR-10b-3p, miR-302a, miR-196a-5p, miR-196b-5p) or decrease (miR-663b, miR-4488, miR-4449) in their expression across grade. In particular, miR-10b-5p was significantly different across all groups, with the exception of the asymptomatic grade 0 brains and we believe this is an issue of statistical power. It is possible that the expression of these miRNAs may relate to *HTT* aggregation or proteasomal degradation, as intranuclear inclusions are observed in pre-symptomatic HD [44] and the density of aggregate formation continues over the course of the disease. Three miRNAs (miR-10b-3p/5p, miR-302a) related to H-V striatal score, independent of the CAG repeat expansion size and for miR-10b-5p, independent of cortical involvement. These results suggest the relationship of miRNA expression to striatal involvement in the disease is independent of cortical involvement, which is a critical finding, because prefrontal cortex was the source of tissue profiled in these studies.

Based on correlation (see Figure 13), up-regulated miRNAs clustered together based on their relationships to clinical features. Generally, these miRNAs had strong, positive associations to striatal and cortical H-V scores,

95

weak positive association with disease duration and strong negative associations to onset and death age. Down-regulated miRNAs clustered together as well but were less defined in their relationships to clinical features. Most down-regulated miRNAs were inversely associated with H-V scores and duration, opposite to up-regulated miRNAs. These patterns suggest that decreasing up-regulated miRNAs and increasing down-regulated miRNA may be beneficial. However, it remains to be determined which altered miRNAs are compensatory and potentially neuroprotective and which are pathological and neurotoxic. Furthermore, it is unknown whether these changes are consequential, revealing important molecular aspects of the disease process, or are simply innocent by-products.

However, using target analysis and GO term enrichment, we observed predicted targets of both up- and down-regulated miRNAs shared many of the same biological processes and overall systems relating to "nervous system development." Both sets contained several transcriptional regulation related terms (transcriptional regulation, DNA-dependent or RNA polymerase II, chromatin remodeling, post-transcriptional gene regulation, chromatin remodeling, etc.). Both sets of genes contained terms on metabolism, apoptosis, metal-binding and ubiquitin. Disruption to any of these systems may affect neuron health. Overall, these finding imply both up- and down-regulated miRNAs many be part of the same or similar biological pathways.

Conclusions

Our findings identify many miRNA alterations in HD brain and a large number of these are related to clinical manifestations of the disease, where the signal is independent of the size of the CAG repeat expansion. The study of Grade 0 cases suggests that miR-10b-5p expression changes may occur pre-symptomatically. Up- and down-regulated miRNAs may target genes in similar biological systems, and these genes are involved in transcriptional regulation, neuronal development and other important aspects surrounding neuron function. These miRNAs represent attractive candidates for predicting onset age and overall health of the striatum in HD. Studies pursuing these miRNAs as potential biomarkers for HD are in progress, as miRNAs may be detectable in peripheral fluids [45] and thus have potential to function as accessible biomarkers for disease stage, rate of progression, treatment efficacy and other important clinical characteristics of HD.

Methods

Sample information. Frozen brain tissue from prefrontal cortex Brodmann Area 9 (BA9) was obtained from the Harvard Brain and Tissue Resource Center McLean Hospital, Belmont MA, Banner Sun Health Research Institute, Sun City, Arizona [46] and Human Brain and Spinal Fluid Resource Center VA, West Los Angeles Healthcare Center, Los Angeles, CA. 26 Huntington's disease (HD) samples, 2 asymptomatic HD gene carriers, and 36 neurologically and neuropathologically normal control samples were selected for

the study. HD subjects had no evidence of other neurological disease based on neuropathological examination. HD samples and controls were not different in postmortem interval (PMI) (*p*-value = 0.69), RNA integrity number (*p*-value = 0.08) or gender (*p*-value = 0.51) but differed in ages at death (HD mean age =59.5, control mean age =68.6; *p*-value = 0.01) (**see Table 1**). Asymptomatic HD samples did not differ in age at death (mean age =67.5) in comparison to HD or control samples (control *p*-value = 0.92; HD *p*-value = 0.40). Information on CAG genotype, onset age, death age, disease duration, Vonsattel grade, Hadzi-Vonsattel striatal and cortical scores for HD samples can be found on GEO. Total RNA was isolated using QIAzol Lysis Reagent and purified using miRNeasy MinElute Cleanup columns. RNA quality for sequencing was assessed using Agilent's BioAnalyzer 2100 system and RNA 6000 Nano Kits to determine RNA Integrity Number or Agilent 2200 TapeStation and Agilent DNA ScreenTape assay RNA Quality Number. For each brain sample, 1 ug of RNA was used to construct sequencing libraries using Illumina's TruSeq Small RNA Sample Prep Kit, according to the manufacturer's protocol, and sequenced using 1x51nt single-end reads on Illumina's HiSeq 2000 system at Tufts University (http://tucf-genomics.tufts.edu/) or the Michigan State sequencing core facility (http://rtsf.natsci.msu.edu/genomics/).

   miRNA sequence analysis. Reads were quality filtered, removing reads below 80% Q20, using FASTX-toolkit *FASTQ quality filter* (version 0.0.13.2, http://hannonlab.cshl.edu/fastx_toolkit/). Adapter sequence (5′-

TGGAATTCTCGGGTGCCAAGG-3′) was removed from the 3′ end of all reads

using cutadapt 1.2.1 (http://code.google.com/p/cutadapt/) and reads less than 15

nucleotides in length were discarded [47]. Reads were collapsed using FASTX-

toolkit *FASTA/Q collapser*. Reads were aligned to the UCSC human reference

genome (build hg19) using Bowtie version 1.0.0, using no mismatch alignments

and a limit of 200 multiple mapping instances [48]. Aligned reads that overlapped

with the human miRNA annotation, miRBase version 20,

(http://www.mirbase.org/ftp.shtml) were identified using BEDTools *IntersectBed*

[49]. Reads longer than 27 bases were removed. miRNA reads were counted if

±4 nucleotides from the mature, annotated 5′ start coordinates. Reads that

mapped to multiple locations, represented by a single mature miRNA, were

recorded as a single miRNA count. Multi-mapped reads represented by multiple

mature miRNA annotations were discarded. R version 3.1.0 and Bioconductor

2.1.4 version were used for differential expression analysis. DESeq2 version

1.40.0 was used for estimation of library size and correction, as well as variance-

stabilizing transformation (VST) [50,51]. miRNAs with a mean less than 2 raw

read counts across all samples were removed. Batch effect was corrected using

ComBat with default options through the Bioconductor package sva 3.10 [52,53].

All samples were included in VST and batch correction. Using 36 controls and 26

HD grades 2–4, differential expression analysis was performed with LIMMA

version 3.20.8 [54,55], adjusting for age at death in the model. *Q*-values were

FDR-adjusted for 938 comparisons. The unprocessed fastq files, normalized

miRNA counts and results from miRNA differential expression analysis have been deposited in NCBI's Gene Expression Omnibus [56], and are accessible through GEO Series accession number GSE64977 (http://www.ncbi.nlm.nih.gov/geo/query/acc.cgi?acc=GSE64977).

Firefly miRNA assay. A panel of 16 differentially expressed miRNAs with moderate to high expression (miR-10b-5p, miR-194-5p, miR-223-3p, miR-132-3p, miR-144-5p, miR-148a-3p, miR-486-5p, miR-363-3p, miR-199a-5p, miR-16-2-3p, miR-142-3p, miR-34c-5p, miR-129-5p, miR-433-3p, miR-885-5p, miR-346) and six stably expressed miRNAs in sequencing (miR-9-5p, miR-92a-3p, miR-98-5p, miR-101-3p, miR-151a-3p, miR-338-3p) was used for validation. In a 96-well filter plate, Firefly Multimix (Firefly BioWorks, www.fireflybio.com) was incubated with 25ul Hybridization Buffer and 25ul total RNA at a concentration of 1 ng/ul at 37°C for 60 minutes. After rinsing to removing unbound RNA, 75ul of Labeling Buffer was added to each well, and the plate was incubated for 60 minutes at room temperature. Adapted-modified miRNAs were released from the particles using 90°C water, and PCR amplified using a fluorescently-label primer set. PCR product was hybridized to fresh Firefly Multimix for 30 minutes at 37°C and re-suspended in Run Buffer for readout. Particles were scanned on an EMD Millipore Guava 8HT flow cytometer. Raw output was background subtracted, normalized using the geometric mean of the six normalizer miRNAs and log-transformed. LIMMA version 3.20.8 [54] was used to calculate significance.

HD feature analysis. For analysis of miRNA expression to Vonsattel grade, Tukey HSD statistics and compact letter display were generated by the multcomp R package [57]. CAG-adjusted age of onset was calculated using the logarithmic model from Djousse et al. 2003 [4]. Hadzi-Vonsattel striatal and cortical scores were measured in 523 HD brain samples as previously described [28]. Samples with greater than 55 repeats or missing CAG information were excluded from analysis, leaving 346 samples. To provide robust residual estimates for the subset of samples included in the sequencing project, H-V striatal score, H-V cortical score, death age and disease duration features were corrected for CAG size by modeling each feature to CAG size within the HD dataset (N = 346) and the residuals from the model were extracted for each sample (see Figure 11) [28]. VST-batch corrected counts were used for all subsequent analyses. CAG-adjusted residuals and miRNA expression relationships were analyzed using linear regressions. Covariates (PMI, RIN, age at death) were not included in linear models, as neither PMI nor RIN were determined to have an effect on the outcome of the results. Age at death could not be included in the analysis due to the relationship of age at death and HD clinical pathology. Q-values were FDR-adjusted for 75 differentially expressed miRNA contrasts for linear regressions were reported.

For the cluster analysis in Figure 13, Pearson correlations for miRNA expression to clinical feature were performed and those miRNAs with p-values < 0.05, without adjustment for multiple comparisons, were reported. Pearson correlation

coefficients were hierarchically clustered using Euclidean distance and unsupervised complete clustering method through the R-package *pheatmap* version 0.7.7.

Target prediction and gene ontology enrichment. Targetscan, release 6.2 [33] was used to select mRNA targets of miRNAs with at least one relationship to clinical feature. Fourteen miRNAs were available on Targetscan and twelve miRNAs had unique seed sequences. Targets were removed with total context scores ≥ −0.1. miRNAs with positive fold change in HD (miR-106a/302a-5p, miR-196a/miR-196b, miR-302a-3p, miR-363, miR-10b, miR-615-3p), and negative fold change in HD (miR-129-3p, miR-129-5p, miR-132-3p, miR-4449, miR-4488, miR-490-5p) were stratified for gene ontology term (GO) enrichment analysis. GO term enrichment for "biological processes," "molecular function," and "cellular component," was performed using topGO [58] with the "weight01" algorithm and Fisher statistic within the R statistical environment. A weighted Fisher p-value < 0.05 threshold was used to select significant GO enrichment. Significant terms were collapsed by semantic similarity using the program REVIGO [59], with p-value included for each term and using the "Small (0.5)" similarity setting. The union of genes from REVIGO "parent" terms was calculated using topGO's *genes.in.term* function.

References

1. HDCRG. A novel gene containing a trinucleotide repeat that is expanded and unstable on Huntington's disease chromosomes. Cell. 1993;72(6):971–83.

2. Myers RH. Huntington's disease genetics. NeuroRx. 2004;1(2):255–62.

3. Li JL, Hayden MR, Almqvist EW, Brinkman RR, Durr A, Dode C, et al. A genome scan for modifiers of age at onset in Huntington disease: the HD MAPS study. Am J Hum Genet. 2003;73(3):682–7.

4. Djousse L, Knowlton B, Hayden M, Almqvist EW, Brinkman R, Ross C, et al. Interaction of normal and expanded CAG repeat sizes influences age at onset of Huntington disease. Am J Med Genet A. 2003;119A(3):279–82.

5. Bartel DP. MicroRNAs: genomics, biogenesis, mechanism, and function. Cell. 2004;116(2):281–97.

6. Bartel DP. MicroRNAs: target recognition and regulatory functions. Cell. 2009;136(19167326):215–33.

7. Alvarez-Garcia I, Miska EA. MicroRNA functions in animal development and human disease. Development. 2005;132(21):4653–62.

8. Schratt GM, Tuebing F, Nigh EA, Kane CG, Sabatini ME, Kiebler M, et al. A brain-specific microRNA regulates dendritic spine development. Nature. 2006;439(7074):283–9.

9. Cao X, Yeo G, Muotri AR, Kuwabara T, Gage FH. Noncoding RNAs in the mammalian central nervous system. Annu Rev Neurosci. 2006;29:77–103.

10. Gascon E, Gao FB. Cause or effect: misregulation of microRNA pathways in neurodegeneration. Front Neurosci. 2012;6:48.

11. Junn E, Mouradian MM. MicroRNAs in neurodegenerative diseases and their therapeutic potential. Pharmacol Ther. 2012;133(2):142–50.

12. Gaughwin PM, Ciesla M, Lahiri N, Tabrizi SJ, Brundin P, Bjorkqvist M. Hsa-miR-34b is a plasma-stable microRNA that is elevated in pre-manifest Huntington's disease. Hum Mol Genet. 2011;20(11):2225–37.

13. Hoss AG, Kartha VK, Dong X, Latourelle JC, Dumitriu A, Hadzi TC, et al. MicroRNAs located in the Hox gene clusters are implicated in huntington's disease pathogenesis. PLoS Genet. 2014;10(2):e1004188.

14. Jin J, Cheng Y, Zhang Y, Wood W, Peng Q, Hutchison E, et al. Interrogation of brain miRNA and mRNA expression profiles reveals a molecular regulatory network that is perturbed by mutant huntingtin. J Neurochem. 2012;123(4):477–90.

15. Johnson R, Zuccato C, Belyaev ND, Guest DJ, Cattaneo E, Buckley NJ. A microRNA-based gene dysregulation pathway in Huntington's disease. Neurobiol Dis. 2008;29(3):438–45.

16. Jovicic A, Roshan R, Moisoi N, Pradervand S, Moser R, Pillai B, et al. Comprehensive expression analyses of neural cell-type-specific miRNAs identify new determinants of the specification and maintenance of neuronal phenotypes. J Neurosci. 2013;33(12):5127–37.

17. Kocerha J, Xu Y, Prucha MS, Zhao D, Chan AW. microRNA-128a dysregulation in transgenic Huntington's disease monkeys. Molecular Brain. 2014;7:46.

18. Lee ST, Chu K, Im WS, Yoon HJ, Im JY, Park JE, et al. Altered microRNA regulation in Huntington's disease models. Exp Neurol. 2011;227(1):172–9.

19. Marti E, Pantano L, Banez-Coronel M, Llorens F, Minones-Moyano E, Porta S, et al. A myriad of miRNA variants in control and Huntington's disease brain regions detected by massively parallel sequencing. Nucleic Acids Res. 2010;38(20):7219–35.

20. Packer AN, Xing Y, Harper SQ, Jones L, Davidson BL. The bifunctional microRNA miR-9/miR-9* regulates REST and CoREST and is downregulated in Huntington's disease. J Neurosci. 2008;28(53):14341–6.

21. Sinha M, Ghose J, Bhattarcharyya NP. Micro RNA −214,-150,-146a and-125b target Huntingtin gene. RNA Biol. 2011;8(6):1005–21.

22. Sinha M, Ghose J, Das E, Bhattarcharyya NP. Altered microRNAs in STHdh (Q111)/Hdh (Q111) cells: miR-146a targets TBP. Biochem Biophys Res Commun. 2010;396(3):742–7.

23. Soldati C, Bithell A, Johnston C, Wong K-Y, Stanton LW, Buckley NJ. Dysregulation of REST-regulated coding and non-coding RNAs in a cellular model of Huntington's disease. J Neurochem. 2013;124(23145961):418–30.

24. Cheng PH, Li CL, Chang YF, Tsai SJ, Lai YY, Chan AW, et al. Yang SH: miR-196a ameliorates phenotypes of Huntington disease in cell, transgenic mouse, and induced pluripotent stem cell models. Am J Hum Genet. 2013;93(2):306–12.

25. Vonsattel JP, Myers RH, Stevens TJ, Ferrante RJ, Bird ED, Richardson Jr EP. Neuropathological classification of Huntington's disease. J Neuropathol Exp Neurol. 1985;44(6):559–77.

26. Gutekunst CA, Li SH, Yi H, Mulroy JS, Kuemmerle S, Jones R, et al. Nuclear and neuropil aggregates in Huntington's disease: relationship to neuropathology. J Neurosci. 1999;19(7):2522–34.

27. Rosas HD, Salat DH, Lee SY, Zaleta AK, Pappu V, Fischl B, et al. Cerebral cortex and the clinical expression of Huntington's disease: complexity and heterogeneity. Brain J Neurol. 2008;131(Pt 4):1057–68.

28. Hadzi TC, Hendricks AE, Latourelle JC, Lunetta KL, Cupples LA, Gillis T, et al. Assessment of cortical and striatal involvement in 523 Huntington disease brains. Neurology. 2012;79(16):1708–15.

29. Sotrel A, Williams RS, Kaufmann WE, Myers RH. Evidence for neuronal degeneration and dendritic plasticity in cortical pyramidal neurons of Huntington's disease: a quantitative Golgi study. Neurology. 1993;43(10):2088–96.

30. Bai G, Cheung I, Shulha HP, Coelho JE, Li P, Dong X, et al. Epigenetic dysregulation of hairy and enhancer of split 4 (HES4) is associated with striatal degeneration in postmortem Huntington brains. Hum Mol Genet. 2015;24(5):1441–56.

31. Langbehn DR, Hayden MR, Paulsen JS. CAG-repeat length and the age of onset in Huntington disease (HD): a review and validation study of statistical approaches. Am J Med Genet B Neuropsychiatr Genet. 2010;153B(2):397–408.

32. Myers RH, Vonsattel JP, Stevens TJ, Cupples LA, Richardson EP, Martin JB, et al. Clinical and neuropathologic assessment of severity in Huntington's disease. Neurology. 1988;38(3):341–7.

33. Lewis BP, Burge CB, Bartel DP. Conserved seed pairing, often flanked by adenosines, indicates that thousands of human genes are microRNA targets. Cell. 2005;120(1):15–20.

34. Lagos-Quintana M, Rauhut R, Yalcin A, Meyer J, Lendeckel W, Tuschl T. Identification of tissue-specific microRNAs from mouse. Current Biol CB. 2002;12(9):735–9.

35. Miska EA, Alvarez-Saavedra E, Townsend M, Yoshii A, Sestan N, Rakic P, et al. Microarray analysis of microRNA expression in the developing mammalian brain. Genome Biol. 2004;5(9):R68.

36. Vo N, Klein ME, Varlamova O, Keller DM, Yamamoto T, Goodman RH, et al. A cAMP-response element binding protein-induced microRNA regulates neuronal morphogenesis. Proc Natl Acad Sci U S A. 2005;102(45):16426–31.

37. McGleenon BM, Dynan KB, Passmore AP. Acetylcholinesterase inhibitors in Alzheimer's disease. Br J Clin Pharmacol. 1999;48(4):471–80.

38. Kozlowska E, Krzyzosiak WJ, Koscianska E. Regulation of huntingtin gene expression by miRNA-137, −214, −148a, and their respective isomiRs. Int J Mol Sci. 2013;14(8):16999–7016.

39. Varendi K, Kumar A, Harma MA, Andressoo JO: miR-1, miR-10b, miR-155, and miR-191 are novel regulators of BDNF. Cellular and molecular life sciences: CMLS 2014

40. Li Y, Yui D, Luikart BW, McKay RM, Li Y, Rubenstein JL, et al. Conditional ablation of brain-derived neurotrophic factor-TrkB signaling impairs striatal neuron development. Proc Natl Acad Sci U S A. 2012;109(38):15491–6.

41. Zuccato C, Cattaneo E. Role of brain-derived neurotrophic factor in Huntington's disease. Prog Neurobiol. 2007;81(5–6):294–330.

42. Zuccato C, Ciammola A, Rigamonti D, Leavitt BR, Goffredo D, Conti L, et al. Loss of huntingtin-mediated BDNF gene transcription in Huntington's disease. Science. 2001;293(5529):493–8.

43. Meseguer S, Mudduluru G, Escamilla JM, Allgayer H, Barettino D. MicroRNAs-10a and -10b contribute to retinoic acid-induced differentiation of neuroblastoma cells and target the alternative splicing regulatory factor SFRS1 (SF2/ASF). J Biol Chem. 2011;286(21118818):4150–64.

44. Gomez-Tortosa E, MacDonald ME, Friend JC, Taylor SA, Weiler LJ, Cupples LA, et al. Quantitative neuropathological changes in presymptomatic Huntington's disease. Ann Neurol. 2001;49(1):29–34.

45. Burgos KL, Javaherian A, Bomprezzi R, Ghaffari L, Rhodes S, Courtright A, et al. Identification of extracellular miRNA in human cerebrospinal fluid by next-generation sequencing. RNA. 2013;19(5):712–22.

46. Beach TG, Sue LI, Walker DG, Roher AE, Lue L, Vedders L, et al. The sun health research institute brain donation program: description and experience, 1987–2007. Cell Tissue Bank. 2008;9(3):229–45.

47. Martin M. Cutadapt removes adapter sequences from high-throughput sequencing reads. EMBnet J. 2011;17(1):10–2.

48. Langmead B, Trapnell C, Pop M, Salzberg SL: Ultrafast and memory-efficient alignment of short DNA sequences to the human genome. Genome Biol 2009, 10 (19261174).

49. Quinlan AR, Hall IM. BEDTools: a flexible suite of utilities for comparing genomic features. Bioinformatics. 2010;26(6):841–2.

50. Anders S, Huber W. Differential expression analysis for sequence count data. Genome Biol. 2010;11(10):R106.

51. Love MI, Huber W, Anders S. Moderated estimation of fold change and dispersion for RNA-seq data with DESeq2. Genome biology. 2014;15(12):550.

52. Johnson WE, Li C, Rabinovic A. Adjusting batch effects in microarray expression data using empirical Bayes methods. Biostatistics. 2007;8(1):118–27.

53. Leek J, Johnson, WE, Parker, HS, Jaffe, AE, Storey, JD: sva: Surrogate variable analysis. In. R package version 3.10.0.

54. Smyth G. Limma: linear models for microarray data. In: Gentleman R, Carey V, Dudoit S, Irizarry R, Huber W, editors. Bioinformatics and computational biology solutions using R and bioconductor. New York: Springer; 2005. p. 397–420.

55. Soneson C, Delorenzi M. A comparison of methods for differential expression analysis of RNA-seq data. BMC Bioinformatics. 2013;14:91.

56. Edgar R, Domrachev M, Lash AE. Gene Expression Omnibus: NCBI gene expression and hybridization array data repository. Nucleic Acids Res. 2002;30(1):207–10.

57. Hothorn T, Bretz F, Westfall P. Simultaneous inference in general parametric models. Biometrical J Biometrische Zeitschrift. 2008;50(3):346–63.

58. Alexa A, Rahnenfuhrer J, Lengauer T. Improved scoring of functional groups from gene expression data by decorrelating GO graph structure. Bioinformatics. 2006;22(13):1600–7.

59. Supek F, Bosnjak M, Skunca N, Smuc T. REVIGO summarizes and visualizes long lists of gene ontology terms. PLoS One. 2011;6(7):e21800.

CHAPTER 4: STUDY OF PLASMA-DERIVED MIRNAS MIMIC DIFFERENCES

IN HUNTINGTON'S DISEASE BRAIN

Introduction

Huntington's disease (HD) is an autosomal dominant inherited movement disorder, caused by an expanded CAG trinucleotide repeat sequence in the huntingtin gene [1]. The emergence of abnormal, choreiform movements, often accompanied by neurophysiological, psychiatric or cognitive impairments [2], defines disease onset and generally occurs around middle age [3]. Neurodegeneration precedes clinical diagnosis. As many as half of the neurons in the caudate nucleus in the striatum are lost by the onset of motor signs of disease [4], and volumetric changes in the striatum occur as early as two decades prior to predicted onset age [5]. Because motor and cognitive impairments correlate with the neuroanatomical changes in the striatum [6], to prevent neuronal loss and thereby prevent or delay disease onset, therapeutic intervention would ideally occur prior to HD manifestation.

While predictive genetic testing can reliable detect HD, the lack of validated biomarkers for HD progression limits the evaluation of preventive and early-stage disease-modifying therapies. Current progressive measures for prodromal and

early-stage HD patients rely on rating of functional decline, which are susceptible to inter-rater variability and limited sensitivity [2].

Large, multicenter, longitudinal studies comparing large cohorts of asymptomatic HD gene carriers and early-stage HD to healthy controls have used a battery of clinical and neuroimaging based assessments, aimed at identifying robust quantitative measures [7, 8]. These studies, among others, have identified a number of image-based biomarkers that may relate to HD progression, such as morphometric changes [7, 9], elevation in the glial cell marker myo-inositol [10], the reduction in the neuronal integrity marker N-acetyl aspartate [10], and recently, the medium spiny neuron marker PDE10A [11]. Although neuroimaging biomarkers are encouraging, prior to clinical adoption, problems in reproducibility across imaging facilities from technical and analytical inconsistencies must first be addressed [12].

Alternatively, the disease mechanisms that are observed in the brain may be detectable in the blood. Research measuring oxidative stress using 8OHdG levels [13], mutant HTT accumulation [14], inflammatory markers [15], and genome-wide RNA changes [16-18], have uncovered a number of concordant changes between brain and blood. While promising, the clinical utility of these measures is yet to be reported.

Recently, we completed comprehensive evaluations of altered miRNA levels obtained through next-generation sequencing technology in human HD and control prefrontal cortex samples to investigate their role in transcriptional

109

dysregulation in this disease [19]. We identified 75 miRNAs significantly altered in HD and several of these showed significant associations to *HTT* CAG repeat-adjusted age at motor onset, or extent of striatal neuropathological involvement [20], including miR-10b-5p, associated with both. Furthermore, among asymptomatic HD gene carriers, levels of miR-10b-5p were distinguishable from both the low expression observed in normal controls and higher levels seen among symptomatic HD patients, suggesting a relationship between cortical levels of miR-10b-5p and disease stage.

Because brain-derived miRNAs may pass through the blood-brain-barrier by exosome transport [21], and because they are remarkably stable [22], the miRNAs identified in our studies of postmortem brain tissue may be detectable in peripheral fluids [23-25], and thus potentially provide accessible biomarkers for disease stage and rate of progression in clinical trials.

The first step in the evaluation of clinical utility is to determine whether the observed HD brain-related miRNA alterations may also be detected in peripheral samples. To evaluate the biomarker potential for miRNAs, we compared the levels of four miRNAs related to HD clinical features in postmortem brains (miR-10b-5p, miR-486-5p, miR-132-3p, and miR-363-3p) in HD, asymptomatic and healthy control plasma samples.

Methods

Study participants (n=38) were recruited through the Boston University Neurological Associates (BUNA) and Tewksbury State Hospital from 2012-2014,

110

with appropriate IRB approval and consent (Protocol Number H-31052) (**see**

Table 7). No significant differences were observed in the age or sex distribution

between any of the 3 groups (HD cases, asymptomatic HD carriers, and

controls). A trained phlebotomist drew blood by standard practice. BD

Vacutainer CPT Mononuclear Cell Preparation Tubes containing 0.1 mL sodium

citrate anticoagulant and 0.1 M Ficoll medium were used to isolate plasma from 8

mL of whole blood.

Table 7. Summary of the samples used for the study.

Condition	N	Age	Onset age	Gender
Control	8	46.1 ± 13.5		3M, 5F
Asymptomatic HD	4	42.5 ± 28.7		1M, 3F
Manifest HD	26	53.0 ± 8.7	47.6 ± 9.9	11M, 15F

One mL of plasma was used for RNA extraction. To minimize platelet

contamination [26], residual platelets were removed by centrifugation, collecting

supernatant after spinning for 5 min at 16,000 x g. 0.22 um filtration was used to

remove heterogeneous, phospholipid membrane bound microparticles, 0.05-1.5

um in size, shed from platelets and other blood cells [27]. RNA was extracted

using Qiazol and miRNeasy RNA isolation kit from Qiagen, according to

manufacturer's protocol. RNA purity and abundance was assessed by

spectrophotometry.

The four miRNAs included in this study were selected based on the

following criteria: (1) All four were altered at genome-wide significant levels in HD

brain [20] (up in HD: miR-10b-5p, miR-486-5p, miR-363-3p; down in HD: miR-

132-3p). (2) All four were readily abundant in both brain and blood [28], and (3) candidate miRNAs showed nominal association in the cortical study (p<0.05) to CAG-adjusted clinical HD features (onset: miR-10b-5p, miR-486-5p miR-363-3p; striatal neuropathological involvement: miR-10b-5p, miR-132-3p).

Exiqon miRCURY LNA Universal RT miRNA PCR was used to assay miR-10b-5p (cat. 205637), miR-486-5p (cat. 204001), miR-132-3p (cat. 204129), and miR-363-3p (cat. 204726), following the manufacturer's protocol. UniSp6 synthetic spike-in was used to evaluate cDNA efficiency. Following cDNA synthesis, samples were diluted to 0.2 ng/ul in RNAse free water. Both SNORD44 (cat. 203902) and miR-451a (cat. 204737) were used for normalization. For quantitative PCR (qPCR), samples were assayed in triplicate across three 384-well plates, using Applied Biosystems 7900HT Real-Time PCR System. For analysis, threshold cycle (C_T) values for triplicate wells were normalized by average RNU44 and miR-451a values. Extreme outlier wells and samples (standard deviations above 10) were removed. miRNA levels were calculated using the $\Delta\Delta C_T$ method [29].

Linear regression analyses predicting $-\Delta\Delta C_T$ were used to test the association between miRNA levels and disease status in HD cases and controls for the four miRNA. One-tailed tests were used to test the a priori hypothesis of consistent direction of effects as observed in the brain study, thus any relationships inconsistent with the cortical findings would not be identified as significant. Bonferroni correction, assuming four comparisons was applied.

For miR-10b-5p, we further examined the relationship between asymptomatic HD gene carriers and HD cases and controls separately using linear regression, again using a one-tailed test of the previously observed relationships. In addition, cumulative logit models using the "ordinal" package in R [30], were applied to test an ordinal relationship between controls, asymptomatic gene carriers and HD cases using a Chisq likelihood-ratio test. Finally, we examined the relationship of miR-10b-5p to age of motor onset in cases using linear regression.

Results

All four miRNAs were detected in plasma at reasonable levels (miR-10b-5p average C_T= 33.8, miR-132-3p average C_T= 32.4, miR-363-3p average C_T= 32.2, miR-486-5p average C_T= 25.7). After calculating -$\Delta\Delta C_T$, levels of candidate miRNAs in the 26 HD patients were compared to the 8 controls to test whether miRNAs alterations in HD plasma resembled changes in observed in HD brain. We observed increased levels of miR-10b-5p (one-sided p= 6.77e-3, β= 2.39) and miR-486-5p (one-sided p= 0.044, β= 1.44) between HD and control subjects. These changes are consistent with the changes observed in the brain [20] where miR-10b-5p and miR-486-5p were also increased (see Table 8). Levels of miR-132-3p in plasma, though not significant, were lower in HD, consistent with the results in brain (one-sided p = 0.92, β= -0.62). miR-363-3p levels were not altered in blood, nor consistent with changes observed in HD brain (one-sided p = 0.99, β= -7.93e-2).

113

Table 8. Comparison of miR-10b-5p, miR-486-5p, miR-132-3p, and miR-363-3p levels in plasma between control and HD patients.
miR-10b-5p and miR-486-5p are significantly increased in HD blood in same direction as changes observed in HD brain. miR-132-5p and miR-363-3p were not altered in HD blood.

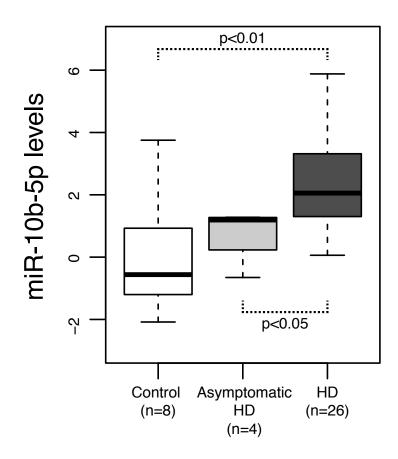| miRNA	Bonferroni corrected one-sided q-value	$-\Delta\Delta C_T$ beta	Direction of effect blood to brain
miR-10b-5p	0.0068	2.39E+00	+ / +
miR-486-5p	0.044	1.44E+00	+ / +
miR-132-3p	0.92	-6.22E-01	- / -
miR-363-3p	0.2	-7.93E-02	- / +

One of the four candidate miRNAs, miR-10b-5p, also showed significant association to age at motor onset and to disease stage in the brain study. Therefore, we focused next on miR-10b-5p and its relationship to HD symptomology. We did not see consistency in the relationship between miR-10b-5p and onset age in blood (one-sided p= 0.99, positive effect) compared to that observed in HD brain (negative effect) although a positive association of miR-10b-5p levels in blood to onset age, opposite to that seen in brain, may exist (two-sided p=3.20e-3, beta=0.13).

Although there was no statistical difference between asymptomatic HD patients and controls in miR-10b-5p levels, (one-sided p= 0.24, β= 0.53), miR-10b-5p levels were significantly elevated from asymptomatic gene carriers to HD patients (one-sided p= 0.049, β= 1.15), and on average, miR-10b-5p levels were lowest in control subjects (mean=0.00), higher in asymptomatic HD gene carriers

(mean=0.75), and highest in HD patients (mean=2.38). Using a cumulative

logistic regression to test the ordinal relationship of miRNA levels between

controls, asymptomatic HD gene carriers and manifest HD patients found a

significant positive association with miR-10b-5p levels (one-sided p= 2.05e-4,

cumulative OR =2.27) (**see Figure 15**), concordant with the direction of the effect

observed in HD prefrontal cortex.

Figure 15. miR-10b-5p has an ordinal association with HD stage.
Boxplot of miR-10b-5p levels (-$\Delta\Delta$Ct) for control (in white), asymptomatic HD
gene carrier (in grey), and manifest HD (in black) subjects. miR-10b-5p had a
significant, upward, ordinal association to disease stage (one-sided p= 2.05e-4,
cumulative OR =2.27). Regression analysis revealed differences between
asymptomatic and HD patients (one-sided p= 0.049, β= 1.15), and differences
between controls and HD (p= 3.39e-3, Bonferroni-corrected one-sided p= 6.77e-
3, β= 2.39), but not difference between controls and asymptomatic HD patients
(one-sided p= 0.24, β= 0.53).

Discussion

The results from this study confirm that two candidate miRNAs, miR-10b-5p and miR-486-5p, are increased in both brain and blood in HD. Levels of miR-10b-5p were significant elevated HD patients compared to asymptomatic HD gene carriers, and while the miR-10b-5p were not significantly different in asymptomatic subjects compared to controls, the ordinal relationship of controls, asymptomatic HD and manifest HD suggest premanifest HD miRNAs changes may exist.

In a previous study, miR-34b was observed significantly increased in both an HD cell model and in plasma from premanifest HD patient [31]. However, miR-34b alterations were not detected in early or late-stage HD and we did not observe a relationship of this miRNA to HD in brain, so it is difficult to interpret the utility of this finding [20].

While we believe our study is beneficial for clinical biomarker discovery, but because of study design limitations, it should be interpreted as a proof-of-concept experiment. We believe increasing our sample size will provide the statistical power for detection of asymptomatic HD gene carriers and controls miR-10b-5p differences. More importantly, our study requires an independent validation. Research of the DNA damage marker, 8-OHdG, in blood, and its relationship to HD progression [13, 32] highlights the importance of biomarker validation, as recent studies have yet to reproduce these results [32].

Commonly, the inherit variation of data from human samples, coupled with the lack of standardization in biological procedures, results in failed cross-validation. To minimize technical inconsistencies due to the vanishingly small RNA quantity in plasma [28], RNA can be directly measured using with RNA extraction-free protocols. Firefly Bioworks, which allows for the multiplex analysis of up to 68 miRNAs, as well as recent advancements in extraction-free, low input, library preparation protocols for miRNA-sequencing, may aid in the orthogonal validation of potential miRNA biomarkers. Moreover, these assays allow for larger input normalization panels (as opposed to miR-451a/SNORD44), as well

as the measurement of miRNA alterations that were detected in HD prefrontal

cortex that could not be assessed in this study [20].

A longitudinal study of miR-10b-5p is critical for assessing the relationship

of miRNA levels to disease progression within the same subjects, as evaluated

by motor and cognitive sections of United Huntington's Disease Ratings Scale

(UHDRS). The relationship of miRNA levels to functional ratings may be

potentially confounded by CAG repeat length, as we observed a relationship of

CAG repeat length to miR-10b-5p levels in brain. Therefore, to establish accurate

prediction of progressive based on miRNA levels, statistical correction of the

CAG length should be applied.

Blood-based biochemical assays are minimally invasive and relatively

simple compared to neuroimaging-based diagnostics. Here, we demonstrate the

strength of this study and overall approach, built from alterations observed in HD

cortex. The miRNA differences in HD blood may resemble changes observed in

HD brain, which provides greater feasibility that these alterations are

representative of the disease process, rather than physiological response to HD-

associated weight loss, which is independent to neurodegeneration and other

disease features [33].

References

1.   Paulsen JS, Long JD, Johnson HJ, Aylward EH, Ross CA, Williams JK, Nance MA, Erwin CJ, Westervelt HJ, Harrington DL et al: Clinical and Biomarker Changes in Premanifest Huntington Disease Show Trial Feasibility: A Decade of the PREDICT-HD Study. Frontiers in aging neuroscience 2014, 6:78.

2.   Vonsattel JP, Myers RH, Stevens TJ, Ferrante RJ, Bird ED, Richardson EP, Jr.: Neuropathological classification of Huntington's disease. J Neuropathol Exp Neurol 1985, 44(6):559-577.

3.   Hoss AG, Kartha VK, Dong X, Latourelle JC, Dumitriu A, Hadzi TC, Macdonald ME, Gusella JF, Akbarian S, Chen JF et al: MicroRNAs located in the Hox gene clusters are implicated in huntington's disease pathogenesis. PLoS Genet 2014, 10(2):e1004188.

4.   Hoss AG, Labadorf A, Latourelle JC, Kartha VK, Hadzi TC, Gusella JF, MacDonald ME, Chen J-F, Akbarian S, Weng Z et al: miR-10b-5p expression in Huntington's disease brain relates to age of onset and the extent of striatal involvement. BMC medical genomics 2015, 8:10.

5.   Weir DW, Sturrock A, Leavitt BR: Development of biomarkers for Huntington's disease. Lancet neurology 2011, 10(6):573-590.

6.   Hersch SM, Rosas HD: Biomarkers to Enable the Development of Neuroprotective Therapies for Huntington's Disease. In: Neurobiology of Huntington's Disease: Applications to Drug Discovery. edn. Edited by Lo DC, Hughes RE. Boca Raton (FL); 2011.

7.   Song SJ, Poliseno L, Song MS, Ala U, Webster K, Ng C, Beringer G, Brikbak NJ, Yuan X, Cantley LC et al: MicroRNA-antagonism regulates breast cancer stemness and metastasis via TET-family-dependent chromatin remodeling. Cell 2013, 154(2):311-324.

8.   Lu M, Zhang Q, Deng M, Miao J, Guo Y, Gao W, Cui Q: An analysis of human microRNA and disease associations. PLoS One 2008, 3(10):e3420.

9.   Sassen S, Miska EA, Caldas C: MicroRNA: implications for cancer. Virchows Archiv : an international journal of pathology 2008, 452(1):1-10.

10.   Unified Huntington's Disease Rating Scale: reliability and consistency. Huntington Study Group. Movement disorders : official journal of the Movement Disorder Society 1996, 11(2):136-142.

11.   Cheng HH, Yi HS, Kim Y, Kroh EM, Chien JW, Eaton KD, Goodman MT, Tait JF, Tewari M, Pritchard CC: Plasma processing conditions substantially influence circulating microRNA biomarker levels. PLoS One 2013, 8(6):e64795.

12.   Simak J, Gelderman MP: Cell membrane microparticles in blood and blood products: potentially pathogenic agents and diagnostic markers. Transfusion medicine reviews 2006, 20(1):1-26.

13.   Burgos KL, Javaherian A, Bomprezzi R, Ghaffari L, Rhodes S, Courtright A, Tembe W, Kim S, Metpally R, Van Keuren-Jensen K: Identification of extracellular miRNA in human cerebrospinal fluid by next-generation sequencing. Rna 2013, 19(5):712-722.

14.   Livak KJ, Schmittgen TD: Analysis of relative gene expression data using real-time quantitative PCR and the 2(-Delta Delta C(T)) Method. Methods 2001, 25(11846609):402-408.

CHAPTER 5: DISTINCT MICRORNA ALTERATIONS OBSERVED IN PARKINSON'S DISEASE PREFRONTAL CORTEX

Abstract

Objective. The goal of this study was to examine the microRNA (miRNA) profile of Parkinson's disease (PD) frontal cortex as compared to normal control brain, allowing for the identification of PD specific signatures as well as the study of disease-related phenotypes, such as onset age or dementia.

Methods. Small RNA sequence analysis was performed from prefrontal cortex for 29 PD samples and 33 control samples. After sample QC, normalization and batch correction, linear regression was used to identify miRNAs altered in PD, and a PD classifier was developed using weighted voting class prediction. The relationship of miRNA levels to onset age and PD with dementia (PDD) was also characterized in case-only analyses.

Results. 125 miRNAs were differentially expressed in PD at a genome-wide level of significance (FDR q<0.05). A set of 29 miRNAs classified PD from non-diseased brain (93.9% specificity, 96.6% sensitivity). The majority of differentially expressed miRNAs (105/125) showed an ordinal relationship from control, to PD without dementia (PDN), to PDD. Among PD brains, 36 miRNAs classified PDD from PDN (sensitivity =81.2%, specificity =88.9%). Among

differential expressed miRNAs, miR-10b-5p had a positive association with onset age (q=4.7e-2).

Conclusions. Based on cortical miRNA levels, PD brains were accurately classified from non-diseased brains. Additionally, the PDD miRNA profile exhibited a more severe pattern of alteration among those differentially expressed in PD. To evaluate the clinical utility of miRNAs as potential clinical biomarkers, brain-related miRNA alterations, in particular, miR-10b-5p, must be further characterized and tested in peripheral biofluids.

Introduction

Parkinson's disease (PD) is a progressive movement disorder, characterized clinically by resting tremor, rigidity, bradykinesia and postural instability [1]. Motor symptoms are accompanied by the loss of dopamine-producing neurons in the substantia nigra pars compacta, and associated with widespread deposition of cytoplasmic protein inclusions, largely composed of insoluble α-synuclein, throughout the brain [2].

PD subtypes can be separated based on distinct, clinical phenotypes. Approximately one-third of patients experience dementia (PDD), which has significant ramifications for quality of life and burden of care [3, 4]. Additionally, there is wide variation in the age of motor onset (ranging from age 20 to age 90) [5], with young-onset occurring before age 50 and representing 5-10% of PD cases [6]. While neuropathological hallmarks contribute to the degeneration of the nigrostriatal dopaminergic system, the etiology, clinical heterogeneity and

fundamental pathological mechanisms by which preferential neuronal loss occurs in PD are largely unknown.

The microRNA (miRNA) profile of diseased brains may offer insight into the molecular and pathological mechanisms that occur in PD. miRNAs are short, noncoding RNAs that inhibit translation through sequence-specific binding of the 3'-untranslated region (3'UTR) of target messenger RNAs (mRNAs). miRNAs can transcriptionally regulate a set or multiple sets of genes simultaneously, and in the brain, their regulatory effects have profound effects on neuronal development, differentiation and maturation [7]. Deregulation of miRNAs has been implicated in neurodegenerative diseases [8], and several studies suggest miRNAs may impact PD pathogenesis [9, 10].

In this study, we performed genome-wide miRNA sequencing of 29 PD cases and 33 neuropathologically-normal controls from prefrontal cortex. As opposed to microarray technologies that can only detect specific sequences that have been chosen *a priori*, high-throughput sequencing provides a relatively unbiased quantification of miRNA molecule abundance. We compared miRNA levels between PD and controls and based on their miRNA profile, classified PD from non-diseased brains. Among the PD brains, we identified miRNAs associated with the presence or absence of dementia and age of motor onset, as well as identified a set of miRNAs altered in both PD and Huntington's disease, which may be relevant to the pathological processes that occur in the PD brain.

Methods

Sample information and small RNA sequencing. Frozen brain tissue from prefrontal cortex Brodmann Area 9 (BA9) for 29 PD samples and 33 control samples was obtained from the Banner Sun Health Research Institute, Sun City, Arizona [11], Harvard Brain and Tissue Resource Center McLean Hospital Belmont MA, and Human Brain and Spinal Fluid Resource Center VA West Los Angeles Healthcare Center, Los Angeles, CA. PD samples had no evidence of Alzheimer's disease comorbidity based on neuropathological examination. Sample information can be found in Table S1 and summarized in Table 1. The medical charts of all 29 PD samples were reviewed to obtain information regarding clinical diagnoses of dementia (PDD n=11, no evidence of dementia (PDN) =18). 21 subjects had information on the age of onset of motor symptoms. All samples were male. Differences in covariates were tested assuming unequal variance. No difference in postmortem interval (PMI) (*p*-value =0.10) or RNA integrity number (*p*-value = 0.08) was observed between PD and controls. PD and controls differed in ages at death (PD mean age = 77.6, control mean age = 68.1; *p*-value = 3.2e-3). Potential confounding by age at death was assessed in subsequent analyses. PDN and PDD samples did not differ in PMI (*p*-value =0.62), RNA integrity number (*p*-value =0.27), age at onset (*p*-value =0.24), duration (*p*-value =0.44), or age at death (*p*-value =0.28).

Total RNA was isolated using QIAzol Lysis Reagent and purified using miRNeasy MinElute Cleanup columns. Samples were prepared using Illumina's

TruSeq Small RNA Sample Prep Kit, according to the manufacturer's protocol,

and sequenced on Illumina's HiSeq 2000 system with 1x51nt single-end reads at

Tufts University and the Michigan State sequencing core facility.

Table 9. Summarized sample information.

Ages at death were significantly different between controls and PD, as indicated
(** $p<0.01$ compared to controls). No differences between PDN and PDD were
observed.

Type	N	Motor Onset	Disease duration	Age at death	Post mortem interval	RNA integrity number
Control	33			68.1 ± 14.8	15.0 ± 8.7	7.6 ± 0.7
All diagnosed PD	29	66.5 ± 9.8	10.5 ± 6.5	77.6 ± 9.0 **	11.1 ± 9.7	7.3 ± 0.7
PD, Non demented	18	64.1 ± 7.2	11.5 ± 6.4	76.1 ± 8.9	11.9 ± 9.2	7.2 ± 0.8
PD with dementia	11	69.8 ± 12.2	9.2 ± 6.7	79.9 ± 9.0	9.9 ± 10.9	7.5 ± 0.5

Statistical analysis. Reads were processed and counted as described in

Hoss et al. 2015 [12]. R version 3.1.0, Bioconductor version 2.1.4, and DESeq2

version 1.40.0 were used for variance stabilizing transformation (VST) of count

data. Batch correction was applied using ComBat using sva 3.10 [13] and LIMMA

version 3.20.8 [14] was used for differential expression analysis of PD cases and

controls. All PD samples were from a single batch, therefore DESeq2

normalized, VST counts from PD samples without batch correction were used for

the PD-only analyses relating miRNA levels to clinical features. Differential

expression analysis was performed with and without adjustment for age at death.

After multiple comparisons correction using a false discovery rate [15], FDR-

adjusted *q*-values<0.05 were reported as significant.

To further evaluate the differential expression patterns between PD cases and controls, unsupervised, Ward hierarchical clustering by Euclidian distance was applied using the heatmap2 function in the gplots R package [16]. Supervised, predictive modeling of case status was performed using the GenePatterns WeightedXVoting module using 29 PD-associated miRNAs with large effects [17].

To determine if miRNAs were associated with PD in the presence or absence of dementia, VST counts for PDN and PDD were compared using LIMMA, adjusting for age at death, and p-values were FDR-adjusted for the number of comparisons. miRNAs nominally associated with PDD were used to classify PD patients with and without dementia, as described above, using the weighted voting method. To determine beta estimates relative to control samples, PDN and PDD were separately compared to controls using LIMMA. In addition, cumulative logit models using the "ordinal" package in R [18], were applied to test whether an ordinal relationship existed across control, PDN and PDD samples. FDR-corrected Chisq likelihood-ratio tests were used to determine significant miRNA associations.

Linear models were used to model the relationship between age of motor onset and miRNA levels among the 21 PD samples with onset data. Tests were performed genome-wide and exclusively among the set of differentially expressed miRNAs. FDR-adjusted q-values<0.05 were reported. Models were run with and without adjustment for age at death.

126

Finally, to determine whether overlap in miRNA alterations exist between PD and HD brain, results from PD differential expression analysis were compared to those of our previously published Huntington's disease (HD) study [12], which contain the same control brains. HD data was accessed from NCBI's Gene Expression Omnibus, series accession number GSE64977 (http://www.ncbi.nlm.nih.gov/geo/query/acc.cgi?acc=GSE64977) and analyzed using the same bioinformatics approach for differential expression analysis as described above (Bioconductor version 2.1.4, DESeq2 version 1.40.0, ComBat sva 3.10, LIMMA version 3.20.8).

Results

miRNA levels are altered in Parkinson's disease compared to non-disease brains. To identify miRNA differences in PD as compared to non-disease subjects, miRNA sequence analysis was performed in prefrontal cortex (Brodmann Area 9) for 33 controls and 29 idiopathic PD samples (see Table 1). Results of differential expression analyses, correcting for sequencing batch effects and with and without adjustment for age at death are shown in Table S2. 125 miRNAs were significantly altered in PD after adjusting for age at death (FDR *q*-value<0.05, see Table S2). Unadjusted results were similar, but confounding by age of death was observed for some miRNA, so adjusted results are reported here. Most miRNA alterations were moderate, with 77% of the differentially abundant miRNAs (96/125) within a ±0.5 log fold change (LFC).

The levels of 64 miRNAs were down-regulated, whereas the levels of 61 miRNAs were up-regulated in PD relative to controls.
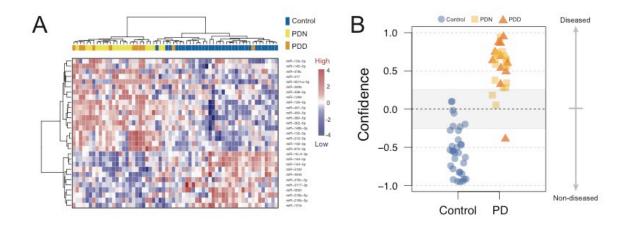
Next, we used classification models to investigate whether the levels of PD-related miRNAs in brain could accurately assign disease status. To select the most informative miRNAs, we filtered on effect size (LFC>0.5 or LFC< -0.5). After filtering, 29 PD-related miRNAs were used in an unsupervised hierarchical cluster analysis. Samples clustered based on disease status with the exception of five PD which clustered with the controls, (see Figure 16A). To further assess whether miRNA levels could differentiate PD and control samples, disease status was predicted using a weighted voting classification with leave-one-out cross-validation. This model is tested by iteratively leaving one sample out, creating a training model by assigning a weighted linear combination based on the levels of the 29 miRNAs, and testing this model on the left out sample. Here, only three errors were observed using 29 miRNAs (two Type I errors, one Type II error), with 93.9% specificity, 96.6% sensitivity and an absolute error rate of 4.8% (see Figure 16B). Both Type I errors were called with low confidence (9.8-10.1%).

miRNA alterations in Parkinson's disease with dementia. To assess whether miRNA differences specific to the PDD subtype were distinguishable from a generalized PD response, we performed a differential expression analysis comparing PDN to PDD using normalized VST count data from 18 PDN and 11 PDD samples. We observed no genome-wide significant (q<0.05) miRNAs associated with dementia in PD, with or without adjustment for age or disease

duration, after multiple correction testing (<mark>see Table S3</mark>). Even when limiting to

the 125 differential expressed miRNAs we saw no significant differences

between PDN and PDD. We however noted stronger directions of effect in PDD

when separately comparing PDN versus control and PDD versus control,

suggesting PDD may represent a more severe version of the PD miRNA profile

spectrum.

Figure 16. miRNA changes related to Parkinson's disease.
A. Heatmap of 29 miRNAs differentially expressed between PD and control prefrontal cortex samples with log fold changes (LFC) greater than 0.5 or less than -0.5. Scaled level values are color-coded according to the legend on the right. The dendrogram on the left depicts hierarchical clustering based on level. The top dendrogram depicts clustering based on the miRNA signal from each sample. The top bar indicates disease status (blue: control, yellow: PD, non-demented (PDN), orange: PD with dementia (PDD)). **B.** Disease prediction using 29 miRNAs. Scores less than zero were called as non-diseased whereas scores above zero were called as PD. Blue circles =control, yellow boxes =PD, orange triangles = PDN.
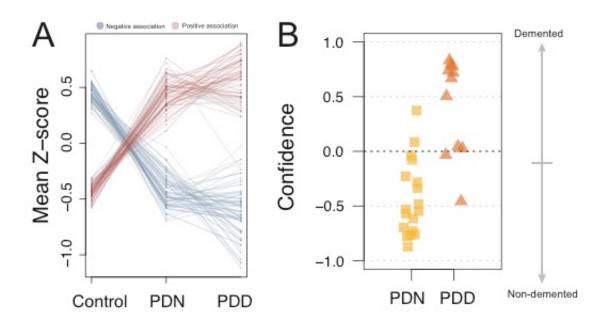
To test whether PDD had increased miRNA alterations in comparison to PDN, we created an ordered categorical variable (controls, PDN, and PDD) and tested the association of this variable to genome-wide miRNA levels. 105 of the 125 differentially expressed miRNAs had a significant ordinal association ($q<0.05$) **(see Table S4, and Figure 2A),** indicating that in the majority of differentially expressed miRNAs in PD, PDD samples exhibit larger differences than PDN cases as compared to controls for the same miRNAs.

Figure 17. miRNA profile for Parkinson's disease with dementia.
A. Line plot for the 125 DE miRNAs in PD. The counts were scaled using Z-transformation, and the means were calculated for each miRNA for each condition (control, PDN, PDD). The line colors correspond to the beta estimates from the ordinal regression analysis, where blue=negative ordered relationship and red=positive ordered relationship. **B.** PDN/PDD class prediction, using the 36 nominally significant miRNAs from PDN/PDD differential expression analysis. Four errors were observed among the 29 samples studied.

We further investigated the clinical utility of these miRNA profiles for the assessment of dementia using classification analyses (WeightedXVoting) [17].

The 36 nominally significant miRNAs (p<0.05) identified in the PDN/PDD

comparison from LIMMA were used to classify disease state (See Figure 2B),

though with more limited accuracy than the PD-control model (absolute error rate

=13.8%, sensitivity =81.2%, specificity =88.9%). Four miRNA features overlap

between the control/PD and PDN/PDD models (miR-132-3p, hsa-miR-132-5p,

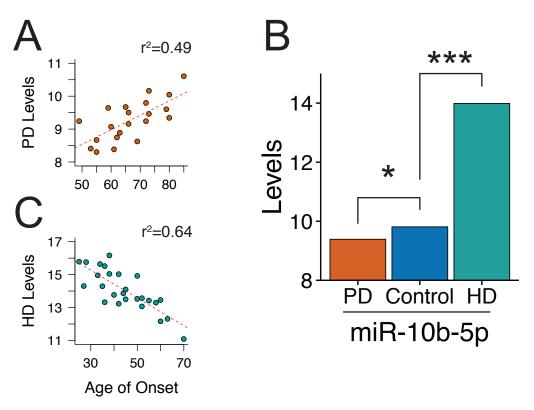hsa-miR-145-5p, hsa-miR-212-5p).

miR-10b-5p levels are associated with the onset of motor symptoms

in both Parkinson's and Huntington's disease. To understand whether

deregulated miRNAs were specific to PD, or a general response to the

neurodegenerative process, we compared miRNA that were significantly altered

in PD to those significantly altered in Huntington's disease (HD). 21 miRNAs

were found differentially expressed in both PD and HD experiments, and of

these, only two miRNAs had opposite directions of effect between diseases

(miR-10b-5p, miR-320b).

Within the PD case sample, we tested the association of age of motor

onset of PD with miRNA levels. Although we did not observe significance in a

genome-wide analysis, restricting our study to the 125 significantly differentially

abundant PD miRNAs revealed miR-10b-5p to have a significant, positive

association to onset age (beta=0.040, *q*-value=4.7e-2, model r^2=0.49, **see**

Figure 3A). Adding death age increased the magnitude of the effect estimate

(death adjusted age of onset beta=0.049, *p*-value onset =3.2e-3, *p*-value death

=0.40), although did not stand up to multiple comparisons corrections (q-value

onset =0.19). While miR-10b-5p is significantly decreased in PD, miR-10b-5p

was observed in our previous HD cortical miRNA study [19] to be massively

increased in HD in comparison to controls (<mark>see Figure</mark> 3B). Intriguingly, PD and

HD also exhibit opposite effects with regard to onset age, where miR-10b-5p has

a strong, negative relationship to age of onset in HD (r^2=0.64; $r^{2=}$0.39 after

accounting for the contribution of HD gene repeat length) and a strong, positive

effect in PD (<mark>see Figure</mark> 3C).

Figure 18. miR-10b-5p levels are associated with motor onset age in both Parkinson's and Huntington's disease.
A. Comparison of miR-10b-5p level in PD and HD. *q<0.05, **q<0.01, ***q<0.001, p-values adjusted for genome-wide comparisons. **B.** Scatterplot of miR-10b-5p levels to motor onset age in Parkinson's disease (PD). In PD, miR-10b-5p levels exhibit a positive association to onset. **C.** Scatterplot of miR-10b-5p levels to motor onset age in Huntington's disease (HD). In HD, miR-10b-5p levels exhibit a negative association to onset.

Discussion

Parkinson's disease related miRNAs. In this study, we identified 125 miRNAs altered at genome-wide levels in PD prefrontal cortex using next-generation sequencing. This is the largest miRNA sequencing analysis performed in PD versus control brain samples (29 versus 33 respectively), the first to provide a detailed miRNA PD profile, classify brains by miRNA levels and to evaluate the relationship of miRNA levels in brain to relevant clinical features.

Reduced levels of miR-133b [9], miR-34b and miR-34c [20], and elevated levels of autophagy-related miRNAs, were previously reported [21], and while these miRNAs were detectable in our study, we did not observe significant changes in their levels. These discrepancies are likely a consequence of the different brain regions that were studied (midbrain versus prefrontal cortex), and the assay technologies that were used to profile miRNA levels (reverse transcriptase quantitative PCR [9, 21], and microarray [20] versus miRNA-sequencing).

Several miRNAs that we report altered in PD brain may interact with PD-related genes. Monogenic forms of PD include mutations within the α-synuclein gene (*SNCA*), Leucine-rich Repeat Kinase 2 (*LRRK2*), one of the most common causes of familial PD [22] and glucocerebrosidase (*GBA*). While we did not observe alterations of *SNCA*-targeting miRNAs, miR-7 and miR-153 [23, 24], two miRNAs shown be regulated by *LRRK2* (let-7i-3p/5p and miR-184 [10]) and one

133

miRNA experimentally shown to target *LRRK2* expression (miR-1224 [25]), were observed to be down-regulated in PD.

Glucocerebrosidase (GBA) deficiency is associated with PD [26]. We observed miR-127-5p, which has been shown to reduce GBA activity [27], to be down-regulated in PD brains, and miR-16-5p which has been shown to correspond to enhanced GBA protein levels [27], was found to up-regulated in brain in our study. It is noteworthy to observe *LRRK2*-related miRNAs, as none of the PD brains in our study had *LRRK2* mutations. This may support a role of *LRRK2* and *GBA* in PD, independent of that produced by the known mutations in these genes.

Classification based on miRNA abundance. We were able to classify PD based on the levels of 29 miRNAs with less than a 5% error rate. Although this classification was performed using postmortem brain samples, we believe this may be relevant for PD biomarker discovery, particularly if these miRNAs are peripherally detectable. We reasonably differentiated PD subtypes (PDN/PDD) based on miRNA levels, and we observed a pattern of increased changes in the PDD samples relative to the PDN samples in the set of altered miRNAs. We observed that the majority of differentially expressed miRNAs had an ordinal relationship to controls and PD cases stratified by the presence or absence of dementia, suggesting PDD may represent a more severe alteration of the PD miRNA profile.

PD-related miRNA changes in biofluids. Our study in PD brains identified profiles of miRNAs that distinguish PD from controls, which if also observed in peripheral biofluids, such as blood or cerebrospinal fluid (CSF), could be valuable in the evaluation of PD diagnosis, prognosis, or progression. The small size (~22 nucleotides) of miRNA may allow for neuropathologically altered miRNA to cross the blood-brain barrier in exosomes [28] and circulate stably in peripheral fluids as cell-free molecules [29]. Although there was no overlap of miRNAs in brain to changes observed in most PD blood studies [30-34], we did observe increased levels in one (miR-29a-3p) of three miRNAs previously reported as increased in blood of PD patients after Levodopa treatment [35]. In Burgos et al. 2014, small RNA sequencing was performed for blood serum and CSF from 67 PD and 78 control subjects [36], five miRNAs were found significantly altered in PD serum and 17 were significantly altered in CSF. Of these 22 miRNAs, five showed consistent overlap with our cortical findings, with one from serum (miR-1294) and four from CSF (miR-132-5p, miR-127-3p, miR-212-3p, miR-1224-5p). Thus, miRNAs detected in CSF may have a stronger relationship with brain miRNAs levels than those detected in serum.

Common miRNA changes in PD and HD. We previously reported 75 miRNAs altered in HD prefrontal cortex [12], and when comparing miRNAs altered in both PD and HD, 21 miRNAs were observed deregulated in both diseases. Among the miRNAs with concordant changes in PD and HD, a several miRNAs correlated with various HD clinical features, such as the extent of striatal

degeneration and duration of the disease [12]. These miRNAs may represent a generalized, neurodegenerative response in the prefrontal cortex, which relate to severity and/or progression across these diseases. However, it is important to recognize that the results from the PD and HD studies are not independent, as they were both analyzed using the same 33 control brains.

Of the two miRNAs with discordance between PD and HD, miR-10b-5p emerged due its relationship to onset in both diseases. miR-10b-5p is markedly increased in HD in comparison to controls, and has a negative association to age of onset for HD, with higher levels of miR-10b-5p corresponding early onset age. In contrast, miR-10b-5p is significantly decreased in PD, and has a positive association to onset age, where higher miRNA levels correspond to later onset ages. In a separate Alzheimer's disease (AD) study, examining miRNA levels in prefrontal cortex, miR-10b-5p levels were significantly reduced in AD [37]. However, at the very earliest stages of AD, miR-10b-5p levels clustered with up-regulated miRNAs whereas at early to middle stages, miR-10b-5p levels appeared to decline [37]. The relationship of miR-10b-5p to these three age-related, neurodegenerative diseases suggests a complicated pattern of miR-10b-5p alteration in response to the neurodegenerative or pathologic protein aggregation processes.

Conclusion

This study provides evidence that miRNA levels are altered in PD prefrontal cortex. These changes are sufficiently consistent that diseased brains

can be discriminated with high confidence from non-diseased brains based on the level of 29 miRNAs. PDD may represent a more severe profile of PD related miRNAs than PDN. 21 miRNAs changes were similar between PD and HD, with the exception of miR-10b-5p, which had opposite direction of effects to disease association and to motor onset age in the two diseases. Further characterization of miR-10b-5p in the neurodegenerative disease context is warranted to better understand if it has clinical potential as a biomarker for disease progress or to identify potential therapeutic targets.

References

1. Damier P, Hirsch EC, Agid Y, Graybiel AM: **The substantia nigra of the human brain. II. Patterns of loss of dopamine-containing neurons in Parkinson's disease**. *Brain : a journal of neurology* 1999, **122 (Pt 8)**:1437-1448.
2. Spillantini MG, Crowther RA, Jakes R, Hasegawa M, Goedert M: **alpha-Synuclein in filamentous inclusions of Lewy bodies from Parkinson's disease and dementia with lewy bodies**. *Proc Natl Acad Sci U S A* 1998, **95**(11):6469-6473.
3. Edwards TL, Scott WK, Almonte C, Burt A, Powell EH, Beecham GW, Wang L, Zuchner S, Konidari I, Wang G *et al*: **Genome-wide association study confirms SNPs in SNCA and the MAPT region as common risk factors for Parkinson disease**. *Ann Hum Genet* 2010, **74**(2):97-109.
4. Breteler MM, de Groot RR, van Romunde LK, Hofman A: **Risk of dementia in patients with Parkinson's disease, epilepsy, and severe head trauma: a register-based follow-up study**. *American journal of epidemiology* 1995, **142**(12):1300-1305.
5. Schrag A, Ben-Shlomo Y, Brown R, Marsden CD, Quinn N: **Young-onset Parkinson's disease revisited--clinical features, natural history, and mortality**. *Movement disorders : official journal of the Movement Disorder Society* 1998, **13**(6):885-894.
6. Golbe LI: **Young-onset Parkinson's disease: a clinical review**. *Neurology* 1991, **41**(2 (Pt 1)):168-173.
7. O'Carroll D, Schaefer A: **General principals of miRNA biogenesis and regulation in the brain**. *Neuropsychopharmacology* 2013, **38**(1):39-54.
8. Chan AW, Kocerha J: **The Path to microRNA Therapeutics in Psychiatric and Neurodegenerative Disorders**. *Front Genet* 2012, **3**:82.

9.   Kim J, Inoue K, Ishii J, Vanti WB, Voronov SV, Murchison E, Hannon G, Abeliovich A: **A MicroRNA feedback circuit in midbrain dopamine neurons**. *Science* 2007, **317**(5842):1220-1224.

10.   Gehrke S, Imai Y, Sokol N, Lu B: **Pathogenic LRRK2 negatively regulates microRNA-mediated translational repression**. *Nature* 2010, **466**(7306):637-641.

11.   Beach TG, Sue LI, Walker DG, Roher AE, Lue L, Vedders L, Connor DJ, Sabbagh MN, Rogers J: **The Sun Health Research Institute Brain Donation Program: description and experience, 1987-2007**. *Cell and tissue banking* 2008, **9**(3):229-245.

12.   Hoss AG, Labadorf A, Latourelle JC, Kartha VK, Hadzi TC, Gusella JF, MacDonald ME, Chen J-F, Akbarian S, Weng Z *et al*: **miR-10b-5p expression in Huntington's disease brain relates to age of onset and the extent of striatal involvement**. *BMC medical genomics* 2015, **8**:10.

13.   Johnson WE, Li C, Rabinovic A: **Adjusting batch effects in microarray expression data using empirical Bayes methods**. *Biostatistics* 2007, **8**(1):118-127.

14.   Smyth G: **Limma: linear models for microarray data**. In: *Bioinformatics and Computational Biology Solutions Using R and Bioconductor.* Edited by Gentleman R, Carey, V, Dudoit, S, Irizarry, R, Huber, W. New York: Springer; 2005: 397-420.

15.   Benjamini Y, Hochberg Y: **Controlling the False Discovery Rate - a Practical and Powerful Approach to Multiple Testing**. *J Roy Stat Soc B Met* 1995, **57**(1):289-300.

16.   Warnes G, Bolker B, Bonebakker I, Gentleman R, Huber W, Liaw A, Lumley T, Maechler M, Magnusson A, Moeller S *et al*: **gplots: Various R Programming Tools for Plotting Data**. In*.* Edited by R, package version 2.16.0 edn; 2015.

17.   Reich M, Liefeld T, Gould J, Lerner J, Tamayo P, Mesirov JP: **GenePattern 2.0**. *Nature genetics* 2006, **38**(5):500-501.

18.   Christensen RHB: **Regression Models for Ordinal Data**. *R package version 20151-21* http://wwwcranr-projectorg/package=ordinal/ 2015.

19.   Hoss AG, Kartha VK, Dong X, Latourelle JC, Dumitriu A, Hadzi TC, Macdonald ME, Gusella JF, Akbarian S, Chen JF *et al*: **MicroRNAs located in the Hox gene clusters are implicated in huntington's disease pathogenesis**. *PLoS Genet* 2014, **10**(2):e1004188.

20.   Minones-Moyano E, Porta S, Escaramis G, Rabionet R, Iraola S, Kagerbauer B, Espinosa-Parrilla Y, Ferrer I, Estivill X, Marti E: **MicroRNA profiling of Parkinson's disease brains identifies early downregulation of miR-34b/c which modulate mitochondrial function**. *Hum Mol Genet* 2011, **20**(15):3067-3078.

21.   Alvarez-Erviti L, Seow Y, Schapira AH, Rodriguez-Oroz MC, Obeso JA, Cooper JM: **Influence of microRNA deregulation on chaperone-**

mediated autophagy and alpha-synuclein pathology in Parkinson's disease. *Cell death & disease* 2013, **4**:e545.

22.   Nalls MA, Pankratz N, Lill CM, Do CB, Hernandez DG, Saad M, DeStefano AL, Kara E, Bras J, Sharma M *et al*: **Large-scale meta-analysis of genome-wide association data identifies six new risk loci for Parkinson's disease**. *Nature genetics* 2014, **46**(9):989-993.

23.   Doxakis E: **Post-transcriptional regulation of alpha-synuclein expression by mir-7 and mir-153**. *J Biol Chem* 2010, **285**(17):12726-12734.

24.   Junn E, Lee KW, Jeong BS, Chan TW, Im JY, Mouradian MM: **Repression of alpha-synuclein expression and toxicity by microRNA-7**. *Proc Natl Acad Sci U S A* 2009, **106**(31):13052-13057.

25.   Sibley CR, Seow Y, Curtis H, Weinberg MS, Wood MJ: **Silencing of Parkinson's disease-associated genes with artificial mirtron mimics of miR-1224**. *Nucleic Acids Res* 2012, **40**(19):9863-9875.

26.   Aharon-Peretz J, Rosenbaum H, Gershoni-Baruch R: **Mutations in the glucocerebrosidase gene and Parkinson's disease in Ashkenazi Jews**. *N Engl J Med* 2004, **351**(19):1972-1977.

27.   Siebert M, Westbroek W, Chen YC, Moaven N, Li Y, Velayati A, Saraiva-Pereira ML, Martin SE, Sidransky E: **Identification of miRNAs that modulate glucocerebrosidase activity in Gaucher disease cells**. *RNA Biol* 2014, **11**(10):1291-1300.

28.   Kalani A, Tyagi A, Tyagi N: **Exosomes: mediators of neurodegeneration, neuroprotection and therapeutics**. *Molecular neurobiology* 2014, **49**(1):590-600.

29.   Mitchell PS, Parkin RK, Kroh EM, Fritz BR, Wyman SK, Pogosova-Agadjanyan EL, Peterson A, Noteboom J, O'Briant KC, Allen A *et al*: **Circulating microRNAs as stable blood-based markers for cancer detection**. *Proceedings of the National Academy of Sciences of the United States of America* 2008, **105**(30):10513-10518.

30.   Botta-Orfila T, Morato X, Compta Y, Lozano JJ, Falgas N, Valldeoriola F, Pont-Sunyer C, Vilas D, Mengual L, Fernandez M *et al*: **Identification of blood serum micro-RNAs associated with idiopathic and LRRK2 Parkinson's disease**. *Journal of neuroscience research* 2014, **92**(8):1071-1077.

31.   Cardo LF, Coto E, de Mena L, Ribacoba R, Moris G, Menendez M, Alvarez V: **Profile of microRNAs in the plasma of Parkinson's disease patients and healthy controls**. *Journal of neurology* 2013, **260**(5):1420-1422.

32.   Khoo SK, Petillo D, Kang UJ, Resau JH, Berryhill B, Linder J, Forsgren L, Neuman LA, Tan AC: **Plasma-based circulating MicroRNA biomarkers for Parkinson's disease**. *Journal of Parkinson's disease* 2012, **2**(4):321-331.

33. Martins M, Rosa A, Guedes LC, Fonseca BV, Gotovac K, Violante S, Mestre T, Coelho M, Rosa MM, Martin ER *et al*: **Convergence of miRNA expression profiling, alpha-synuclein interacton and GWAS in Parkinson's disease**. *PLoS One* 2011, **6**(10):e25443.

34. Soreq L, Salomonis N, Bronstein M, Greenberg DS, Israel Z, Bergman H, Soreq H: **Small RNA sequencing-microarray analyses in Parkinson leukocytes reveal deep brain stimulation-induced splicing changes that classify brain region transcriptomes**. *Frontiers in molecular neuroscience* 2013, **6**:10.

35. Serafin A, Foco L, Zanigni S, Blankenburg H, Picard A, Zanon A, Giannini G, Pichler I, Facheris MF, Cortelli P *et al*: **Overexpression of blood microRNAs 103a, 30b, and 29a in l-dopa-treated patients with PD**. *Neurology* 2015, **84**(7):645-653.

36. Burgos K, Malenica I, Metpally R, Courtright A, Rakela B, Beach T, Shill H, Adler C, Sabbagh M, Villa S *et al*: **Profiles of extracellular miRNA in cerebrospinal fluid and serum from patients with Alzheimer's and Parkinson's diseases correlate with disease status and features of pathology**. *PLoS One* 2014, **9**(5):e94839.

37. Lau P, Bossers K, Janky R, Salta E, Frigerio CS, Barbash S, Rothman R, Sierksma AS, Thathiah A, Greenberg D *et al*: **Alteration of the microRNA network during the progression of Alzheimer's disease**. *EMBO molecular medicine* 2013, **5**(10):1613-1634.

Conclusion

Summary of Aims

miRNAs are altered in HD brain, several of which relate to clinical phenotypes, such as onset age and striatal degeneration. This effect is CAG-independent, and likely independent of both death age and cortical involvement. In particular, miR-10b-5p levels have the strongest associations to these features, where increased levels in HD brain predict earlier onset age and more striatal involvement. Levels of miR-10b-5p are increased in asymptomatic and grade 2 brains, indicating the levels of this miRNA are increased pre-clinically or within the early stages of the disease process.

In plasma, we found two miRNAs (miR-10b-5p and miR-486-5p) that were significantly altered. These same miRNAs exhibited nominal association ($p<0.05$) to CAG-adjusted onset (miR-10b-5p and miR-486-5p) and to CAG-adjusted striatal involvement (miR-10b-5p) in the HD cortical study. Levels of both miRNAs were elevated in both HD plasma and brain. miR-10b-5p levels were observed to be slightly elevated in asymptomatic HD and significantly increased in manifest HD compared to healthy controls, which suggests miR-10b-5p changes occur in HD, and may increase in plasma during the transition from premotor to manifest HD.

We identified significant differences in miRNA levels in PD brain and based on a set of deregulated miRNAs, we were able to classify PD and non-diseased brains with high accuracy. The miRNA profile of PDD suggests PDD

has a more extreme molecular phenotype than PDN. A comparison with our previous Huntington's disease (HD) study, which used the same set of control brains, revealed a set of miRNAs altered in both PD and HD. When testing for the association of differentially expressed miRNAs to age at onset, miR-10b-5p had a significant, positive relationship. In contrast to HD, miR-10b-5p was slightly decreased in PD and increased levels of miR-10b-5p were observed in individuals with late-onset.

Overall conclusion

These studies provide a detailed miRNA profile for HD and PD brain, identify miRNAs associated with disease pathology and suggest miRNA changes observed in brain can be detected in blood. Together, these findings support the potential of miRNA biomarkers for the diagnosis and assessment of progression for neurodegenerative diseases.

APPENDIX

Table S2.1. miRNA RT-qPCR validation study results.

Table S2.2. Sample information for eight Huntington's disease brains used for RT-qPCR replication study.

Table S2.3. Sample information for eight control brains used for RT-qPCR replication study.

Table S2.4. miRNA RT-qPCR replication study results.

Table S2.5. Sample information for fourteen Parkinson's disease brains used for RT-qPCR replication study.

Table S2.6. Read statistics for miRNA-sequence analysis.

Table S2.7. Mean and standard deviation inner-distance estimates for TopHat2 alignment.

Table S2.8. Read statistics for mRNA-sequence analysis.

Table S3.1. Sample information for 36 control brains used for miRNA-sequencing.

Table S3.2. Sample information for 28 Huntington's disease brains used for miRNA-sequencing.

Table S3.3. Read statistics for miRNA-sequence analysis.

Table S3.4. Correlation of differentially expressed miRNA precursor pairs.

Table S3.5. Summary statistics for Firefly BioWorks assay.

Table S3.6. Linear regression analysis modeled the relationship of miRNA expression and Vonsattel grade.

Table S5.1. Detailed sample information.
Missing information is designated as "NA".

Table S5.2. Results from miRNA differential expression analysis in Parkinson's disease.

BIBLIOGRAPHY

1.   Gusella JF, Wexler NS, Conneally PM, Naylor SL, Anderson MA, Tanzi RE, Watkins PC, Ottina K, Wallace MR, Sakaguchi AY: **A polymorphic DNA marker genetically linked to Huntington's disease**. *Nature* 1983, **306**:234-238.

2.   **Unified Huntington's Disease Rating Scale: reliability and consistency. Huntington Study Group**. *Movement disorders : official journal of the Movement Disorder Society* 1996, **11**(2):136-142.

3.   Harper PS: **The epidemiology of Huntington's disease**. *Human genetics* 1992, **89**(4):365-376.

4.   Group THsDCR: **A novel gene containing a trinucleotide repeat that is expanded and unstable on Huntington's disease chromosomes.** *Cell* 1993, **72**:971-983.

5.   Duyao M, Ambrose C, Myers R, Novelletto A, Persichetti F, Frontali M, Folstein S, Ross C, Franz M, Abbott M: **Trinucleotide repeat length instability and age of onset in Huntington's disease**. *Nature Genetics* 1993, **4**:387-392.

6.   Hendricks AE, Latourelle JC, Lunetta KL, Cupples LA, Wheeler V, MacDonald ME, Gusella JF, Myers RH: **Estimating the Probability of de novo HD cases from Transmissions of Expanded Penetrant CAG Alleles in the Huntington Disease Gene from Male Carriers of High Normal Alleles (27–35 CAG)**. *American journal of medical genetics Part A* 2009, **149A**:1375-1381.

7.   Myers RH: **Huntington's Disease Genetics**. *NeuroRx* 2004, **1**:255-262.

8.   Djousse L, Knowlton B, Hayden M, Almqvist EW, Brinkman R, Ross C, Margolis R, Rosenblatt A, Durr A, Dode C *et al*: **Interaction of normal and expanded CAG repeat sizes influences age at onset of Huntington disease**. *American Journal of Medical Genetics Part A* 2003, **119A**(3):279-282.

9.   Vonsattel JP, Myers RH, Stevens TJ, Ferrante RJ, Bird ED, Richardson EP: **Neuropathological classification of Huntington's disease**. *Journal of Neuropathology and Experimental Neurology* 1985, **44**:559-577.

10.   Hadzi TC, Hendricks AE, Latourelle JC, Lunetta KL, Cupples LA, Gillis T, Mysore JS, Gusella JF, MacDonald ME, Myers RH *et al*: **Assessment of cortical and striatal involvement in 523 Huntington disease brains**. *Neurology* 2012, **79**:1708-1715.

11.   Rosas HD, Hevelone ND, Zaleta AK, Greve DN, Salat DH, Fischl B: **Regional cortical thinning in preclinical Huntington disease and its relationship to cognition**. *Neurology* 2005, **65**:745-747.

12.   Aylward EH, Sparks BF, Field KM, Yallapragada V, Shpritz BD, Rosenblatt A, Brandt J, Gourley LM, Liang K, Zhou H *et al*: **Onset and rate of striatal atrophy in preclinical Huntington disease**. *Neurology* 2004, **63**(1):66-72.

13.   Hadzi TC, Hendricks AE, Latourelle JC, Lunetta KL, Cupples LA, Gillis T, Mysore JS, Gusella JF, MacDonald ME, Myers RH *et al*: **Assessment of cortical and striatal involvement in 523 Huntington disease brains**. *Neurology* 2012, **79**(16):1708-1715.

14.   Sotrel A, Paskevich PA, Kiely DK, Bird ED, Williams RS, Myers RH: **Morphometric analysis of the prefrontal cortex in Huntington's disease**. *Neurology* 1991, **41**:1117-1117.

15.   Cudkowicz M, Kowall NW: **Degeneration of pyramidal projection neurons in Huntington's disease cortex**. *Annals of Neurology* 1990, **27**:200-204.

16.   DiFiglia M, Sapp E, Chase KO, Davies SW, Bates GP, Vonsattel JP, Aronin N: **Aggregation of huntingtin in neuronal intranuclear inclusions and dystrophic neurites in brain**. *Science* 1997, **277**(5334):1990-1993.

17.   Scherzinger E, Lurz R, Turmaine M, Mangiarini L, Hollenbach B, Hasenbank R, Bates GP, Davies SW, Lehrach H, Wanker EE: **Huntingtin-encoded polyglutamine expansions form amyloid-like protein aggregates in vitro and in vivo**. *Cell* 1997, **90**(3):549-558.

18.   Gutekunst C-A, Li S-H, Yi H, Mulroy JS, Kuemmerle S, Jones R, Rye D, Ferrante RJ, Hersch SM, Li X-J: **Nuclear and Neuropil Aggregates in Huntington's Disease: Relationship to Neuropathology**. *The Journal of Neuroscience* 1999, **19**:2522-2534.

19.   Li SH, Li XJ: **Huntingtin and its role in neuronal degeneration**. *Neuroscientist* 2004, **10**(5):467-475.

20.   Di Prospero NA, Tagle DA: **Normal and mutant huntingtin: partners in crime**. *Nature Medcine* 2000, **6**(11):1208-1209.

21.   Steffan JS, Kazantsev A, Spasic-Boskovic O, Greenwald M, Zhu YZ, Gohler H, Wanker EE, Bates GP, Housman DE, Thompson LM: **The Huntington's disease protein interacts with p53 and CREB-binding protein**

and represses transcription. *Proceedings of the National Academy of Sciences of the United States of America* 2000, **97**(12):6763-6768.

22.   Li SH, Cheng AL, Zhou H, Lam S, Rao M, Li H, Li XJ: **Interaction of Huntington disease protein with transcriptional activator Sp1**. *Molecular and Cell Biology* 2002, **22**(5):1277-1287.

23.   van Roon-Mom WM, Reid SJ, Jones AL, MacDonald ME, Faull RL, Snell RG: **Insoluble TATA-binding protein accumulation in Huntington's disease cortex**. *Molecular Brain Research* 2002, **109**(1-2):1-10.

24.   Zuccato C, Tartari M, Crotti A, Goffredo D, Valenza M, Conti L, Cataudella T, Leavitt BR, Hayden MR, Timmusk T *et al*: **Huntingtin interacts with REST/NRSF to modulate the transcription of NRSE-controlled neuronal genes**. *Nature Genetics* 2003, **35**(1):76-83.

25.   Cha JH: **Transcriptional dysregulation in Huntington's disease**. *Trends in Neuroscience* 2000, **23**(9):387-392.

26.   Marcora E, Kennedy MB: **The Huntington's disease mutation impairs Huntingtin's role in the transport of NF-?B from the synapse to the nucleus**. *Human Molecular Genetics* 2010, **19**:4373-4384.

27.   Godavarthi SK, Narender D, Mishra A, Goswami A, Rao SNR, Nukina N, Jana NR: **Induction of chemokines, MCP-1, and KC in the mutant huntingtin expressing neuronal cells because of proteasomal dysfunction**. *Journal of Neurochemistry* 2009, **108**:787-795.

28.   Sharp AH, Loev SJ, Schilling G, Li S-H, Li X-J, Bao J, Wagster MV, Kotzuk JA, Steiner JP, Lo A *et al*: **Widespread expression of Huntington's disease gene (IT15) protein product**. *Neuron* 1995, **14**:1065-1074.

29.   Trottier Y, Devys D, Imbert G, Saudou F, An I, Lutz Y, Weber C, Agid Y, Hirsch EC, Mandel JL: **Cellular localization of the Huntington's disease protein and discrimination of the normal and mutated form**. *Nature Genetics* 1995, **10**:104-110.

30.   Bessert DA, Gutridge KL, Dunbar JC, Carlock LR: **The identification of a functional nuclear localization signal in the Huntington disease protein**. *Molecular Brain Research* 1995, **33**:165-173.

31.   Caviston JP, Zajac AL, Tokito M, Holzbaur EL: **Huntingtin coordinates the dynein-mediated dynamic positioning of endosomes and lysosomes**. *Molecular Biology of the Cell* 2011, **22**(4):478-492.

32.   Li SH, Gutekunst CA, Hersch SM, Li XJ: **Interaction of huntingtin-associated protein with dynactin P150Glued**. *Journal of Neuroscience* 1998, **18**(4):1261-1269.

33.   Colin E, Zala D, Liot G, Rangone H, Borrell-Pages M, Li XJ, Saudou F, Humbert S: **Huntingtin phosphorylation acts as a molecular switch for anterograde/retrograde transport in neurons**. *EMBO Journal* 2008, **27**(15):2124-2134.

34.   Savas JN, Ma B, Deinhardt K, Culver BP, Restituito S, Wu L, Belasco JG, Chao MV, Tanese N: **A role for huntington disease protein in dendritic RNA granules**. *Journal of Biological Chemistry* 2010, **285**(17):13142-13153.

35.   Ma B, Culver BP, Baj G, Tongiorgi E, Chao MV, Tanese N: **Localization of BDNF mRNA with the Huntington's disease protein in rat brain**. *Molecular Neurodegeneration* 2010, **5**:22.

36.   Tong Y, Ha TJ, Liu L, Nishimoto A, Reiner A, Goldowitz D: **Spatial and temporal requirements for huntingtin (Htt) in neuronal migration and survival during brain development**. *Journal of Neuroscience* 2011, **31**(41):14794-14799.

37.   Nasir J, Floresco SB, O'Kusky JR, Diewert VM, Richman JM, Zeisler J, Borowski A, Marth JD, Phillips AG, Hayden MR: **Targeted disruption of the Huntington's disease gene results in embryonic lethality and behavioral and morphological changes in heterozygotes**. *Cell* 1995, **81**(5):811-823.

38.   Träger U, Andre R, Magnusson-Lind A, Miller JRC, Connolly C, Weiss A, Grueninger S, Silajdžić E, Smith DL, Leavitt BR *et al*: **Characterisation of immune cell function in fragment and full-length Huntington's disease mouse models**. *Neurobiology of Disease* 2014, **73C**:388-398.

39.   Consortium HDi: **Induced pluripotent stem cells from patients with Huntington's disease show CAG-repeat-expansion-associated phenotypes**. *Cell Stem Cell* 2012, **11**(2):264-278.

40.   Koroshetz WJ, Jenkins BG, Rosen BR, Beal MF: **Energy metabolism defects in Huntington's disease and effects of coenzyme Q10**. *Annals of Neurology* 1997, **41**(2):160-165.

41.   Cattaneo E, Rigamonti D, Goffredo D, Zuccato C, Squitieri F, Sipione S: **Loss of normal huntingtin function: new developments in Huntington's disease research**. *Trends in Neuroscience* 2001, **24**(3):182-188.

42.   Ravikumar B, Vacher C, Berger Z, Davies JE, Luo S, Oroz LG, Scaravilli F, Easton DF, Duden R, O'Kane CJ *et al*: **Inhibition of mTOR induces autophagy and reduces toxicity of polyglutamine expansions in fly and mouse models of Huntington disease**. *Nature Genetics* 2004, **36**(6):585-595.

43.   Wang J, Wang CE, Orr A, Tydlacka S, Li SH, Li XJ: **Impaired ubiquitin-proteasome system activity in the synapses of Huntington's disease mice**. *Journal of Cell Biology* 2008, **180**(6):1177-1189.

44.   Usdin MT, Shelbourne PF, Myers RM, Madison DV: **Impaired synaptic plasticity in mice carrying the Huntington's disease mutation**. *Human Molecular Genetics* 1999, **8**(5):839-846.

45.   Liang ZQ, Wang XX, Wang Y, Chuang DM, DiFiglia M, Chase TN, Qin ZH: **Susceptibility of striatal neurons to excitotoxic injury correlates with basal levels of Bcl-2 and the induction of P53 and c-Myc immunoreactivity**. *Neurobiology of Disease* 2005, **20**(2):562-573.

46.   Wellington CL, Ellerby LM, Hackam AS, Margolis RL, Trifiro MA, Singaraja R, McCutcheon K, Salvesen GS, Propp SS, Bromm M *et al*: **Caspase cleavage of gene products associated with triplet expansion disorders generates truncated fragments containing the polyglutamine tract**. *Journal of Biological Chemistry* 1998, **273**(15):9158-9167.

47.   Kim YJ, Yi Y, Sapp E, Wang Y, Cuiffo B, Kegel KB, Qin ZH, Aronin N, DiFiglia M: **Caspase 3-cleaved N-terminal fragments of wild-type and mutant huntingtin are present in normal and Huntington's disease brains, associate with membranes, and undergo calpain-dependent proteolysis**. *Proceedings of the National Academy of Sciences of the United States of America* 2001, **98**:12784-12789.

48.   Scherzinger E, Sittler A, Schweiger K, Heiser V, Lurz R, Hasenbank R, Bates GP, Lehrach H, Wanker EE: **Self-assembly of polyglutamine-containing huntingtin fragments into amyloid-like fibrils: implications for Huntington's disease pathology**. *Proceedings of the National Academy of Sciences of the United States of America* 1999, **96**(8):4604-4609.

49.   Wellington CL, Ellerby LM, Gutekunst CA, Rogers D, Warby S, Graham RK, Loubser O, van Raamsdonk J, Singaraja R, Yang YZ *et al*: **Caspase cleavage of mutant huntingtin precedes neurodegeneration in Huntington's disease**. *Journal of Neuroscience* 2002, **22**(18):7862-7872.

50.   Parkinson J: **An essay on the shaking palsy. 1817**. *The Journal of neuropsychiatry and clinical neurosciences* 2002, **14**(2):223-236; discussion 222.

148

51.   Spillantini MG, Crowther RA, Jakes R, Hasegawa M, Goedert M: **alpha-Synuclein in filamentous inclusions of Lewy bodies from Parkinson's disease and dementia with lewy bodies**. *Proceedings of the National Academy of Sciences of the United States of America* 1998, **95**(11):6469-6473.

52.   Stefanis L: **alpha-Synuclein in Parkinson's disease**. *Cold Spring Harbor perspectives in medicine* 2012, **2**(2):a009399.

53.   Braak H, Del Tredici K, Rub U, de Vos RA, Jansen Steur EN, Braak E: **Staging of brain pathology related to sporadic Parkinson's disease**. *Neurobiology of aging* 2003, **24**(2):197-211.

54.   Sacino AN, Brooks M, Thomas MA, McKinney AB, Lee S, Regenhardt RW, McGarvey NH, Ayers JI, Notterpek L, Borchelt DR *et al*: **Intramuscular injection of alpha-synuclein induces CNS alpha-synuclein pathology and a rapid-onset motor phenotype in transgenic mice**. *Proceedings of the National Academy of Sciences of the United States of America* 2014, **111**(29):10732-10737.

55.   Mosharov EV, Staal RG, Bove J, Prou D, Hananiya A, Markov D, Poulsen N, Larsen KE, Moore CM, Troyer MD *et al*: **Alpha-synuclein overexpression increases cytosolic catecholamine concentration**. *Journal of Neuroscience* 2006, **26**(36):9304-9311.

56.   Mosharov EV, Larsen KE, Kanter E, Phillips KA, Wilson K, Schmitz Y, Krantz DE, Kobayashi K, Edwards RH, Sulzer D: **Interplay between cytosolic dopamine, calcium, and alpha-synuclein causes selective death of substantia nigra neurons**. *Neuron* 2009, **62**(2):218-229.

57.   Betarbet R, Sherer TB, MacKenzie G, Garcia-Osuna M, Panov AV, Greenamyre JT: **Chronic systemic pesticide exposure reproduces features of Parkinson's disease**. *Nature neuroscience* 2000, **3**(12):1301-1306.

58.   Jenner P: **Oxidative stress in Parkinson's disease**. *Annals of Neurology* 2003, **53 Suppl 3**:S26-36; discussion S36-28.

59.   Janda E, Isidoro C, Carresi C, Mollace V: **Defective autophagy in Parkinson's disease: role of oxidative stress**. *Molecular neurobiology* 2012, **46**(3):639-661.

60.   Dexter DT, Jenner P: **Parkinson disease: from pathology to molecular disease mechanisms**. *Free radical biology & medicine* 2013, **62**:132-144.

61.   Nalls MA, Pankratz N, Lill CM, Do CB, Hernandez DG, Saad M, DeStefano AL, Kara E, Bras J, Sharma M *et al*: **Large-scale meta-analysis of**

149

genome-wide association data identifies six new risk loci for Parkinson's disease. *Nature genetics* 2014, **46**(9):989-993.

62.   Simon-Sanchez J, Schulte C, Bras JM, Sharma M, Gibbs JR, Berg D, Paisan-Ruiz C, Lichtner P, Scholz SW, Hernandez DG *et al*: **Genome-wide association study reveals genetic risk underlying Parkinson's disease**. *Nature genetics* 2009, **41**(12):1308-1312.

63.   Nishioka K, Hayashi S, Farrer MJ, Singleton AB, Yoshino H, Imai H, Kitami T, Sato K, Kuroda R, Tomiyama H *et al*: **Clinical heterogeneity of alpha-synuclein gene duplication in Parkinson's disease**. *Annuals of Neurology* 2006, **59**(2):298-309.

64.   Kruger R, Kuhn W, Muller T, Woitalla D, Graeber M, Kosel S, Przuntek H, Epplen JT, Schols L, Riess O: **Ala30Pro mutation in the gene encoding alpha-synuclein in Parkinson's disease**. *Nature genetics* 1998, **18**(2):106-108.

65.   Zarranz JJ, Alegre J, Gomez-Esteban JC, Lezcano E, Ros R, Ampuero I, Vidal L, Hoenicka J, Rodriguez O, Atares B *et al*: **The new mutation, E46K, of alpha-synuclein causes Parkinson and Lewy body dementia**. *Annals of Neurology* 2004, **55**(2):164-173.

66.   Singleton AB, Farrer M, Johnson J, Singleton A, Hague S, Kachergus J, Hulihan M, Peuralinna T, Dutra A, Nussbaum R *et al*: **alpha-Synuclein locus triplication causes Parkinson's disease**. *Science* 2003, **302**(5646):841.

67.   Polymeropoulos MH, Lavedan C, Leroy E, Ide SE, Dehejia A, Dutra A, Pike B, Root H, Rubenstein J, Boyer R *et al*: **Mutation in the alpha-synuclein gene identified in families with Parkinson's disease**. *Science* 1997, **276**(5321):2045-2047.

68.   Lin MK, Farrer MJ: **Genetics and genomics of Parkinson's disease**. *Genome medicine* 2014, **6**(6):48.

69.   Hamza TH, Payami H: **The heritability of risk and age at onset of Parkinson's disease after accounting for known genetic risk factors**. *Journal of human genetics* 2010, **55**(4):241-243.

70.   Barrett MJ, Hac NE, Yan G, Harrison MB, Wooten GF: **Relationship of age of onset and family history in Parkinson disease**. *Movement disorders : official journal of the Movement Disorder Society* 2015.

71.   Harris GJ, Pearlson GD, Peyser CE, Aylward EH, Roberts J, Barta PE, Chase GA, Folstein SE: **Putamen volume reduction on magnetic resonance**

imaging exceeds caudate changes in mild Huntington's disease. *Annals of Neurology* 1992, **31**(1):69-75.

72.   Tabrizi SJ, Scahill RI, Owen G, Durr A, Leavitt BR, Roos RA, Borowsky B, Landwehrmeyer B, Frost C, Johnson H *et al*: **Predictors of phenotypic progression and disease onset in premanifest and early-stage Huntington's disease in the TRACK-HD study: analysis of 36-month observational data**. *The Lancet Neurology* 2013, **12**(7):637-649.

73.   Paulsen JS, Langbehn DR, Stout JC, Aylward E, Ross CA, Nance M, Guttman M, Johnson S, MacDonald M, Beglinger LJ *et al*: **Detection of Huntington's disease decades before diagnosis: the Predict-HD study**. *Journal of Neurology, Neurosurgery & Psychiatry* 2008, **79**(8):874-880.

74.   Wolf RC, Vasic N, Schonfeldt-Lecuona C, Landwehrmeyer GB, Ecker D: **Dorsolateral prefrontal cortex dysfunction in presymptomatic Huntington's disease: evidence from event-related fMRI**. *Brain : a journal of neurology* 2007, **130**(Pt 11):2845-2857.

75.   Pavese N, Gerhard A, Tai YF, Ho AK, Turkheimer F, Barker RA, Brooks DJ, Piccini P: **Microglial activation correlates with severity in Huntington disease: a clinical and PET study**. *Neurology* 2006, **66**(11):1638-1643.

76.   Tai YF, Pavese N, Gerhard A, Tabrizi SJ, Barker RA, Brooks DJ, Piccini P: **Microglial activation in presymptomatic Huntington's disease gene carriers**. *Brain : a journal of neurology* 2007, **130**(Pt 7):1759-1766.

77.   Bjorkqvist M, Wild EJ, Thiele J, Silvestroni A, Andre R, Lahiri N, Raibon E, Lee RV, Benn CL, Soulet D *et al*: **A novel pathogenic pathway of immune activation detectable before clinical onset in Huntington's disease**. *Journal of Experimental Medicine* 2008, **205**(8):1869-1877.

78.   Niccolini F, Politis M: **Neuroimaging in Huntington's disease**. *World journal of radiology* 2014, **6**(6):301-312.

79.   Kimura H, McGeer EG, McGeer PL: **Metabolic alterations in an animal model of Huntington's disease using the 14C-deoxyglucose method**. *Journal of neural transmission Supplementum* 1980(16):103-109.

80.   Kuhl DE, Phelps ME, Markham CH, Metter EJ, Riege WH, Winter J: **Cerebral metabolism and atrophy in Huntington's disease determined by 18FDG and computed tomographic scan**. *Annals of Neurology* 1982, **12**(5):425-434.

81.   Young AB, Penney JB, Starosta-Rubinstein S, Markel DS, Berent S, Giordani B, Ehrenkaufer R, Jewett D, Hichwa R: **PET scan investigations of Huntington's disease: cerebral metabolic correlates of neurological features and functional decline**. *Annals of Neurology* 1986, **20**(3):296-303.

82.   Mazziotta JC, Phelps ME, Pahl JJ, Huang SC, Baxter LR, Riege WH, Hoffman JM, Kuhl DE, Lanto AB, Wapenski JA *et al*: **Reduced cerebral glucose metabolism in asymptomatic subjects at risk for Huntington's disease**. *New England Journal of Medicine* 1987, **316**(7):357-362.

83.   Herben-Dekker M, van Oostrom JC, Roos RA, Jurgens CK, Witjes-Ane MN, Kremer HP, Leenders KL, Spikman JM: **Striatal metabolism and psychomotor speed as predictors of motor onset in Huntington's disease**. *Journal of neurology* 2014, **261**(7):1387-1397.

84.   Browne SE, Bowling AC, MacGarvey U, Baik MJ, Berger SC, Muqit MM, Bird ED, Beal MF: **Oxidative damage and metabolic dysfunction in Huntington's disease: selective vulnerability of the basal ganglia**. *Annals of Neurology* 1997, **41**(5):646-653.

85.   Hersch SM, Gevorkian S, Marder K, Moskowitz C, Feigin A, Cox M, Como P, Zimmerman C, Lin M, Zhang L *et al*: **Creatine in Huntington disease is safe, tolerable, bioavailable in brain and reduces serum 8OH2'dG**. *Neurology* 2006, **66**(2):250-252.

86.   Chen CM, Wu YR, Cheng ML, Liu JL, Lee YM, Lee PW, Soong BW, Chiu DT: **Increased oxidative damage and mitochondrial abnormalities in the peripheral blood of Huntington's disease patients**. *Biochemical and biophysical research communications* 2007, **359**(2):335-340.

87.   Long JD, Matson WR, Juhl AR, Leavitt BR, Paulsen JS, Investigators P-H, Coordinators of the Huntington Study G: **8OHdG as a marker for Huntington disease progression**. *Neurobiology of disease* 2012, **46**(3):625-634.

88.   Borowsky B, Warner J, Leavitt BR, Tabrizi SJ, Roos RA, Durr A, Becker C, Sampaio C, Tobin AJ, Schulman H: **8OHdG is not a biomarker for Huntington disease state or progression**. *Neurology* 2013, **80**(21):1934-1941.

89.   Russell D, Jennings D, Barret O, Tamagnan G, Carroll V, Alagille D, Morley T, Papin C, Seibyl J, Marek K: **Monitoring loss of striatal phosphodiesterase 10A (PDE10A) with [18F]MNI-659 and PET: A biomarker of early Huntington disease (HD) progression**. *Neurology* 2015, **84**(14):Supplement S15.004.

90.   McArthur RA: **Translational neuroimaging : tools for CNS drug discovery, development and treatment**. London ; Waltham, MA: Academic Press; 2013.

91.   Weiss A, Trager U, Wild EJ, Grueninger S, Farmer R, Landles C, Scahill RI, Lahiri N, Haider S, Macdonald D *et al*: **Mutant huntingtin fragmentation in immune cells tracks Huntington's disease progression**. *The Journal of clinical investigation* 2012, **122**(10):3731-3736.

92.   Wild EJ, Boggio R, Langbehn D, Robertson N, Haider S, Miller JR, Zetterberg H, Leavitt BR, Kuhn R, Tabrizi SJ *et al*: **Quantification of mutant huntingtin protein in cerebrospinal fluid from Huntington's disease patients**. *The Journal of clinical investigation* 2015.

93.   Mastrokolias A, Ariyurek Y, Goeman JJ, van Duijn E, Roos RA, van der Mast RC, van Ommen GB, den Dunnen JT, t Hoen PA, van Roon-Mom WM: **Huntington's disease biomarker progression profile identified by transcriptome sequencing in peripheral blood**. *European journal of human genetics : EJHG* 2015.

94.   Borovecki F, Lovrecic L, Zhou J, Jeong H, Then F, Rosas HD, Hersch SM, Hogarth P, Bouzou B, Jensen RV *et al*: **Genome-wide expression profiling of human blood reveals biomarkers for Huntington's disease**. *Proceedings of the National Academy of Sciences of the United States of America* 2005, **102**(31):11023-11028.

95.   Aarsland D, Zaccai J, Brayne C: **A systematic review of prevalence studies of dementia in Parkinson's disease**. *Movement disorders : official journal of the Movement Disorder Society* 2005, **20**(10):1255-1263.

96.   Chahine LM, Stern MB: **Characterizing Premotor Parkinson's Disease: Clinical Features and Objective Markers**. *Movement disorders clinical practice* 2014, **1**(4):299-306.

97.   Doty RL, Deems DA, Stellar S: **Olfactory dysfunction in parkinsonism: a general deficit unrelated to neurologic signs, disease stage, or disease duration**. *Neurology* 1988, **38**(8):1237-1244.

98.   Abbott RD, Petrovitch H, White LR, Masaki KH, Tanner CM, Curb JD, Grandinetti A, Blanchette PL, Popper JS, Ross GW: **Frequency of bowel movements and the future risk of Parkinson's disease**. *Neurology* 2001, **57**(3):456-462.

99.   Abbott RD, Ross GW, White LR, Tanner CM, Masaki KH, Nelson JS, Curb JD, Petrovitch H: **Excessive daytime sleepiness and subsequent development of Parkinson disease**. *Neurology* 2005, **65**(9):1442-1446.

100.   Boeve BF: **Idiopathic REM sleep behaviour disorder in the development of Parkinson's disease**. *The Lancet Neurology* 2013, **12**(5):469-482.

101.   Ross GW, Petrovitch H, Abbott RD, Tanner CM, Popper J, Masaki K, Launer L, White LR: **Association of olfactory dysfunction with risk for future Parkinson's disease**. *Annals of Neurology* 2008, **63**(2):167-173.

102.   Movement Disorder Society Task Force on Rating Scales for Parkinson's D: **The Unified Parkinson's Disease Rating Scale (UPDRS): status and recommendations**. *Movement disorders : official journal of the Movement Disorder Society* 2003, **18**(7):738-750.

103.   Miller DB, O'Callaghan JP: **Biomarkers of Parkinson's disease: present and future**. *Metabolism: clinical and experimental* 2015, **64**(3 Suppl 1):S40-46.

104.   Iranzo A, Lomena F, Stockner H, Valldeoriola F, Vilaseca I, Salamero M, Molinuevo JL, Serradell M, Duch J, Pavia J *et al*: **Decreased striatal dopamine transporter uptake and substantia nigra hyperechogenicity as risk markers of synucleinopathy in patients with idiopathic rapid-eye-movement sleep behaviour disorder: a prospective study [corrected]**. *The Lancet Neurology* 2010, **9**(11):1070-1077.

105.   Shannon KM, Keshavarzian A, Mutlu E, Dodiya HB, Daian D, Jaglin JA, Kordower JH: **Alpha-synuclein in colonic submucosa in early untreated Parkinson's disease**. *Movement disorders : official journal of the Movement Disorder Society* 2012, **27**(6):709-715.

106.   Maarouf CL, Beach TG, Adler CH, Shill HA, Sabbagh MN, Wu T, Walker DG, Kokjohn TA, Roher AE, Arizona PDC: **Cerebrospinal fluid biomarkers of neuropathologically diagnosed Parkinson's disease subjects**. *Neurological research* 2012, **34**(7):669-676.

107.   Hall S, Surova Y, Ohrfelt A, Zetterberg H, Lindqvist D, Hansson O: **CSF biomarkers and clinical progression of Parkinson disease**. *Neurology* 2015, **84**(1):57-63.

108.   Soreq L, Bergman H, Goll Y, Greenberg DS, Israel Z, Soreq H: **Deep brain stimulation induces rapidly reversible transcript changes in Parkinson's leucocytes**. *Journal of cellular and molecular medicine* 2012, **16**(7):1496-1507.

109.   Soreq L, Guffanti A, Salomonis N, Simchovitz A, Israel Z, Bergman H, Soreq H: **Long non-coding RNA and alternative splicing modulations in Parkinson's leukocytes identified by RNA sequencing**. *PLoS computational biology* 2014, **10**(3):e1003517.

110.   Santiago JA, Potashkin JA: **Network-based metaanalysis identifies HNF4A and PTBP1 as longitudinally dynamic biomarkers for Parkinson's disease**. *Proceedings of the National Academy of Sciences of the United States of America* 2015, **112**(7):2257-2262.

111.   Lavut A, Raveh D: **Sequestration of highly expressed mRNAs in cytoplasmic granules, P-bodies, and stress granules enhances cell viability**. *PLoS Genetics* 2012, **8**(2):e1002527.

112.   Martino S, di Girolamo I, Orlacchio A, Datti A, Orlacchio A: **MicroRNA implications across neurodevelopment and neuropathology**. *Journal of biomedicine & biotechnology* 2009, **2009**:654346.

113.   Junn E, Mouradian MM: **MicroRNAs in neurodegenerative diseases and their therapeutic potential**. *Pharmacology & therapeutics* 2012, **133**(2):142-150.

114.   Packer AN, Xing Y, Harper SQ, Jones L, Davidson BL: **The bifunctional microRNA miR-9/miR-9* regulates REST and CoREST and is downregulated in Huntington's disease**. *Journal of Neuroscience* 2008, **28**(53):14341-14346.

115.   Marti E, Pantano L, Banez-Coronel M, Llorens F, Minones-Moyano E, Porta S, Sumoy L, Ferrer I, Estivill X: **A myriad of miRNA variants in control and Huntington's disease brain regions detected by massively parallel sequencing**. *Nucleic Acids Research* 2010, **38**(20):7219-7235.

116.   Johnson R, Zuccato C, Belyaev ND, Guest DJ, Cattaneo E, Buckley NJ: **A microRNA-based gene dysregulation pathway in Huntington's disease**. *Neurobiology of disease* 2008, **29**(3):438-445.

117.   Sinha M, Ghose J, Bhattarcharyya NP: **Micro RNA -214,-150,-146a and-125b target Huntingtin gene**. *RNA Biology* 2011, **8**(6):1005-1021.

118.   Cheng PH, Li CL, Chang YF, Tsai SJ, Lai YY, Chan AW, Chen CM, Yang SH: **miR-196a Ameliorates Phenotypes of Huntington Disease in Cell, Transgenic Mouse, and Induced Pluripotent Stem Cell Models**. *American journal of human genetics* 2013.

119.   Lee ST, Chu K, Im WS, Yoon HJ, Im JY, Park JE, Park KH, Jung KH, Lee SK, Kim M *et al*: **Altered microRNA regulation in Huntington's disease models**. *Experimental Neurology* 2011, **227**(1):172-179.

120.   Jin J, Cheng Y, Zhang Y, Wood W, Peng Q, Hutchison E, Mattson MP, Becker KG, Duan W: **Interrogation of brain miRNA and mRNA expression profiles reveals a molecular regulatory network that is perturbed by mutant huntingtin**. *Journal of neurochemistry* 2012, **123**(4):477-490.

121.   Savas JN, Ma B, Deinhardt K, Culver BP, Restituito S, Wu L, Belasco JG, Chao MV, Tanese N: **A role for huntington disease protein in dendritic RNA granules**. *Journal of Biological Chemistry* 2010, **285**(17):13142-13153.

122.   Savas JN, Makusky A, Ottosen S, Baillat D, Then F, Krainc D, Shiekhattar R, Markey SP, Tanese N: **Huntington's disease protein contributes to RNA-mediated gene silencing through association with Argonaute and P bodies**. *Proceedings of the National Academy of Sciences of the United States of America* 2008, **105**(31):10820-10825.

123.   Kim J, Inoue K, Ishii J, Vanti WB, Voronov SV, Murchison E, Hannon G, Abeliovich A: **A MicroRNA feedback circuit in midbrain dopamine neurons**. *Science* 2007, **317**(5842):1220-1224.

124.   de Mena L, Coto E, Cardo LF, Diaz M, Blazquez M, Ribacoba R, Salvador C, Pastor P, Samaranch L, Moris G *et al*: **Analysis of the Micro-RNA-133 and PITX3 genes in Parkinson's disease**. *American Journal of Medical Genetics B Neuropsychiatry Genetrics* 2010, **153B**(6):1234-1239.

125.   Sotiriou S, Gibney G, Baxevanis AD, Nussbaum RL: **A single nucleotide polymorphism in the 3'UTR of the SNCA gene encoding alpha-synuclein is a new potential susceptibility locus for Parkinson disease**. *Neuroscience Letter* 2009, **461**(2):196-201.

126.   Junn E, Lee KW, Jeong BS, Chan TW, Im JY, Mouradian MM: **Repression of alpha-synuclein expression and toxicity by microRNA-7**. *Proceedings of the National Academy of Sciences of the United States of America* 2009, **106**(31):13052-13057.

127.   Doxakis E: **Post-transcriptional regulation of alpha-synuclein expression by mir-7 and mir-153**. *Journal of Biological Chemistry* 2010, **285**(17):12726-12734.

128.   Rhinn H, Qiang L, Yamashita T, Rhee D, Zolin A, Vanti W, Abeliovich A: **Alternative alpha-synuclein transcript usage as a convergent mechanism in Parkinson's disease pathology**. *Nature communications* 2012, **3**:1084.

129. Minones-Moyano E, Porta S, Escaramis G, Rabionet R, Iraola S, Kagerbauer B, Espinosa-Parrilla Y, Ferrer I, Estivill X, Marti E: **MicroRNA profiling of Parkinson's disease brains identifies early downregulation of miR-34b/c which modulate mitochondrial function**. *Human Molecular Genetics* 2011, **20**(15):3067-3078.

130. Botta-Orfila T, Morato X, Compta Y, Lozano JJ, Falgas N, Valldeoriola F, Pont-Sunyer C, Vilas D, Mengual L, Fernandez M *et al*: **Identification of blood serum micro-RNAs associated with idiopathic and LRRK2 Parkinson's disease**. *Journal of neuroscience research* 2014, **92**(8):1071-1077.

131. Cardo LF, Coto E, de Mena L, Ribacoba R, Moris G, Menendez M, Alvarez V: **Profile of microRNAs in the plasma of Parkinson's disease patients and healthy controls**. *Journal of neurology* 2013, **260**(5):1420-1422.

132. Khoo SK, Petillo D, Kang UJ, Resau JH, Berryhill B, Linder J, Forsgren L, Neuman LA, Tan AC: **Plasma-based circulating MicroRNA biomarkers for Parkinson's disease**. *Journal of Parkinson's disease* 2012, **2**(4):321-331.

133. Martins M, Rosa A, Guedes LC, Fonseca BV, Gotovac K, Violante S, Mestre T, Coelho M, Rosa MM, Martin ER *et al*: **Convergence of miRNA expression profiling, alpha-synuclein interacton and GWAS in Parkinson's disease**. *PLoS One* 2011, **6**(10):e25443.

134. Soreq L, Salomonis N, Bronstein M, Greenberg DS, Israel Z, Bergman H, Soreq H: **Small RNA sequencing-microarray analyses in Parkinson leukocytes reveal deep brain stimulation-induced splicing changes that classify brain region transcriptomes**. *Frontiers in molecular neuroscience* 2013, **6**:10.

135. Serafin A, Foco L, Zanigni S, Blankenburg H, Picard A, Zanon A, Giannini G, Pichler I, Facheris MF, Cortelli P *et al*: **Overexpression of blood microRNAs 103a, 30b, and 29a in l-dopa-treated patients with PD**. *Neurology* 2015, **84**(7):645-653.

136. Burgos K, Malenica I, Metpally R, Courtright A, Rakela B, Beach T, Shill H, Adler C, Sabbagh M, Villa S *et al*: **Profiles of extracellular miRNA in cerebrospinal fluid and serum from patients with Alzheimer's and Parkinson's diseases correlate with disease status and features of pathology**. *PLoS One* 2014, **9**(5):e94839.

137. Gantier MP, McCoy CE, Rusinova I, Saulep D, Wang D, Xu D, Irving AT, Behlke MA, Hertzog PJ, Mackay F *et al*: **Analysis of microRNA turnover in mammalian cells following Dicer1 ablation**. *Nucleic Acids Research* 2011, **39**(13):5692-5703.

138. Kalani A, Tyagi A, Tyagi N: **Exosomes: mediators of neurodegeneration, neuroprotection and therapeutics**. *Molecular neurobiology* 2014, **49**(1):590-600.

139. Mitchell PS, Parkin RK, Kroh EM, Fritz BR, Wyman SK, Pogosova-Agadjanyan EL, Peterson A, Noteboom J, O'Briant KC, Allen A *et al*: **Circulating microRNAs as stable blood-based markers for cancer detection**. *Proceedings of the National Academy of Sciences of the United States of America* 2008, **105**(30):10513-10518.

CURRICULUM VITAE

ANDREW HOSS

PERSONAL
Birth year: 1984
Home address: 203-205 Elm Street #3, Cambridge, MA 02139
Phone: 617-913-2875
Email: andrewghoss@gmail.com

EDUCATION
Ph.D. Genetics & Genomics, Boston University School of Medicine, Boston, MA, June 2015 (expected)
M.S. Biology, Tufts University, 2011
B.A. Biological Sciences & Psychology, Binghamton University, 2006

RESEARCH EXPERIENCE

BOSTON UNIVERSITY, DEPARTMENT OF NEUROLOGY, Boston, MA
Doctoral candidate, *Richard H. Myers Lab*, 2011-2015

Project #1: Neurodegenerative disease transcriptomic profiling

- Utilized small RNA and large RNA sequence analysis from human brain to identify biomarkers of Huntington's and Parkinson's disease progression
- Extensive background in bioinformatics analysis (Tuxedo, bedtools, samtools, fastx toolkit, novoalign, miRDeep, R/Bioconductor) and data interpretation (differential expression profiling, multivariate statistics, predictive modeling, regression analysis)
- Independently established a funded collaboration with Firefly Bioworks to develop their novel flow cytometer-based miRNA detection platform
- Created *in vitro* Huntington's disease models and custom image analysis scripts using ImageJ to assess cell death and the extent of aggregate formation for functional validation of miRNAs

Project #2: Characterization of cyclin-g associated kinase (GAK) in Parkinson's disease

- Evaluated the *GAK* locus using targeted sequencing in 425 familial Parkinson's disease cases to identify the functional variants ultimately responsible for the association to the disease

WORK EXPERIENCE

BROAD INSTITUTE OF MIT AND HARVARD, Cambridge, MA
Process Development Associate I/II, Special Projects Group, 2009 – 2011

- Led R&D and process improvement efforts in Ion Torrent/Life Technologies collaboration
- First external user of Ion Torrent, performing over 1000 sequencing runs prior to commercial release
- Helped patent on-bead paired-end sequencing by reducing the invention to practice
- Maintained platform infrastructure by managing protocols, databases, reagent supply chains, software and machine upgrades
- Frequently applied molecular biology techniques and various nucleic acid quantification methods for sequencing chemistry optimization

Process Technician I/II, Production Sequencing Group, 2007 – 2009
- Participated in the evaluation, implementation and scale-up of 454 FLX/Titanium technologies for numerous long-term initiatives including the Human Microbiome Project
- Expert knowledge of NGS workflows and data analysis for 454, Helicos, Illumina and SOLiD platforms
- Scripted liquid handling robots and engineered several plate-based modules to streamline the 454 sequencing process

Process Technician Assistant, Core Sequencing, 2007
- Operated automated laboratory equipment to clone, amplify, purify, and prepare DNA libraries for cycle sequencing reactions
- Experienced in cloning, transformation, colony plating and picking techniques
- Prepared quality control validations and maintained LIMS records
- Executed process development projects to improve ultra-high throughput Sanger sequencing

OTHER EXPERIENCE
- LEANGEN PARTNERS, Cambridge, MA, *Consultant*, 2011
- CORNELL UNIVERSITY, Ithaca, NY, *Field Technician*, Dr. Anne Clark Laboratory, 2006
- BINGHAMTON UNIVERSITY, *Teaching Assistant*, Organic Chemistry I & II, 3 semesters, 2006
- BINGHAMTON UNIVERSITY, *Undergraduate Assistant*, Fetal Alcohol Laboratory, 2004

CERTIFICATIONS
- Six Sigma Green Belt (*final project to improve sequence quality saved $136,000/year*)
- JMP ANOVA
- SAS I & II

PRESENTATIONS AND AWARDS
- FIREFLY FRONTIERS GRANT, Firefly Bioworks, 2013
- BUSM Evans Day, Poster Award, 2013
- BUSM Genome Science Institute, Poster Award, 2014
- BUSM Genome Science Institute, Poster Award, 2015
- Society for Neuroscience, Poster Presentation, 2013
- Huntington's Study Group, Poster Selection, 2014
- Advances in Genome Biology and Technology Meeting, Poster Selection, 2011
- Advances in Genome Biology and Technology Meeting, Poster Selection, 2008

PUBLICATIONS

Hoss AG, Kartha VK, Dong X, Latourelle JC, Dumitriu A, Hadzi TC, Macdonald ME, Gusella JF, Akbarian S, Chen JF, Weng Z, Myers RH. MicroRNAs located in the Hox gene clusters are implicated in huntington's disease pathogenesis. *PLoS Genetics.* 2014, 10(2):e1004188.

Hoss AG, Labadorf A, Latourelle JC, Kartha VK, Hadzi TC, Gusella JF, Macdonald ME, Chen JF, Akbarian S, Weng Z, Myers RH. miR-10b-5p expression in Huntington's disease brain relates to age of onset and the extent of striatal involvement. *BMC Medical Genomics.* 2015, 8:10.

Bai G, Cheung I, Shulha HP, Coelho JE, Li P, Dong X, Jakovcevski M, Wang Y, Grigorenko A, Jiang Y *Hoss A*, Patel K, Zheng M, Rogaev E, Myers RH, Weng Z, Akbarian S, Chen JF. Epigenetic dysregulation of hairy and enhancer of split 4 (HES4) is associated with striatal degeneration in postmortem Huntington brains. Hum Mol Genet 2015, 24(5):1441-1456.

Labadorf A, *Hoss AG*, Myers RH. Neuroimmune Response and Inflammation in Huntington's disease. In *Neuroimmune Pharmacology, 2nd Edition*. Springer 2015.

Labadorf A, *Hoss AG*, Lagomarsino V, Latourelle JC, Hadzi TC, Macdonald ME, Gusella JF, Chen JF, Akbarian S, Weng Z, Myers RH. Integrated geneset enrichment analysis of high-throughput RNA sequencing data reveals the human Huntington disease brain experiences extensive increased inflammation and developmental gene expression. PLoS One. In Press.

Hoss, AG, Lagomarsino V, Frank S, Hadzi TC, Latourelle JC, Myers RH. Pilot study of plasma-derived miRNAs mimic differences in Huntington's disease brain. Movement Disorders. doi: 10.1002/mds.26457.

Hoss, AG, Labadorf A, Hadzi TC, Beach TG, Myers RH, Latourelle JC. Distinct microRNA alterations observed in Parkinson's disease prefrontal cortex. Frontiers of Aging Neuroscience. In Submission.

PATENTS

Myers, RH, *Hoss, AG*, Kartha, VK. Methods and assays relating to Huntington's disease and Parkinson's disease. U.S. Patent Application 14/595,783, filed January 2015. Patent Pending.

162